Lehigh University
Lehigh Preserve

Theses and Dissertations

2014

Signals and Molecular Mechanisms Involved in Gap Junction Internalization

John Fong
Lehigh University

Follow this and additional works at: http://preserve.lehigh.edu/etd

Part of the Molecular Biology Commons

Recommended Citation
Fong, John, "Signals and Molecular Mechanisms Involved in Gap Junction Internalization" (2014). *Theses and Dissertations.* Paper 1485.

This Dissertation is brought to you for free and open access by Lehigh Preserve. It has been accepted for inclusion in Theses and Dissertations by an authorized administrator of Lehigh Preserve. For more information, please contact preserve@lehigh.edu.

Signals and Molecular Mechanisms Involved in Gap Junction Internalization

by

John T. Fong

A Dissertation

Presented to the Graduate and Research Committee

of Lehigh University

in Candidacy for the Degree of

Doctor of Philosophy

in

Cell & Molecular Biology

Lehigh University

January 2014

© 2013 Copyright

John T. Fong

All Rights Reserved

Approved and recommended for acceptance as a dissertation in partial fulfillment of the requirements for the degree of Doctor of Philosophy

John T. Fong

Signals and Molecular Mechanisms Involved in Gap Junction Internalization

_____

Defense Date

_____

Matthias Falk, Ph.D.

Dissertation Advisor

(Must Sign with Blue Ink)

_____

Approved Date

Committee Members:

_____

Lynne Cassimeris, Ph.D.

_____

Kathy Iovine, Ph.D.

_____

Wojtek Auerbach, Ph.D.

Abbreviatons Used:

AGJ = annular gap junction

AP-2 = adaptor protein complex-2

CHC = clathrin heavy chain

CHX = cycloheximide

CME = clathrin-mediated endocytosis

Cx = connexin

Dab2 = Disabled-2

EGF = epidermal growth factor

GFP = green fluorescent protein

GJ = gap junction

GJIC = gap junction intercellular communication

MAPK = mitogen activated protein kinase

MEF = mouse embryonic fibroblast

mESC = mouse embryonic stem cell

PBS = phosphate buffer saline

PCR = polymerase chain reaction

PKC = protein kinase C

PM = plasma membrane

SDS-PAGE = sodium dodecyl sulfate poly arcrylamide gel electrophoresis

TBS = tris buffered saline

Acknowledgements

I would like to thank my advisor, Dr. Matthias Falk, for guiding me throughout my Ph.D. work. Thanks for spending time to troubleshoot and improve my experiments. I am grateful to have the opportunity to work in his lab.

I extend my gratitude to my committee: Dr. Matthias Falk, Dr. Lynne Cassimeris, Dr. Kathy Iovine, and Dr. Wojtek Auerbach for their critical scientific advice, and comment. Thanks for training me on the confocal microscope and the micro-injector.

I thank Dr. Matthias Falk and Dr. Lynne Cassimeris for the advice on career planning, and for strongly recommending me for post-doctoral training.

I thank Dr. Wojtek Auerbach for inspiring me to pursue a Ph.D. degree. Also thanks for strongly recommending me for post-doctoral training.

I appreciate former Falk lab members – Dr. Anna Gumpert, Dr. Susan Baker, and Dr. Jutta Marzillier - for all of the technical training; current Falk lab members – Dr. Anastasia Thevenin, Dr. Wutigri Nimlamool, Tia Kowal, Rachael Kells, and Charles Fisher - for all of their critical comments and scientific discussions. I am thankful to work with you all in the lab.

Office staff - Maria, Vicki, and Heather for their administrative support.

Graduate students in the department for taking this journey with me.

List of Figures

Figure 1: Amino acid sequence and protein topology of Cx43

Figure 2: Schematic representation of connexins, connexons, and gap junctions

Figure 3: Schematic representation of classical clathrin mediated endocytosis

Figure 4: Schematic representation of gap junction formation and degradation

Figure 5: Cx43 mutants that interfere with AP-2/clathrin binding

Figure 6: Cx43 mutants with AP-2 binding sites S2 or S3 mutated, co-precipitate reduced amounts, while mutants with both sites mutated (S2+3) no longer co-precipitate clathrin and clathrin accessory proteins

Figure 7: The accessory clathrin adaptor protein, Dab2, interacts indirectly with Cx43 via AP-2

Figure 8: AP-2 binding-deficient Cx43 mutants have more GJ channels in their apposed PMs

Figure 9: GJ plaques assembled by AP-2 binding-deficient Cx43 mutants are internalization impaired

Figure 10: AP-2 binding deficient Cx43 mutant proteins exhibit longer half-lives

Figure 11: AP-2 binding-deficient Cx43 mutants become donor cells

Figure 12: Model of Cx43 recruiting clathrin and endocytic clathrin-adaptors

Figure 13: Schematic representation of PCR site-specific mutagenesis

Figure 14: Illustration of ImageJ analysis of gap junction plaque size

Figure 15: EGF induces inhibition of GJIC

Figure 16: EGF induces Cx43 phosphorylation at Ser262, Ser279/282, and Ser368 by activating MAPK and PKC

Figure 17: EGF induces GJ internalization in mES cells

Figure 18: Cx43 in EGF treated mES cells co-immunoprecipitates more clathrin

Figure 19: Schematic representation of EGF phosphorylating Cx43 and inducing GJ internalization

Table of Contents

Abbreviations used

Acknowledgements

List of figures

Abstract...……..…..……..1

1. Chapter 1: Introduction

   1.1. Connexins and gap junction……...…….....3

   1.2. Gap junction intercellular communication (GJIC)……..5

   1.3. Gap junction internalization and degradation……..7

   1.4. Figures……..……..12

2. Chapter 2: Two tyrosine-based sorting signals in the Cx43 C-terminus cooperate to mediate gap junction endocytosis

   2.1. Abstract……..18

   2.2. Introduction……19

   2.3. Results

      2.3.1. Design and construction of Cx43 mutants that interfere with AP-2/clathrin binding……...20

      2.3.2. Cx43 with both AP-2 binding sites (S2+3) mutated no-longer co-precipitate clathrin and clathrin-adaptors……...23

      2.3.3. Cx43/Dab2 interaction is indirect and mediated via AP-2…….25

2.3.4. Cells expressing Cx43 with AP-2/clathrin binding sites mutated have more GJ channels in their apposing plasma membranes……27

2.3.5. GJ plaques formed by AP-2/clathrin binding deficient Cx43 mutants are internalization impaired……....28

2.3.6. AP-2/clathrin binding-deficient Cx43 mutant proteins exhibit longer half-lives…….30

2.3.7. Cells expressing AP-2/clathrin binding deficient Cx43 mutants become donor cells when paired with wt Cx43 expressing cells…...31

2.4. Discussion…….…….33

2.5. Materials and methods

2.5.1. PCR mutagenesis and cDNA construction…….39

2.5.2. Cell culture and transfections…….…41

2.5.3. Immunofluorescence microscopy and image analyses……..42

2.5.4. Duolink in situ protein colocalization assays…….43

2.5.5. Live-cell imaging……...44

2.5.6. Western blot analyses…….44

2.5.7. Co-immunoprecipitation assays…….45

2.5.8. Cx43 protein half-life analyses……..46

2.5.9. Transfection and co-culture of cells expressing wt and mutant Cx43 constructs…….……...46

2.5.10. Statistical analyses…….……47

2.6. Figures……48

3. Chapter 3: Cx43 phosphorylation is the signal for GJ internalization

3.1. Abstract……..65

3.2. Introduction……65

3.3. Results

3.3.1. EGF treatment inhibits GJIC in mES cells via activation of the MAPK signaling cascade……...…67

3.3.2. EGF activates MAPK and PKC in mES cells to phosphorylate Cx43 at serine 262,279/282, and 368……...……69

3.3.3. EGF induces GJ endocytosis in mES cells……69

3.3.4. More clathrin is recruited to Cx43 in EGF induced GJ-endocytosis.71

3.4. Discussion…….….73

3.5. Materials and Methods

3.5.1. Cell culture…….76

3.5.2. Dye transfer assays…….77

3.5.3. Immunofluorescence microscopy and image analyses……..78

3.5.4. Electron microscopic analyses…….…..78

3.5.5. Western blot analyses…….....79

3.5.6. Co-immunoprecipitation assays…….80

3.5.7. Statistical analyses……..……80

3.6. Figures……81

4. Chapter 4: Conclusion and future perspectives……..….89

5. References……...96

6. Supplemental data……..……108

7. Appendix

7.1. Primers used for PCR mutagenesis……..……111

7.2. pEGFP-N1 vector map…….113

7.3. Buffers, solutions, and media used……..114

7.4. Antibodies used……...….116

8. Curriculum Vitae……..…117

Abstract

A gap junction (GJ) is formed when two hemi-channels from two apposed cells dock in the extracellular space. GJs mediate cell-cell communication by allowing direct transfer of molecules (<1.5 kDa) from one cell to the other through these channels. Direct intercellular communication mediated by gap junction channels is a hallmark of normal cell and tissue physiology. In addition, GJs are likely to significantly contribute to physical cell-cell coupling. Clearly, these cellular functions require precise modulation. Defects in GJ intercellular communication lead to serious illnesses. Interestingly, docked GJ channels cannot be separated under physiological conditions. We previously described that cells efficiently internalize their GJs in a clathrin-mediated endocytic process to form double-membrane vesicles termed annular gap junctions (AGJs) or connexosomes (Baker et al., 2008; Gumpert et al., 2008; Piehl et al., 2007). How this complex process is achieved mechanistically in a cell is still unclear. In this dissertation, (1) I elucidate the signals and molecular mechanisms that are involved in GJ internalization. By mutagenesis, I identified two functional tyrosine-based sorting signals (YXXΦ) in the Cx43 (a GJ protein) C-terminal domain that interact with the classical clathrin adaptor protein, adaptor protein complex-2 (AP-2), to recruit clathrin to the plasma membrane (PM), followed by GJ endocytosis. Mutating these two YXXΦ sorting motifs results in inhibition of AP-2 binding, increased accumulation of GJ channels in the PM, impairment of GJ internalization, and increased Cx43 protein half-life. (2) In order to understand the Cx43 protein modifications that initiate GJ endocytosis, I treated mouse embryonic stem cells

(mES) with epidermal growth factor (EGF) and analyzed Cx43 phosphorylation. I found that EGF activates MAPK and PKC to phosphorylate Cx43 at Ser262, Ser279/282, and Ser368. These phosphorylation events induce inhibition of GJIC and trigger GJ internalization. Pharmacological inhibition of MAPK counteracts with EGF to maintain GJIC and to inhibit EGF-induced GJ internalization. Work conducted during my PhD contributed to three primary research papers (two published, one submitted) and three review articles.

Chapter 1:

Introduction

1.1.Connexins and gap junctions

In general, cells do not function as an individual (except solitary cells such as red blood cells, sperm, etc.) in multi-cellular organisms. They tend to come together to form tissues and organs. In a tissue, many cells of the same type are linked to each other via cell-cell junctions and cell-matrix interactions. The four major cell junctions that are well described include adherens junctions, tight junctions, gap junctions, and desmosomes. Among those cell-cell junctions, gap junctions (GJs) are the only junction type that allows direct cell-cell communication via the transfer of molecules between cells.

Connexins (Cxs) are the four spanning trans-membrane proteins that form gap junction (GJ) channels. A Cx protein consists of 4 trans-membrane domains, 2 extracellular loops, and 1 intracellular loop. Both the N- terminus and C-terminus of Cxs are located in the cytosol. Cx genes are highly conserved. Twenty-one different Cx isoforms have been identified in humans and twenty Cx isoforms have been identified in mouse. They are named Cx, followed by the predicted molecular weight of the protein. They are structurally conserved; the main difference is the size of the C-terminus – an example of Cx43 topology is shown in (**Figure 1**). Like most of the trans-membrane proteins, Cxs are synthesized and inserted co-translationally by endoplasmic reticulum (ER) bound ribosomes. Comparable isoforms of Cxs are oligomerized either in the ER or

Golgi to form hemichannels (also termed connexons). Misfolded Cx polypeptides will be degraded in the proteosome, while correctly oligomerized connexons will be trafficked to the plasma membrane (PM) along microtubules via the secretory pathway. The first ten to fifteen residues of the C-terminus adjacent to the fourth trans-membrane domain have been shown to play a crucial role in connexon trafficking to the PM. Mutating or truncating these amino acids will severely inhibit GJ formation. Connexons from two apposed cells can recognize each other and dock in the extracellular space to form complete GJ channels. (reviewed in Segretain and Falk, 2004) (**Figure 4**). Among all Cx isoforms, Cx43 is the most abundant and most studied Cx type. The Cx43 C-terminus can interact with many different proteins via different domains to regulate many different functions (reviewed in Thevenin et al., 2013). A few examples of these binding partners include adaptor protein complex-2 (AP-2), kinases, zonula occludens-1 (ZO-1) and other scaffolding proteins, microtubules, etc. Cx43 is a phospho-protein. Many of its serine and tyrosine residues in the C-terminal domain can be phosphorylated by CK1, PKA, and Akt to increase gap junction intercellular communication (GJIC), whereas, PKC, MAPKs, Src, and CDC2 are known to phosphorylate Cx43 to reduce GJIC. A more detailed discussion of Cx43 phosphorylation by MAPK to reduce GJIC and induce GJ internalization is given in chapter 3.

As described earlier, six Cx polypeptides oligomerize to form a hemi-channel (termed connexon). Recent findings indicate that connexons might function on their own as channels in the non-junctional region of the PM

(Carnarius et al., 2012). One study reported that connexons might have a physiological function in modulation of cell volume by regulating extracellular calcium-dependent isomotic volume (Quist et al., 2000). In addition, ATP and glutamate have been reported to be released through connexons, which can serve as transmitters between cells (Bennett 2012). Complete double-membrane spanning GJ channels are formed when two connexons of apposed cells dock head-on in the extracellular space (**Figure 2**). It is possible that adherens junctions play a role in bringing the two PMs close together to enhance connexon docking. Published evidences suggest that GJ assembly and disassembly may be regulated by signals that are initiated by E-cadherin and N-cadherin, respectively (Govindarajan et al., 2010). Typically tens to many thousands of GJ channels cluster together to form an arrays of channels, termed GJ plaques. GJ plaque size is known to be regulated by interaction of ZO-1 to the PDZ domain of Cx43 C-terminus (Hunter et al., 2005; Rhett et al., 2011). Cx43-GFP fusion proteins have been shown to inhibit ZO-1 binding, which results in unusually large GJ plaques (Hunter et al., 2003). GJs, based on their tightly sealed, double-membrane spanning configuration are likely to also significantly contribute to physical cell-to-cell adhesion.

1.2. Gap junction intercellular communication (GJIC)

GJ channels electrically and chemically couple neighboring cells and mediate intercellular communication (GJIC) by allowing direct transfer of small hydrophilic molecules (less than 1.5k Da, e.g. second messengers such as cAMP

and IP3, ions, metabolites, and potentially small functional RNA molecules) to pass through the channels via passive diffusion. Gap junction intercellular communication (GJIC) has been shown to play a crucial role for all aspects of multi-cellular life, including embryonic development, tissue functions and cellular homeostasis. For example, Cx proteins are found in early embryos, and during all stages of their development. Functional GJIC was observed as early as the eight-cell stage (De Sousa et al., 1993; Lo and Gilula, 1979), and was demonstrated in blastocysts (Houghton, 2005) of which embryonic stem cells are derived. GJIC has also been described in mouse and human ES cells by (Huettner et al., 2006; Worsdorfer et al., 2008), respectively. Recently, GJIC has been shown to play a very important role in maintaining ES cells in their pluripotent state (Kim et al., 2013; Todorova et al., 2008), also Ke et al., 2013 demonstrated that GJIC is required for the generation of induced pluripotent stem cells (iPS) from fibroblasts (Ke et al., 2013) . Mutations in Cxs have been linked to a number of severe diseases. For example, mutations in the GJB2 gene (which encodes for Cx26) are one of the major causes for inherited and sporadic nonsyndromic hearing impairment (Kenneson et al., 2002; Morell et al., 1998). Many mutations of the GJB1 gene (which encodes for Cx32) were found in X-Linked-Charcot-Marie-Tooth syndrome (CMTX) neuropathy patients (Lee et al., 2002). Mutations in Cx46 and Cx50 cause eye-lens cataracts (Gong et al., 1997; White et al., 1998). In the cardiovascular system, functional GJ channels are important in mediating the spread of electrical impulses that trigger synchronized contraction of the cardiac chambers. In mammalian heart, GJs are built of Cx40, Cx43, and Cx45, in

which Cx43 is the predominant Cx type. Mutations in GJA1 (which encodes for Cx43) lead to serious cardiac diseases, such as hypertrophy, ischemia, and heart failure (Fontes et al., 2012), as well as cranio-facial bone defects (oculodentodigital dysplasia, ODDD syndrome) and a number of acute skin disorders (reviewed in (Batra et al., 2012; Xu and Nicholson, 2013)), supporting the crucial role of GJIC in multi-cellular life. Clearly, all these examples illustrate that GJ channel assembly and degradation needs to be regulated precisely to ensure accurate physiological functions.

1.3.Gap junction internalization and degradation

Elegant studies by Goodenough and Gilula, and Ghoshroy et al. revealed that docked GJ channels are inseparable into hemi-channels under physiological conditions (Ghoshroy et al., 1995; Goodenough and Gilula, 1974). Yet, actively proliferating cells, including embryonic and somatic stem cells, are known to un-couple from their neighbors in order to undergo mitosis (Boassa et al., 2011); and modulation of cellular uncoupling and re-coupling plays an important role in many additional physiological and pathological conditions, such as cell migration during development and wound healing, apoptosis, leukocyte extravasation, ischemia, hemorrhage, edema, and cancer metastasis. Furthermore, channels of GJ plaques have been shown to be constitutively endocytosed (Falk et al., 2009), correlating with the short half-life of 1-5 hours reported for Cx proteins and GJs (Beardslee et al., 1998; Falk et al., 2009; Fallon and Goodenough, 1981). How then are GJs endocytosed? We and others previously showed that GJ

internalization resembles a clathrin-mediated endocytosis (CME) process that involves the coat-protein, clathrin itself, the classical PM clathrin-adaptor, AP-2 (adaptor protein complex-2), the alternative clathrin adaptor protein, Dab2 (Disabled-2), the GTPase dynamin2, the retrograde actin motor, myosin-VI, and actin filament assembly (Baker et al., 2008; Gilleron et al., 2011; Gilleron et al., 2008; Gumpert et al., 2008; Johnson et al., 2013b; Piehl et al., 2007). Clathrin normally does not bind directly to its cargo (here the Cx43 protein). Instead, it requires adaptor proteins to link the cargo to the clathrin coat. A schematic representation to illustrate the classical CME process is shown in **Figure 3**. Both, AP-2 and Dab2, have been shown previously to be involved in GJ internalization, and knocking down AP-2 and Dab2 protein levels using RNAi technology significantly reduced GJ internalization (Gumpert et al., 2008; Piehl et al., 2007). To better understand how clathrin and clathrin-adaptors may internalize GJs, we analyzed the Cx43 amino acid sequence for potential AP-2 and Dab2 interaction sites, mutated putative sites by generating a set of amino acid exchange and deletion constructs, and analyzed their impact on GJ internalization. We found that apparently two separate AP-2 binding sites located in the Cx43 C-terminus interact with and recruit AP-2, Dab2, and clathrin to the Cx43 C-terminus. A more detailed description of AP-2 dependent clathrin mediated Cx43 GJ endocytosis will be presented in chapter 2.

GJ endocytosis generates cytoplasmic double-membrane vesicles termed annular gap junctions (AGJs) or connexosomes (Falk et al., 2009; Gaietta et al., 2002; Jordan et al., 2001; Lauf et al., 2002; Piehl et al., 2007). Degradation of

these double-membrane vesicles is a complex process for the cell. There are three known degradation pathways in cells that are described in the literature: proteosomal, endo-/lysosomal, and autophagosomal pathways. Proteosomal degradation in general degrades short-lived, misfolded, and unwanted polypeptides, while endo-/lysosomal and autophagosomal degradation pathways allow the degradation of more complex protein structures that are either endocytosed from the PM, or are present in the cytoplasm. In both endo-/lysosomal as well as autophagosomal degradation pathways, lysosomal fusion plays a key role in mediating final degradation. In addition, autophagy is known to be the pathway for a cell to maintain its minimal source of nutrients for survival by degrading its own organelles under starvation conditions. GJ proteins have been shown to be degraded by the ubiquitin proteosome pathway (Laing and Beyer, 1995; Qin et al., 2003). However, considering the size and complexity of GJ and AGJs, it is unlikely that AGJs will be degraded in proteosome; while misfolded Cx polypeptides and endocytosed connexons are more likely to be degraded in proteosomes and endo-/lysosome, respectively.

AGJs subsequent to internalization were found to be degraded by endo-/lysosomal pathways in cells that were treated with phorbol ester 12-o-tetradecanonylphorbol-13-acetate (TPA), an analog of secondary messenger diacylglyrecrol (Fykerud et al., 2012; Leithe et al., 2009). In these studies, authors reported that TPA induced Cx43 hyper-ubiquitination and to remain ubiquitinated while being trafficked to the endosome. A HECT E3 ubiquitin ligase smad ubiquitination regulatory factor-s (Smurf2) was found to be recruited to Cx43 GJs

in response to TPA treatment, suggesting a role of Smurf2 in Cx43 ubiquitination. Two proteins: ubiquitin-binding protein Hrs (hepatocyte growth factor-regulated tyrosine kinase substrate) and Tsg101 (tumor susceptibility gene 101) were identified to play a crucial role in Cx43 ubiquitination and phosphorylation to regulate trafficking of AGJs to the lysosome. These findings provide insight to understand how AGJs are degraded in the lysosome. However, an important question arises: How is it possible for a double membrane vesicle that consists of tightly bonded membrane layers and densely packed GJ channels to fuse with a single-membrane endosome? Interestingly, by electron microscopy, we found that AGJ may include a small domain where the two membranes are void of GJ channels – single membrane domain (reviewed in Falk et al., 2012). We postulate that this nonjuntional membrane domain allows fusion of double-membrane AGJ and single membrane endosomes that then may be followed by endo-/lysosomal degradation (reviewed in Falk et al., 2012).

Note that lysosomal inhibitors (leupeptin, chloroquine, NH_4Cl, and E-64) that have been used in earlier studies investigating GJ degradation (Berthoud et al., 2004; Laing et al., 1997; Musil et al., 2000; Qin et al., 2003) will inhibit both endo-/lysosomal as well as autophagic degradation pathway (**Figure 4B**). Therefore, obtained results do not specify target endo-/lysosomal versus autophagosomal pathways. We and others have recently described that, internalized AGJs are degraded by autophagy (Bejarano et al., 2012; Fong et al., 2012; Hesketh et al., 2010; Lichtenstein et al., 2011). Robust colocalization of Cx43 and autophagic markers (LC3/Atg8, Rab5, p62/SQSTM1) but only

insignificantly colocalization of Cx43 and endosomal markers (EEA1, Rab7) were demonstrated by Fong et al., 2012 (Fong et al., 2012). Depleting these autophagosomal markers either by RNAi knock down or inhibiting autophagy using pharmacological inhibitors resulted in a significant increase in the level of Cx43 protein, and a significantly increased accumulation of cytoplasmic AGJs. Together, multiple lines of evidence from different laboratories suggest that autophagy is a more logical, and likely default pathway for AGJ degradation. Base on current published knowledge, it is possible that cells may utilize either endo-/lysosomal or autophagosomal degradation pathways (**Figure 4B**). When cells respond to distinct stimuli or extracellular cues, potential sorting signals that may result from protein modifications of the cargo (phophorylation, ubiquitination, etc.) may determine which degradation pathway the cells will be committed to. However, at steady state, autophagy appears to be the default AGJ degradation pathway that regulates GJs turnover. Under physiological conditions, internalized AGJs, similar to cellular organelles, cytoplasmic protein aggregates, and other macromolecular protein-complexes, such as the mitotic ring, are cleared from the cytoplasm and degraded by autophagy.

1.4 Figures

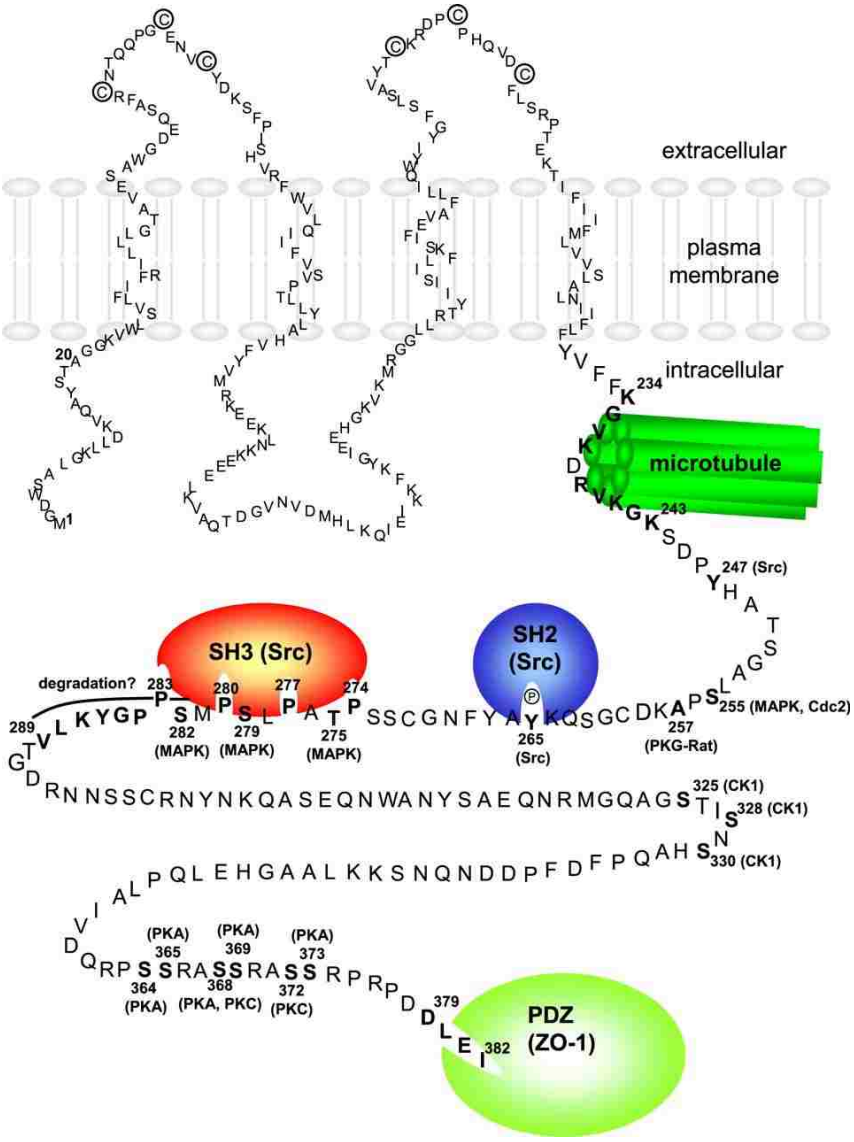

Figure 1: Cx43 amino acid sequence and topology (Giepmans et al., 2004). Cx43 is a four spanning trans-membrane protein in which both N-terminus and C-terminus are in the cytosol. Cx43 can interact with many different proteins, such as AP-2, Kinases, ZO-1, etc. to regulate functions. Many serines and tyrosine

residues in the C-terminus can be phosphorylated or dephosphorylated to regulate gap junction intercellular communication and gap junction turnover.

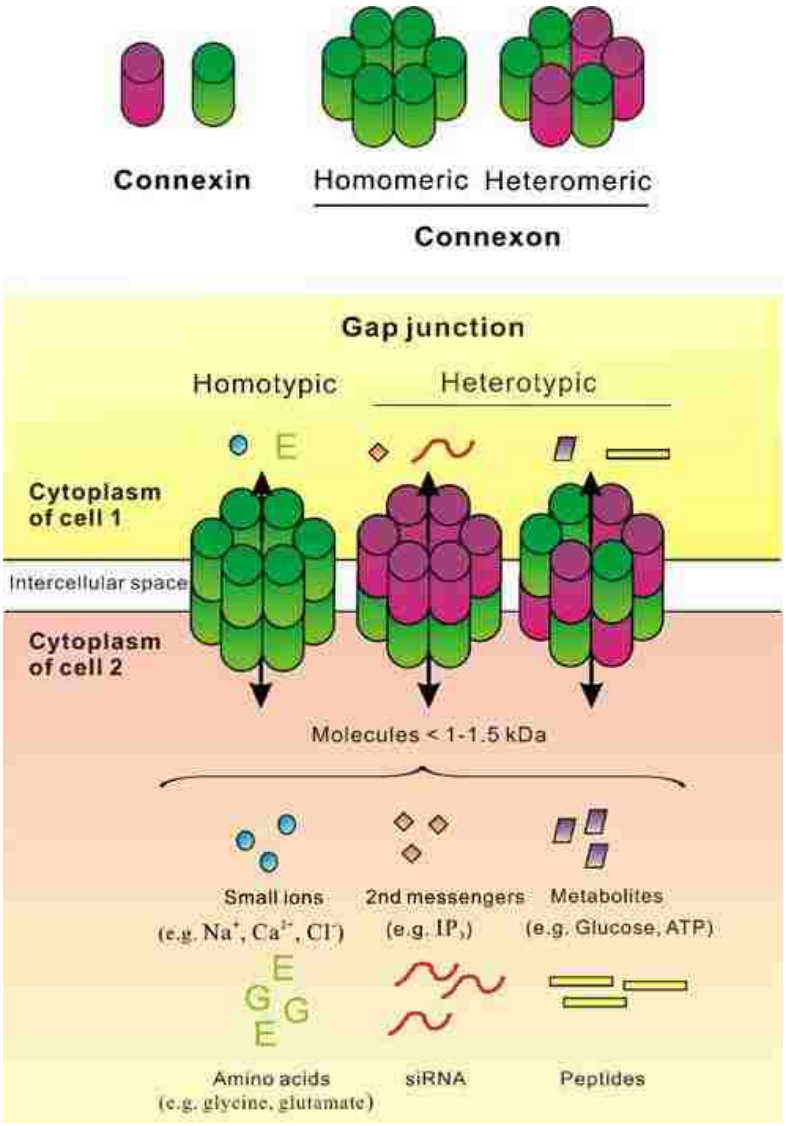

Figure 2: Schematic representation of connexins, connexons, and gap junctions (adopted from Wong et al., 2008).

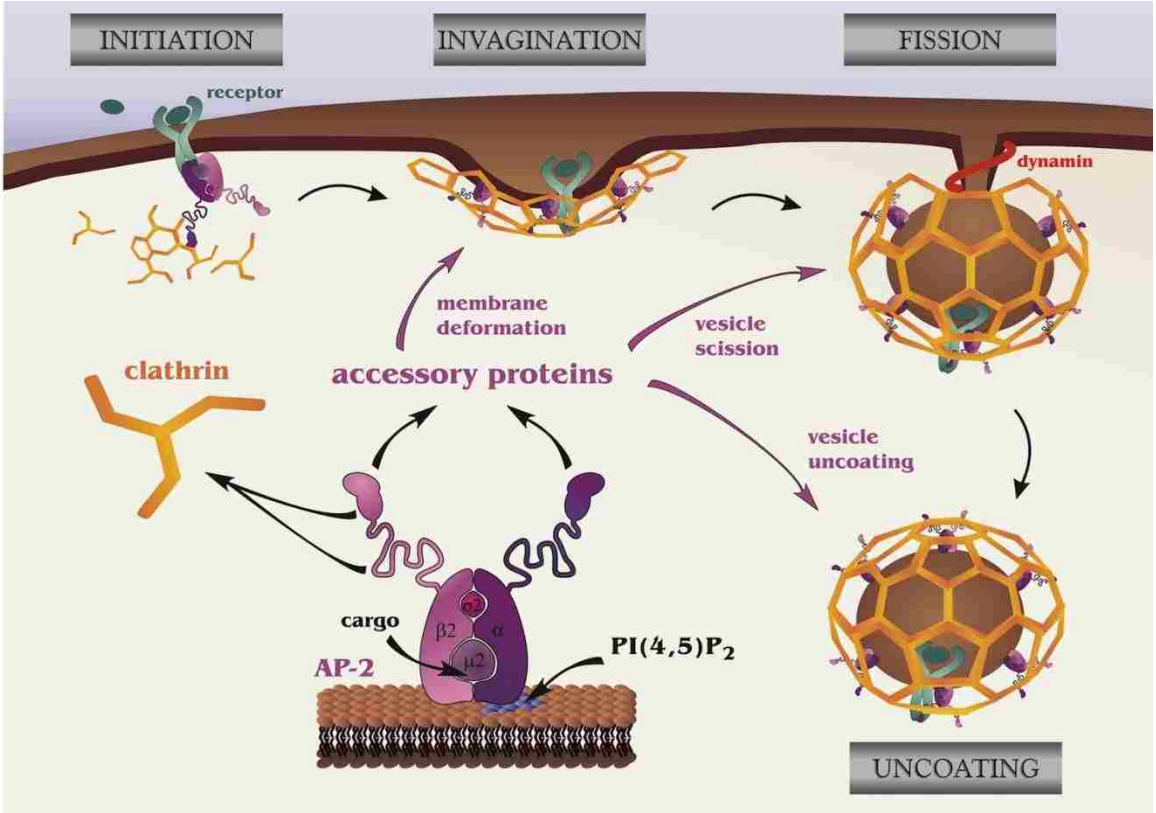

Figure 3: Schematic representation of classical clathrin-mediated endocytosis

During vesicle initiation, adaptor proteins (AP-2) are re-localized to the plasma membrane through interacting with PI(4,5)P_2. AP-2 interacts with the cargo via dileucine or tyrosine-based sorting signals. AP-2 also interacts and recruits other accessory proteins (Dab2, Eps15, etc.) and clathrin to the site of vesicle formation. The GTPase – dynamin – is required to pinch off the coated vesicle from the plasma membrane. (Adopted from McPherson et al. 2009 modified http://www.bumc.bu.edu/biochemistry/files/2012/05/model-CME.jpg)

A

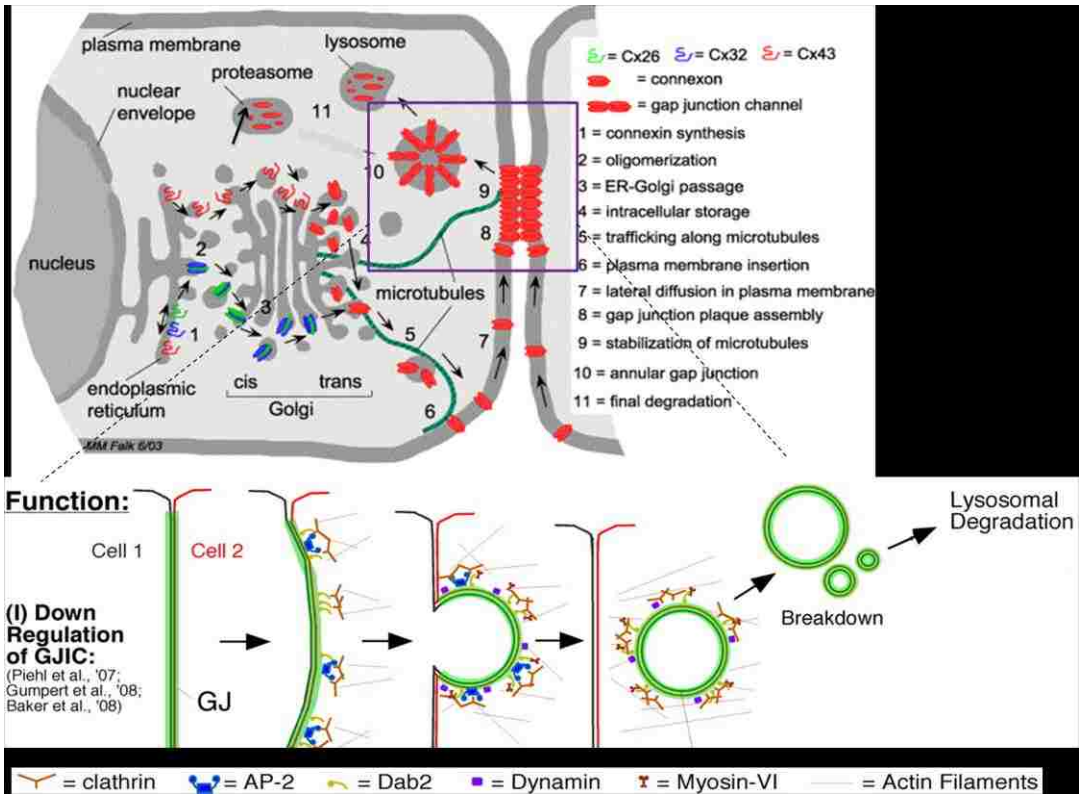
plasma membrane
lysosome
proteasome
nuclear envelope
nucleus
endoplasmic reticulum
cis
trans
Golgi
microtubules
= Cx26
= Cx32
= Cx43
= connexon
= gap junction channel
1 = connexin synthesis
2 = oligomerization
3 = ER-Golgi passage
4 = intracellular storage
5 = trafficking along microtubules
6 = plasma membrane insertion
7 = lateral diffusion in plasma membrane
8 = gap junction plaque assembly
9 = stabilization of microtubules
10 = annular gap junction
11 = final degradation
Function:
Cell 1
Cell 2
(I) Down Regulation of GJIC:
(Piehl et al., '07; Gumpert et al., '08; Baker et al., '08)
GJ
Breakdown
Lysosomal Degradation
= clathrin
= AP-2
= Dab2
= Dynamin
= Myosin-VI
= Actin Filaments

B

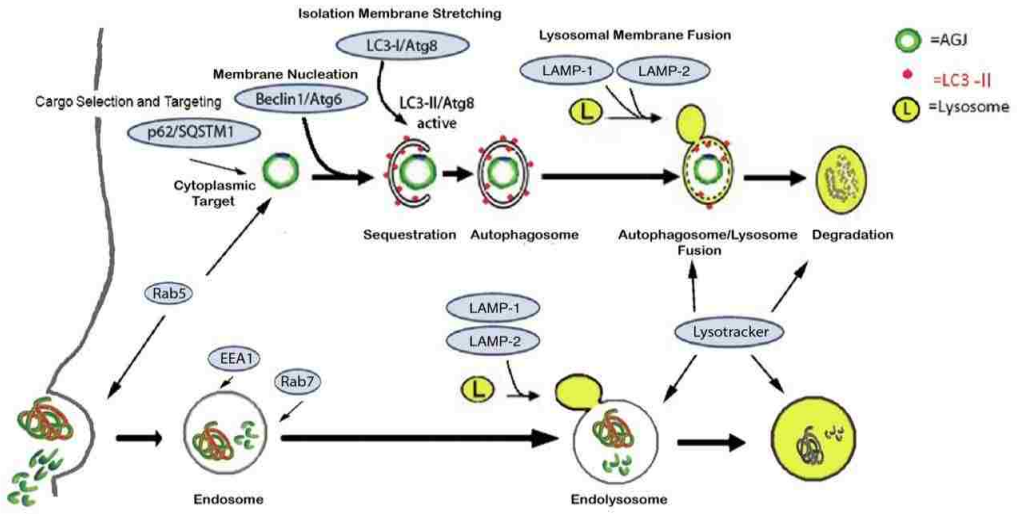
Isolation Membrane Stretching
LC3-I/Atg8
Lysosomal Membrane Fusion
LAMP-1
LAMP-2
=AGJ
=LC3 -II
=Lysosome
Membrane Nucleation
Beclin1/Atg6
Cargo Selection and Targeting
p62/SQSTM1
LC3-II/Atg8 active
Cytoplasmic Target
Sequestration
Autophagosome
Autophagosome/Lysosome Fusion
Degradation
Rab5
LAMP-1
LAMP-2
Lysotracker
EEA1
Rab7
Endosome
Endolysosome

Figure 4: (A) Schematic representation of gap junction formation and degradation. (Falk et al., 2009; Gumpert et al., 2008; Segretain and Falk, 2004 modified). (B) Schematic representation of phago-/lysomal and endo-/lysosomal cellular degradation pathways and respective marker proteins (Falk et al., 2002; Fong et al., 2012 modified).

Chapter 2:

Two tyrosine-based sorting signals in the Cx43 C-terminus cooperate to mediate gap junction endocytosis

(Fong et al. 2013, *Mol Biol Cell*, 24(18), p. 2834-48)

2.1. Abstract

Gap junction (GJ) channels, that electrically and chemically couple neighboring cells, are formed when two hemi-channels (connexons) of apposed cells dock head-on in the extracellular space. Remarkably, docked connexons are inseparable under physiological conditions and we, and others have shown that GJs are internalized in whole utilizing the endocytic clathrin machinery. Endocytosis generates double-membrane vesicles (annular GJs or connexosomes) in the cytoplasm of one of the apposed cells that are degraded by autophagosomal and potentially endo-/lysosomal pathways. Here we investigated the structural motifs that mediate Cx43 GJ endocytosis. We identified three canonical tyrosine-based sorting signals of the type 'YXXΦ' in the Cx43 C-terminus, two of which function cooperatively as AP-2 binding sites. We generated a set of GFP-tagged and untagged Cx43 mutants that either targeted these two sites individually or together. Mutating both sites completely abolished Cx43-AP-2/Dab2/clathrin interaction, resulted in increased GJ plaque size, longer Cx43 protein half-lives, and impaired GJ internalization. Interestingly, Dab2, an accessory clathrin-

adaptor found earlier to be important for GJ endocytosis, interacts indirectly with Cx43 via AP-2, permitting the recruitment of up to four clathrin-complexes per Cx43 protein. Our analyses provide a mechanistic model for clathrin to efficiently internalize large PM structures such as GJs.

2.2. Introduction

As mentioned in the Introduction section, elegant studies by Goodenough and Gilula, and Ghoshroy et al. revealed that connexons once docked cannot be separated back into connexons under physiological conditions (Ghoshroy et al., 1995; Goodenough and Gilula, 1974). Furthermore, channels of GJ plaques have been shown to be constitutively endocytosed to form AGJs (Falk et al., 2009), correlating with the short half-life of 1-5 hours reported for Cx proteins and GJs (Beardslee et al., 1998; Falk et al., 2009; Fallon and Goodenough, 1981). However, the signals and mechanisms that trigger GJ endocytosis remain unclear. We and others found that cells remove their GJ plaques from the plasma membrane (PM) by an endocytic process that resembles clathrin-mediated endocytosis (CME) and involves the coat-protein clathrin itself, the classical PM clathrin-adaptor AP-2 (adaptor protein complex-2), the alternative clathrin adaptor protein Dab2 (Disabled-2), the GTPase dynamin2, the retrograde actin motor myosin-VI, and actin filament assembly (Baker et al., 2008; Gilleron et al., 2011; Gilleron et al., 2008; Gumpert et al., 2008; Johnson et al., 2013a; Piehl et al., 2007). To better understand how clathrin and clathrin-adaptors may internalize GJs, we analyzed the Cx43 amino acid sequence for potential AP-2

and Dab2 interaction sites, mutated putative sites by generating a set of amino acid exchange and deletion constructs, and analyzed their impact on GJ internalization. We found that two separate AP-2 binding sites located in the Cx43 C-terminus interact with and recruit AP-2, Dab2, and clathrin to the Cx43 C-terminus, and that deletion or mutation of these sites impaired GJ internalization if only one site was mutated or completely abolished it if both sites were mutated together. Interestingly, our analyses revealed the potential recruitment of up to four clathrin triskelia per Cx43 polypeptide, suggesting a potential molecular mechanism for the efficient CME of large PM structures such as GJs.

2.3. Results

2.3.1. Design and construction of Cx43 mutants that interfere with AP-2/clathrin binding.

GJ internalization was found to utilize the clathrin-mediated endocytosis (CME) machinery (Gumpert et al., 2008; Johnson et al., 2013a; Piehl et al., 2007), correlating with earlier observations of clathrin colocalizing with vesicular, cytoplasmic GJ structures (Larsen et al., 1979). Clathrin typically does not interact directly with its cargo (here the Cx43 protein), but instead requires adaptor proteins to link the cargo to the clathrin coat. As noted above, both clathrin adaptors, AP-2 and Dab2 have been shown previously to be involved in GJ internalization, and knocking down AP-2 and Dab2 protein levels using RNAi technology significantly reduced GJ internalization (Gumpert et al., 2008; Piehl et

al., 2007). AP-2 is a well-characterized CME adaptor protein complex consisting of α-Adaptin, β2, σ2, and μ2-subunits that is known to bind to PM-localized cargo proteins via three different binding motifs: two types of tyrosine-based sorting signals with either (1) YXXΦ (where Y is tyrosine, an essential residue which cannot be substituted even by structurally related phenylalanine or phospho-tyrosine residues, X which can be any amino acid, and Φ which is an amino acid with a bulky hydrophobic side chain such as F, M, L, I, or V) or (2) NPXY-sequence (where N is asparagine, P is proline, X is any amino acid, Y is tyrosine) that bind to the μ2-subunit, or (3) via a di-leucine based sorting signal [D/E]XXXL[L/I] that can bind to both, μ2 and β2 subunits (reviewed in Bonifacino and Traub, 2003). Dab2 is also known to bind to NPXY sequences (Mishra et al., 2002; Morris and Cooper, 2001; Motley et al., 2003). We did not find any NPXY signals in the Cx43 sequence suggesting that Dab2 may interact indirectly with Cx43 (see Results in section 2.3.3 below), and consistent with the observation that NPXY motifs are typically only present in single-spanning membrane proteins (reviewed in Bonifacino and Traub, 2003). We also did not find any di-leucine based sorting signals in the Cx43 sequence, however di-leucine based sorting signals are present in the C-terminus of a number of other Cxs (reviewed in Thevenin et al., 2013). We found three conserved YXXΦ consensus sequences in the Cx43 C-terminus located at positions Y^{230}VFF, Y^{265}AYF, and Y^{286}KLV. These sites were named sorting signals, S1, S2, and S3, respectively (**Figure 5A**). Endocytic YXXΦ signals normally are located at least 10 amino acid residues away from a transmembrane domain to allow sufficient

space for AP-2 access (Collins et al., 2002; reviewed in Bonifacino and Traub, 2003). Sorting signal S1 (Y^{230}VFF) is located immediately adjacent to transmembrane domain 4 (TM4), which makes it unlikely that S1 would serve as a functional AP-2 binding site. Indeed, we did not gain any evidence that suggests that this site in Cx43 interacts with AP-2 (see results of mutants with sites S2 and S3 [S2+3] mutated/deleted presented below). We generated over 20 different Cx43 mutants (all either untagged or tagged with GFP on the C-terminus) including, 15 point mutations (Y to H; or F to A), 7 small (3-7 amino acids) and 2 large (36 and 128 amino acids) deletion mutants that targeted the putative S1, S2 and S3 AP-2 binding sites and rendered them non-functional. Both deletion as well as point mutants were constructed and tested to reduce the potential impact of side effects. Selected constructs characterized here are shown in **Figure 5A**. Note, that the sorting signal S3 is a portion of a larger, previously identified regulatory sequence (termed proline-rich region) that consists of the S3 signal and a directly upstream, overlapping PY motif that both were found to influence GJ stability, however without additive effect (Thomas et al., 2003) (see Discussion for further detail). To avoid potential interference of these two signals, 7 amino acid residues including the PY-motif and the S3 sorting signal were deleted in S3 and S2+3 mutants (mutants 6. to 8. in **Figure 5A**). Also note, that the Y286 (knocking out both signals) was mutated in the S3 motif, while F268 of the S2 motif was mutated (mutants 2., 4., and 5. in **Figure 5A**). The Y265 in the S2 motif is a well-known c-Src phosphorylation site (Postma et al., 1998; Solan and Lampe, 2008; reviewed in Thevenin et al., 2013), and mutation of this amino acid

residue was expected to generate severe site-effects. Mutating either Y or Φ of the canonical YXXΦ motif was found to abolish its function (reviewed in (Bonifacino and Traub, 2003)). When transfected into HeLa cells, all constructs produced Cx43 proteins that migrated on SDS-polyacrylamide gels according to their predicted molecular weight (shown for GFP-tagged constructs in **Figure 5B**). Also, all constructs assembled into GJ plaques in apposing membranes of transfected cells, as shown for selected constructs in **Figures 7, 8, 9, and 11.**

2.3.2. Cx43 mutants with both AP-2 binding sites (S2+3) mutated no longer co-precipitate clathrin and clathrin-adaptors.

In order to test for protein/protein interactions between Cx43 and CME-components, co-immunoprecipitation assays were performed, both with GFP-tagged and untagged Cx43 mutants (**Figure 6A, B**). Wild type Cx43, as well as Cx43 constructs with sorting signals S2, S3, S2+3, and S1+2+3 mutated were transfected into HeLa cells. Cx43 was immunoprecipitated using anti-GFP (**Figure 6A**) or anti-Cx43 magnetic beads (**Figure 6B**). Cx43 binding partners were detected by Western blot analyses using respective antibodies. Representative immunoprecipitations for selected constructs are shown on the left (lanes 1-7), and quantitative analyses of three independent experiments each are shown on the right. Results show that wt Cx43 co-precipitated AP-2 (using anti α-Adaptin subunit antibodies), Dab2, and clathrin (using anti clathrin heavy chain [CHC] antibodies) (**Figure 6, A and B,** lane 1), consistent with previously published observations (Gumpert et al., 2008; Piehl et al., 2007). Cx43 constructs

with either binding motif S2 or S3 mutated also co-precipitated these endocytic proteins (**Figure 6, A and B,** lanes 2, 3), although only to about 50% of wt, while mutants with both (S2+3, lanes 4, 5), or all three binding motifs mutated (S1+2+3, lanes 6, 7) no longer co-precipitated any, or only minor amounts (≤10 ± 8% compared to wt) of these endocytic proteins. Thus, abolishing Cx43-AP-2 binding also abolished Dab2 and clathrin binding. No detectable differences in co-precipitation efficiencies were found between GFP-tagged and untagged Cx43 constructs, or between mutants with all three, or only binding sites S2+3 mutated, indicating that the GFP-tag did not significantly affect Cx43-endocytic protein interaction, and that the binding motif S1 does not bind AP-2 or recruit these endocytic proteins. HeLa cell lysates and immunobeads only were analyzed in control (**Figure 6, A and B**, lanes 8, 9), and α-tubulin was analyzed as lysate input and loading control. Note that the amount of precipitated Cx43 proteins increases with one (S2 or S3) or two (S2+3) AP-2 binding motifs mutated (**Figure 6, A and B** rows 1), correlating with the increased half-live of these mutants (see Results in section 2.3.6 below and **Figure 10**). Unexpectedly, a weak protein band was detected in the HeLa cell lysates using Cx43 antibodies under our experimental conditions (**Figure 6B**, lane 9, top row), suggesting that small amounts of endogenous Cx43 were present in the CCL-2 HeLa cell clone that we purchased from ATCC for these analyses. Quantitative analyses indicated that the content of endogenous Cx43 is minor, only amounting to about 1-2% compared to a 100% efficient exogenous (transient or stable) expression (see **Figure S1**). Taken together, these results identify the tyrosine-based sorting signals, S2

(Y^{265}AYF) and S3 (Y^{286}KLV) in the Cx43 C-terminus as direct AP-2 binding sites. Both sites can interact with AP-2 and may work jointly to recruit AP-2 adaptors to the Cx43 C-terminus. Both Dab2 and clathrin neither bind, nor interact with Cx43 directly but appear to require the AP-2 complex for their indirect interaction with Cx43.

2.3.3. Cx43/Dab2 interaction is indirect and mediated via AP-2.

Disabled-2 (Dab2), an alternative clathrin adaptor that initially was characterized in AP-2 depleted cells (Mishra et al., 2002; Morris and Cooper, 2001; Motley et al., 2003; Traub, 2003), was also found to play a role in Cx43 GJ internalization (Gumpert et al., 2008; Piehl et al., 2007). As mentioned above, Dab2 interacts with its cargo (such as LDL receptor) via a minimal sequence motif that conforms to tyrosine-based sorting signals of the NPXY type (Mishra et al., 2002; Morris and Cooper, 2001; Traub, 2003; Traub, 2005). However, we did not find any NPXY motifs in Cx43, only cryptic 'PXY' sequences (two in the rat, one in the human Cx43 sequence) (Piehl et al., 2007), making a direct interaction between Dab2 and Cx43 unlikely (reviewed in Thevenin et al., 2013). Yet, Dab2 was found previously by immunofluorescence staining to robustly colocalize with Cx43, both in GJ plaques as well as in AGJs, even in cell lines that express very little amounts of Dab2 (Piehl et al., 2007); and Dab2 was shown by RNAi-knockdown to play a considerable role in GJ internalization (Gumpert et al., 2008). In addition, as found in this study and shown in **Figure 6** above**,** Dab2 robustly co-immunoprecipitated with GFP-tagged and untagged Cx43 when

expressed in HeLa cells, while its co-immunoprecipitation was reduced or lost when AP-2 binding sites were mutated. Dab2 is known to be able to interact with the α-subunit of AP-2 and the C-terminal domain of clathrin heavy chain (reviewed in Bonifacino and Traub, 2003), further suggesting that the interaction between Dab2 and Cx43 is indirect and mediated via AP-2. To substantiate this hypothesis further we performed Duolink® in-cell colocalization assays (**Figure 7**). The Duolink-assay allows for visualization of protein/protein interactions, as long as the two proteins are within 40 nm of each other inside fixed cells (Gullberg M., 2011). Results obtained with wt Cx43, and the S2+3 mutants Cx43$\Delta L^{254\text{-}290}$-GFP and Cx43$\Delta L^{254\text{-}CT}$-GFP are shown. Cx43 and Dab2 antibodies were utilized for the Duolink colocalization reaction (red fluorescent puncta in wt Cx43 and in the Cx43$\Delta L^{254\text{-}290}$ construct, **Figure 7A**, panels a, b). Note that the used Cx43 antibody is directed against a C-terminally located sequence and therefore does not recognize the Cx43$\Delta^{254\text{-}CT}$-GFP mutant protein, thus serving as a negative Duolink control (no red puncta in **Figure 7A**, panel c). GJs were visualized by their Cx43-GFP fluorescence. Duolink-based Cx43/Dab2 colocalization was quantified by comparative red-channel pixel intensity analyses. Results show that the AP-2 binding deficient Cx43$\Delta L^{254\text{-}290}$-GFP (S2+3) mutant, as expected does not colocalize significantly with Dab2 inside cells when compared to wild type Cx43 (reduced to 27%, SEM ± 16.4, $n = 25$, $p < 0.0001$) (**Figure 7B**). As for results presented in Figures S1, 2, and 7 (below), a small amount of Duolink® signal detected in S2+3 mutant expressing cells (av. ~27%, middle bar in **Figure 7B**) may be generated by small amounts of endogenous wt

Cx43 that may have hetero-oligomerized with the mutant Cx43 and thus recruited some AP-2 to these heteromeric connexons. Together, data presented here using *in situ* Duolink colocalization assays and co-immunoprecipitation assays presented above (**Figure 6, A and B**) firmly support the conclusion that the interaction between Cx43 and Dab2 is indirect and mediated via the classical clathrin-adaptor, AP-2.

2.3.4. Cells expressing Cx43 with AP-2/clathrin binding sites mutated have more GJ channels in their apposing plasma membranes.

Since GJ plaque-size has been reported to be regulated by binding of the scaffolding protein, ZO-1 (Hunter et al., 2005; Rhett et al., 2011), and GFP-tagged Cxs are unable to bind to ZO-1 (Hunter et al., 2003; Thevenin et al., 2013), untagged Cx43 wild type and mutants were transiently transfected into HeLa cells, followed by immunofluorescence staining using primary antibodies against Cx43 and Alexa488 (green)-labeled secondary antibodies. mCherry-tagged histone H_2B (mCherry-H_2B) (red) was co-transfected into the cells to identify transfected cell pairs. Of each group, over 30 cell pairs were imaged and analyzed. Representative images are shown in **Figure 8A**. As fluorescence intensity above the threshold is directly proportional to the number of GJ channels in the PM, the number of channels (more channels correlate with larger GJ plaques) of each group was assessed by quantitatively measuring and comparing Alexa488 (GJ) pixel quantity and intensity located in the apposing PMs of transfected cell pairs (see Materials and Methods in section 2.5). Results indicate

that cells that expressed S2 and S3 mutants, in average had double as many GJ channels in their apposing PMs compared to wt Cx43 expressing cells, as indicated by the doubled pixel intensity ($p < 0.0001$; shown for $F^{268}A$ and $Y^{286}H$ mutants, **Figure 4A,** panels a-c, and **4B,** blue and green bars); while cells expressing S2+3 double mutants ($F^{268}A+Y^{286}H$; $\Delta Y^{265}AY+\Delta P^{283}PGYKLV$) had about three times as many GJ channels in their apposing PMs ($p \leq 0.001$; **Figure 8A,** panels d, e and **8B,** orange/red bars), indicating a significant internalization-impairment of the AP-2 binding deficient Cx43 mutants. Taken together, these results again suggest that AP-2 is recruited to Cx43 GJs and that AP-2 regulates GJ endocytosis. Since mutating sites S2 and S3 individually caused a less significant increase in PM GJ channel number compared to mutating both AP-2 binding sites S2+3 together (either by mutating critical residues of the signal sequence or by deleting the signal), these results further support the conclusion that AP-2 interacts with both sites, S2 and S3, in Cx43 polypeptides.

2.3.5. GJ plaques formed by AP-2/clathrin binding-deficient Cx43 mutants are internalization impaired.

As shown in **Figure 8** and described above, cells expressing AP-2/clathrin binding deficient Cx43 mutants exhibit increased amounts of GJ channels in their apposing PMs. In order to examine whether this increase is indeed caused by inefficient GJ internalization, we investigated HeLa cells expressing wt and respective Cx43 mutants for extended time periods (up to 72 hours) by live-cell time-lapse microscopy. Representative image frame sequences are shown in

Figure 9A. Results indicate that wt Cx43-GFP expressing cells constitutively internalized/turned over their plaques with a time-constant of about 5 ± 1.0 hours (n = 16) counted from visual onset of GJ plaque formation to completion of GJ internalization (**Figure 9A,** column 1; **B**, green bar; Supplementary **Table S1**; Supplementary **Movie S1**). Single AP-2 binding site mutants, S2 (F^{268}A-GFP) and S3 (Y^{286}H-GFP, and ΔP^{283}PGYKLV-GFP) were still able to internalize their plaques, however at a much slower rate determined to be 18 ± 3.7 (n = 7), and 19 ± 1.3 (n = 17) hours (**Figure 9A,** columns 2, 3, shown for F^{268}A-GFP and Y^{286}H-GFP; **B**, blue bars; Supplementary **Table S1**; Supplementary **Movies S2, S3**). S2+3 double-mutants (F^{268}A+Y^{286}H-GFP, ΔY^{265}AY+ΔP^{283}PGYKLV-GFP, and $\Delta L^{254\text{-}290}$-GFP, Cx43-$\Delta L^{254\text{-}CT}$-GFP) were found very inefficient/unable to internalize their plaques since they were present for 30 ± 2.7 (n = 9), or even more hours in the case of the $\Delta L^{254\text{-}CT}$-GFP mutant (**Figure 9A,** columns 4, 5, shown for F^{268}A+Y^{286}H-GFP and $\Delta L^{254\text{-}290}$-GFP; **B**, red bar; Supplementary **Table S1**; Supplementary **Movies S4, S5**). The fact that double-site mutants (S2+3) were observed to remove GJs at all, albeit only after prolonged time periods, again may be explained by small amounts of endogenously expressed Cx43 that may hetero-oligomerized with the expressed mutant proteins. Alternatively, other yet uncharacterized cellular processes may have accommodated GJ removal under these conditions. Together, these results indicate that GJ plaques assembled from AP-2/clathrin binding deficient Cx43 mutants are internalization-impaired.

2.3.6. AP-2/clathrin binding-deficient Cx43 mutant proteins exhibit longer half-lives.

To further investigate whether impaired GJ plaque internalization correlates with extended mutant Cx43 protein half-life, we analyzed the half-lives of GFP-tagged and untagged wt and mutant Cx43 proteins in HeLa cells in which protein biosynthesis was blocked pharmacologically (**Figure 10**). Connexins in general are known to exhibit short half-lives of 1 to 5 hours (Beardslee et al., 1998; Falk et al., 2009; Fallon and Goodenough, 1981). Channels in GJ plaques are dynamic and at steady state are constitutively internalized from plaque centers, while newly synthesized GJ channels are accrued along the outer edges of plaques (Falk et al., 2009; Gaietta et al., 2002; Lauf et al., 2002). HeLa cells were transfected with GFP-tagged and untagged wild-type Cx43, S2, S3, and double S2+3 mutants. The next day, cells were treated with cycloheximide, lysed at indicated times, and Cx protein levels were determined using GFP-antibodies and Western blot analyses. Representative blots for GFP-tagged and untagged wt and mutant constructs are shown (**Figure 10A, C**). Quantitative analyses (by stripping blots and re-probing for α-tubulin) showed that wt Cx43-GFP exhibited a short half-life of about 1 hour (**Figure 10A, B** and **C, D,** green curve) consistent with previous results (Beardslee et al., 1998; Falk et al., 2009; Fallon and Goodenough, 1981), whereas single site mutants, S2 and S3 exhibited extended half-lives of about 2 hours (**Figure 10A, B** and **C, D**, blue and purple curves), and about 4 hours for the S2+3 double-site mutants (**Figure 10A, B** and **C, D**, orange and red curves), respectively. All protein half-life experiments were repeated at least 3

times. Although, no significant differences were observed between GFP-tagged and untagged constructs, untagged Cx43 proteins in general appeared somewhat more stable compared to GFP-tagged constructs. Note that cycloheximide treatment in these experiments may generate considerable cytotoxic side effects that may have caused recorded Cx43 protein half-lives to be shorter compared to experiments performed in untreated cells (in Results 2.3.5). Together, these results further support our hypothesis that GJs are internalized in an AP-2 dependent, clathrin-driven process.

2.3.7. Cells expressing AP-2/clathrin binding deficient Cx43 mutants become donor cells when paired with wt Cx43 expressing cells.

To further support our finding that mutating the AP-2 binding sites in Cx43 generates internalization impaired GJs, we paired cells expressing wt Cx43 with cells expressing AP-2 binding site mutants. We transfected HeLa cells separately with wt Cx43-mApple (red fluorescence) and wt or mutant Cx43-GFP (green fluorescence) by electroporation as described in Materials and Methods. Transfected cells were mixed at a 1:1 ratio, seeded and co-cultured on glass cover slips overnight. Cells were fixed, analyzed and quantified for the location of heterotypic wt/mutant AGJs. Heterotypic GJs formed between Cx43-mApple/Cx43-GFP expressing cell pairs were comprised of mApple-labeled connexons on one side, and GFP-labeled connexons on the other, resulting in GJ plaques exhibiting yellow fluorescence on the red and green overlay images (**Figure 11A**). Cytoplasmic AGJ vesicles formed by the internalization of these

heterotypic GJ plaques also appeared yellow (labeled with arrows in **Figure 11A**). Counting the number of heterotypic AGJs and recording their location allow for evaluation of how efficient the mutant expressing cells can internalize their plaques. In three independent experiments, when wt Cx43-GFP expressing cells were co-cultured with wt Cx43-mApple expressing cells, 46 cell pairs with a total of 249 heterotypic AGJ vesicles were analyzed. No overall bias in directionality of GJ internalization was observed in these cell pairs (50:50 ratio, **Figure 11, A**, panel a; and **B**, bar 1). In contrast, single (S2, S3) and double (S2+3) AP-2 binding site mutant expressing cells were found to be significantly less efficient in internalizing the assembled heterotypic GJ plaques, and instead became donor cells (shown for Cx43-F^{268}A-GFP, [S2]; Cx43-Y^{286}H-GFP, [S3] and Cx43-F^{268}A+Y^{286}H-GFP, [S2+3] in **Figure 11, A,** panels b-d**;** and **B**, bars 2-4). In Cx43-F^{268}A-GFP (S2) / wtCx43-mApple cell-pairing experiments, 72 cell pairs with a total of 475 heterotypic AGJ vesicles were analyzed. Only 130 (28% SEM ± 2.9, $p = 0.0004$) were found in the S2 mutant expressing cells. In Cx43-Y^{286}H-GFP (S3) / wt Cx43-mApple cell-pairing experiments, 101 cell pairs with a total of 507 heterotypic AGJ vesicles were analyzed. Only 148 (29%, SEM ± 1.5, $p < 0.001$) were found in the S3 mutant expressing cells. In Cx43-F^{268}A+Y^{286}H-GFP (S2+3) / Cx43-mApple cell-pairing experiments, 75 cell pairs with a total of 425 AGJs were analyzed, and only 125 (21%, SEM ± 6.4, $p = 0.003$) were found in the S2+3 mutant expressing cells (**Figure 11B**). Note that small amounts of heterotypic AGJs detected in S2+3 mutant expressing cells (~20%, **Figure 11B**, bar 4) may again be generated by small amounts of endogenous wt Cx43 (see

Figure S1) that may have hetero-oligomerized with mutant Cx43, and/or may have been generated by potential other AP-2-independent internalization processes (see Discussion). The impaired ability of S2, S3, and S2+3 mutant expressing cells to endocytose these heterotypic GJ plaques further supports the conclusion that both sorting signals, S2 and S3 function in Cx43 GJ internalization, which is consistent with results obtained by other assays described above.

2.4. Discussion

In 2003, Thomas et al. identified a proline-rich region consisting of amino acid residues P^{280}MSPPGYKLVTG^{291} in the Cx43 C-terminus that when mutated increased the steady-state pool and half-life of Cx43 (Thomas et al., 2003). Since then it was assumed that Cx43 GJ internalization and turnover is regulated by this sequence. More recently, Wayakanon et al. (Wayakanon et al., 2012), using Cx43 constructs with progressively truncated C-termini, identified critical regions in the Cx43 C-terminus that regulate plaque size (C^{271}-N^{302}) and direction of GJ internalization (T^{325}-Q^{342}) (Wayakanon et al., 2012). However, while these authors spatially located the region/s important for Cx43 GJ internalization, they did not provide any information on possible mechanisms that may lead to GJ internalization. Here, we report the identification of three tyrosine-based sorting signals with the general consensus sequence YXXΦ (Y^{230}VFF, Y^{265}AYF and Y^{286}KLV) located in the Cx43 C-terminus that we termed sorting signals S1, S2 and S3. YXXΦ signals are known to bind physically to the μ2 subunit of

phosphorylation-activated AP-2 complexes (Collins et al., 2002; Ohno et al., 1995). Sorting signal S3 (Y^{286}KLV) is identical to the signal located within the proline-rich region that Thomas et al. identified previously. Sorting signals S1 or S2 at positions Y^{230}VFF and Y^{265}AYF that we identified in addition, have not been revealed by Thomas et al., and were not examined experimentally in their study (Thomas et al., 2003). We found that sorting signals S2 and S3 both recruit the classical PM clathrin adaptor complex AP-2, the alternative clathrin adaptor protein Dab2, and clathrin to mediate GJ endocytosis. A very recent study that examined Cx43/AP-2 binding by applying a yeast two-hybrid screen using the Cx43 C-terminus as bait and the AP-2 μ2-subunit as prey suggests that the Cx43 C-terminus may require specific post-translational modifications (that did not occur in the yeast host) to render the S2 binding site accessible to AP-2 (Johnson et al., 2013a). Sorting signal S1, due to its close juxtaposed transmembrane domain 4 (TM4) location, and consistent with previously published findings (Collins et al., 2002; reviewed in Bonifacino and Traub, 2003), was not found to serve as an AP-2 interaction/recruitment site.

We characterized the identified internalization motifs by generating and analyzing a set of Cx43 mutants comprised of large and small deletions and critical amino acid exchanges. Cx43 mutants with both sorting signals S2 and S3 (S2+3) mutated no longer co-precipitated AP-2, Dab2, or clathrin. These mutants formed more and/or larger GJ plaques, exhibited longer protein-half lives, and double-mutants exhibited severe impairment of GJ plaque internalization. Interestingly, mutants with only one of the two sorting signals mutated (either S2

or S3) were also internalization impaired. However, the internalization of these mutants was affected less severely (by approximately one-half when compared with the double S2+3 mutants) (**Figures 6, 8-11**). We also found that Dab2 interacts with Cx43 indirectly via AP-2 (**Figures 6, 7**). Collectively, our results suggest that the Cx43 sorting signals S2 and S3, work together to endocytose Cx43 GJs; and they evoke a possible model for clathrin to achieve the efficient internalization of double-membrane spanning GJs. Compared to other PM receptors such as transferrin-, LDL-, receptor-tyrosine kinases (EGF-, VEGF-, PDGF-), and G-protein coupled receptors (GPCRs) that are endocytosed by the clathrin machinery, GJs are large PM structures and their endocytosis may pose a greater challenge to the cellular endocytic machinery (reviewed in Pauly and Drubin, 2007) In our model, schemed in **Figure 12**, AP-2 interacts with the Cx43 sorting signals S2 and S3 via its μ2 subunit as the first step of Cx43 GJ endocytosis. Once Cx43 and AP-2 interaction has been established, AP-2 may either recruit clathrin directly via its β2-subunit appendage and/or clathrin-bound Dab2 via its α subunit appendage. In this model, the interaction between AP-2 and Dab2 is an important step as recruitment of Dab2 to GJ plaques may allow multiple (up to four) clathrin triskelia to be recruited to a single Cx43 of a GJ plaque (**Figure 12**). AP-2, Dab2 and other clathrin adaptors have all been found to be present concurrently in endocytic clathrin-coated vesicles (Keyel et al., 2006), suggesting that they play a cooperative/synergistic role in clathrin and clathrin-machinery component recruitment. Thus, recruitment of multiple adaptors and clathrin complexes per Cx43 cargo molecule may facilitate efficient

endocytosis of these large PM structures. Furthermore, acute GJ internalization in response to certain stimuli (Baker et al., 2008) might, in addition to AP-2, require extra clathrin adaptors (e.g. Dab2) to achieve highly efficient internalization, while constitutive GJ plaque turnover (Falk et al., 2009) may be achieved by AP-2 alone. This, for example is known to occur in GPCR endocytosis, where constitutive endocytosis of un-stimulated receptors is achieved via AP-2 binding, while rapid ligand-stimulated GPCR internalization requires AP-2 plus an additional clathrin adaptor, e.g. β-arrestin or epsin-1 (Chen et al., 2011; Moore et al., 2007; Wolfe and Trejo, 2007). Lastly, recent elegant studies from the Kirchhausen lab indicate that clathrin triskelia, to successfully initiate coat formation need to interact with two AP-2 complexes simultaneously. These interaction typically are mediated via PM-anchored PI-4,5-P_2 (PIP_2) interactions (Cocucci et al., 2012). However, significantly less, or even no PIP_2 is present within GJ plaques, suggesting that Cx43 may have two AP-2 binding sites per Cx43 polypeptide to allow for efficient AP-2 binding/clathrin recruitment to successfully initiate clathrin coat formation and GJ internalization. Future research will be needed to further address these exciting possibilities.

Interestingly, the sequence $SP^{283}PGYKLV^{289}$ that Thomas et al. (2003) identified indeed consists of two overlapping signals, a proline-rich PY motif ($XP^{283}PXY^{286}$) and the YXXΦ tyrosine-rich sorting signal S3 ($Y^{286}KLV^{289}$), and both may play discrete functions in clathrin-dependent and clathrin-independent GJ internalization mechanisms. For example, in addition to clathrin-dependent internalization, clathrin-independent has been reported for EGF receptors.

Clathrin-independent EGF-receptor internalization is reliant on ubiquitination and is regulated by the amount of stimulated receptors that are present in the PM (Sigismund et al., 2005; reviewed in Aguilar and Wendland, 2005). The proline-rich PY motif ($XP^{283}PXY^{286}$) in Cx43 has been reported to interact with the HECT E3 ubiquitin ligase, Nedd4, via its WW2 domain (Leykauf et al., 2006). Nedd4-mediated ubiquitination of Cx43 allows recruitment of Eps15, a multi-functional ubiquitin-interacting endocytic protein to GJs (Catarino et al., 2011; Girao et al., 2009). Eps15 is a component of clathrin-coated pits and vesicles, and it has been reported to interact directly with AP-2 (Benmerah et al., 1998). However, Eps15 also performs an important function in coupling ubiquitinated cargo to clathrin-independent internalization (reviewed in (Aguilar and Wendland, 2005)). Thus, ubiquitinated Cx43 may also be recognized by Eps15 through its ubiquitin-interacting motif, possibly resulting in Eps15-mediated clathrin-independent GJ endocytosis. Also, Leithe et al. identified Cx43 ubiquitination as a potential signal for Cx43 GJ internalization (Leithe et al., 2009), and Fykerud et al. recently identified another ubiquitin ligase, Smurf2, that ubiquitinates Cx43 and prepares GJs for internalization and endo-/lysosomal degradation in TPA-treated cells (Fykerud et al., 2012). We too found that cells that expressed the double-sorting signal mutants S2+3, eventually were able to remove their GJ plaques (**Figure 9, Movies S1-5**), while GJ internalization in the Cx43-$\Delta L^{254\text{-}CT}$-GFP mutant was abolished entirely. However, GJ removal in these S2+3 mutants appeared very different and followed a different spatial and temporal pattern, potentially implying a different, yet uncharacterized cellular

mechanism. Together, these findings suggest that cells may utilize more than one pathway to remove GJ plaques. Different functional requirements and different upstream cell signaling events leading to different Cx43 modifications (e.g. phosphorylation, ubiquitination, SUMOylation, etc.) might dictate which cellular pathway eventually might be utilized (reviewed in (Falk et al., 2012; Thévenin et al., 2013). As stated above, the PY motif ($P^{283}PX\mathbf{Y}^{\mathbf{286}}$) that mediates Nedd4 binding overlaps with the YXXΦ-tyrosine-based sorting signal S3 ($\mathbf{Y}^{\mathbf{286}}KLV^{289}$) since the Y^{286} is essential for both signals. Thomas et al. (2003) separately mutated the $XP^{283}XXY^{286}$ and the $Y^{286}XXV^{289}$ signals by substituting P^{283} with leucine (L) and V^{289} with aspartic acid (D) and found that mutating the latter (YXXΦ) signal resulted in a more significant increase in the steady state pool of Cx43 (3.5 versus 1.7 fold, respectively). When both, the PXXY and the YXXΦ signals were mutated together by either mutating P^{283} to L and V^{289} to D, or by mutating Y^{286} to A, no additive effect was observed. The double mutants behaved similar to the single YXXΦ mutant, suggesting a primarily AP-2 mediated CME-based mechanism for GJ internalization.

Several Cxs, including Cx43, Cx32, Cx36, and Cx46 were reported to interact with Caveolin-1 suggesting the possibility that Cx proteins can localize to lipid rafts (Lin et al., 2003; Schubert et al., 2002). However, the size of typical GJ plaques is much larger than the size of lipid rafts (about 50 nm) (Helms and Zurzolo, 2004; Yuan et al., 2002), making it unlikely for GJs to localize to and internalize utilizing a caveolae-dependent endocytosis mechanism. Caveolae-

dependent endocytosis, however, may be utilized for the internalization of PM localized Cx hemichannels.

In this study, we provide multiple lines of independent evidence that suggest a predominantly AP-2-and clathrin-driven pathway for the internalization of Cx43-based GJs. The alternative clathrin-adaptor Dab2 may also be recruited to Cx43 GJs via AP-2 interaction, most likely to enhance the efficacy of this endocytic process. Interestingly, our analyses uncovered two AP-2 binding sites in the Cx43 C-terminus that are both used to convey the binding of up to four clathrin triskelia per Cx43 polypeptide (via the binding of two AP-2 complexes and two Dab2 proteins), suggesting a potential molecular mechanism for clathrin to mediate the internalization of PM structures that can be 50-times larger than typical clathrin-coated vesicles. Future research will need to address which signals regulate access of AP-2 (and of other endocytic adaptors) to Cxs of endocytosis-primed GJs, and how many Cx polypeptides per connexon/GJ channel need to bind to AP-2 to successfully initiate GJ endocytosis. Post-translational modifications of Cx43, such as phosphorylation and ubiquitination that for example are required for GPCR endocytosis (Chen et al., 2011; Moore et al., 2007; Wolfe and Trejo, 2007), binding/release of regulatory proteins as observed for adherens junctions (Nanes et al., 2012), or conformational changes of the Cx43 C-terminus (Solan and Lampe, 2005) are all enticing possibilities.

2.5. Materials and methods

2.5.1. PCR mutagenesis and cDNA construction

Cx43-GFP mutants were generated by site-specific mutagenesis. Full-length rat Cx43-GFP (previously cloned into pEGFP-N1 vector as described in Falk, (2000) was used as a template for PCR mutagenesis. Primer sequences are listed below. Site-directed mutagenesis of the Cx43 sequence was performed using an overlap extension polymerase chain reaction (PCR) mutagenesis procedure **(Figure 13)** developed by Higuchi et al. (1988).

PCR mutagenesis reactions were done using proofreading Pfu Ultra II polymerase (Stratagene, Cat. No. 600670-51). PCR settings were as the following:

	Stock [ ]	**Vol. used (μl)**	**Final [ ]**
Template DNA	0.5 μg/μl	1	0.5 μg
Pfu buffer	10 X	5	1 X
Pfu Ultra II Polymerase		1	
Forward primer	1 mg/ml	0.5	500 ng
Reverse Primer	1 mg/ml	0.5	500 ng
dNTP	10 mM	1	200 μM
H_2O		41	
Total		50	

Mutated PCR-amplified cDNA fragments were restriction endonuclease-digested with EcoRI and BamHI , and ligated into the full length Cx43-GFP containing vector to replace the wild type sequence with the mutated sequence.

Untagged Cx43 mutants were generated by QuikChange™ site-direct mutagenesis. Cx43-GFP mutants were used as templates for PCR amplification. A pair of mutagenic primers reintroducing the authentic Cx43 TAA STOP-codon behind the last Cx43 amino acid (I^{382}) was used. PCR amplification (using proofreading Pfu Ultra II polymerase) (Stratagene, Cat. No. 600670-51) generated nicked, circular strands. Template DNA (methylated) was digested using *Dpn*I restriction endonuclease. Constructs were then transformed into DH5α competent *E. coli* cells. Plasmids were purified using Qiagen Midi-/Maxiprep plasmid DNA purification kits (Qiagen, Cat. No. 12243, and 12163). All constructs were verified via DNA sequence analyses. Plasmids containing histone mCherry-H2B and Cx43-mApple (generous gifts of Michael W. Davidson, The Florida State University, Tallahassee, FL, USA) were used to identify Cx43-cotransfected cell pairs (**Figure 8**), and in Cx43-GFP/Cx43-mApple co-culture experiments (**Figure 11**).

2.5.2. Cell culture and transfections

HeLa cells (ATCC, Cat. No. CCL2) were maintained under standard conditions in a humidified atmosphere containing 5% CO_2 at 37°C in high glucose Dulbecco's modified Eagles's medium (DMEM). Media were supplemented for a final concentration of 10% with fetal bovine serum (FBS) (Atlanta Biologicals,

Cat. No. S11050), 2mM L-glutamine (Thermo Scientific, Hyclone, Cat. No. SH30034.01, stock 200mM) and 50 I.U/ml penicillin and 50μg/ml streptomycin (Cellgro, Cat. No. 30-001-CI). Cells were passaged the day prior to transfection, cultured to 50-75% confluency and transfected with SuperFect® (Qiagen, Cat. No. 301307) transfection reagent according to manufacturer's recommendations.

2.5.3. Immunofluorescence microscopy and image analyses

Cells were either grown in glass bottom dishes or on glass cover slips pre-treated with poly L-lysine (Sigma, Cat. No. P8920). Cells were fixed with 3.7% formaldehyde and permeabilized with 0.2% Triton X-100 in PBS. Cells were blocked with 10% FBS in PBS at room temperature for 1 hour. Cells were incubated with rabbit polyclonal anti-Cx43 primary antibodies (Cell Signaling Technology, Cat. No. 3512) at 1:500 dilution at 4°C overnight. Secondary antibodies (goat anti-rabbit Alexa488, Molecular Probes/Invitrogen, Cat. No. A11008) were used at 1:500 dilution at room temperature for 1 hour. Cell nuclei were stained with 1μg/ml DAPI. Cells were mounted using Fluoromount-G™ (SouthernBiotech, Cat. No. 0100-01).

Wide-field fluorescence microscopy was performed on a Nikon Eclipse TE 2000E inverted fluorescence microscope equipped with a 60x, NA 1.4, Plan Apochromat oil immersion objective. Images were acquired using MetaVue software version 6.1r5 (Molecular Devices, Sunnyvale, CA), Quantitative analyses were performed using ImageJ version 1.43u (National Institutes of Health, USA). Adobe Photoshop version 8.0 was used to process images.

2.5.4. Duolink® *in situ* protein co-localization assays

HeLa cells were either transfected with wt Cx43-GFP, or with Cx43-$\Delta L^{254-290}$-GFP and Cx43-ΔL^{254-CT}-GFP constructs with putative AP-2 binding sites deleted. Cells were fixed, permeabilized, and blocked as described above. Cells were then incubated with mouse anti-Dab2 and rabbit anti-Cx43 antibodies at 1:500 dilution at 4°C overnight. Unbound primary antibodies were removed by washing 3 times with 1x PBS. Cells were incubated with secondary antibodies conjugated with PLA-specific oligonucleotide probes (Duolink *in situ* starter kit, Olink Bioscience, Uppsala, Sweden, Cat. No. 92101) at 37°C for 1 hour. Unbound antibodies were removed by washing 3 times with wash buffer A. Ligase enzyme and ligation buffer were added according to manufacturer's recommendation in order to hybridize the two PLA-probes and to form a closed DNA circle, a reaction that according to the manufacturer can only occur if the two PLA-probes are located in close proximity to each other ($\leq$ 40 nm). Samples were then washed 3 times with wash buffer A. Amplification solution containing deoxyribonucleotides and Texas Red-analogue fluorescent-labeled oligonucleotides ($\lambda_{ex.}$ 594 nm, $\lambda_{em.}$ 624 nm) were added together with DNA polymerase. Amplification reactions were performed at 37°C for 90 minutes. This will initiate rolling-circle amplification reactions to occur that generate concatemeric DNA strands onto which the fluorescent-labeled oligonucleotide detection probes hybridize. Unbound labeled oligonucleotides were removed by

washing the samples 3 times with buffer B before embedding samples in Duolink mounting medium and microscopic observation.

2.5.5. Live-cell imaging

HeLa cells were transfected with wild type Cx43-GFP, or with Cx43-GFP mutants as described above. Cells were analyzed 24 hours post-transfection, and extended live-cell recordings (up to 72 hours; phase contrast and fluorescence) as shown in Figure 4 were performed on a Nikon BioStation IM Cell-S1 system using a 40x air-objective and glass-bottom dishes. Images were acquired every 2 or 5 minutes. Time-lapse image sequences were than annotated using NIS Elements AR 3.0, SP6, Hotfix 7.

2.5.6. Western blot analyses

Denatured protein samples derived from Cx43 wt and mutant-expressing HeLa cells were analyzed on 10% or 12% SDS-PAGE mini-gels (BioRad). Biotinylated protein ladder (Cell Signaling Technology, Cat. No. 7727S) was used as a molecular weight marker. Proteins were transferred onto nitrocellulose membranes (Whatman, Cat. No. 10439396) on ice at 120 V for 1 hour before blocking with 5% non-fat dry milk in TBST at room temperature for 1 hour. Membranes were then incubated with primary antibodies at 4°C overnight. Antibodies used were: mouse anti-Cx43 (Zymed, Cat. No. 138300) at 1:2000 dilution, rabbit anti-Cx43 (Cell Signaling Technology, Cat. No. 3512) at 1:2500 dilution, mouse anti-α-Adaptin (an AP-2 subunit) (BD Transduction Laboratories,

Cat. No. 610501) at 1:2000 dilution, mouse anti-Dab2 (p96) (BD Transduction Laboratories, Cat. No. 610501, 610464) at 1:2000 dilution, mouse anti-clathrin heavy chain (BD Transduction Laboratories, Cat. No. 610499), at 1:2000 dilution, mouse anti-dynamin2 (BD Transduction Laboratories, Cat. No. 610245) at 1:2000 dilution, mouse anti-GFP-HRP (Miltenyi Biotec, Cat. No. 130-091-833) at 1:2500 dilution, and mouse anti-□-tubulin (Sigma, Cat. No. T9026) at 1:5000 dilution. Membranes were washed 3 times with TBST followed by incubation with HRP-conjugated secondary antibodies at 1:5000 dilution (Zymed Laboratories, Cat. No. 81-6520 or 81-6120) at room temperature for 1 hour. Proteins were detected with ECL plus (GE Healthcare, Cat. No. RPN2132). The NIH ImageJ software package was used to quantify intensity of protein bands.

2.5.7. Co-immunoprecipitation assays

Cx43 transfected HeLa cells were lysed with 1x SDS-free RIPA buffer (Cell Signaling Technology, Cat. No. 9806) supplemented with protease and phosphatase inhibitor cocktail (Cell Signaling Technology, Cat. No. 5872). Supernatants were incubated either with covalently linked anti-GFP magnetic beads (Miltenyi Biotec, Cat. No. 130-091-288), or with rabbit anti-Cx43 antibodies together with Dynabeads® protein-G magnetic beads (Invitrogen, Cat. No.10003) at 4°C overnight, or at room temperature for 2 hours. Beads were washed 3 times with 1x TBS. Cx43 and bound proteins were eluted from the beads using hot SDS-PAGE sample buffer containing 50 mM DTT. Samples were analyzed by Western blot as described above.

2.5.8. Cx43 protein half-life analyses

HeLa cells were cultured and transfected with GFP-tagged wild type or mutant Cx43 constructs in multiple 3.5 cm dishes as described above. Cells were treated with 50ug/ml of cycloheximide (Sigma, Cat. No. C-6255) the following day to inhibit protein biosynthesis, and cells were lysed and harvested with 500 µl of 1x SDS-PAGE sample buffer at 15 and 30 minutes, 1, 2, and 4 hours post treatment. Samples were heated at 95°C for 5 minutes. Cx43 protein levels of each lysate were examined by Western blot analyses using mouse anti-GFP-HRP antibody as described above (15 µl of each protein sample was analyzed). Membranes were stripped with stripping buffer (Boston Bioproducts, Cat. No. BP-96) followed by a stringent wash in TBST before re-probing with mouse anti-α-tubulin antibody (Sigma, Cat. No. T9026). Protein amount of each band was quantified using NIH ImageJ. Cx43 amounts were corrected for uneven loading by comparing with the amount of α-tubulin.

2.5.9. Transfection and co-culture of cells expressing wt and mutant Cx43 constructs

HeLa cells were cultured to 70-80% confluency. Cells were dislocated using 0.25% trypsin/EDTA, washed 3 times with 1x PBS and pelleted. Cell pellets were re-suspended in electroporation buffer (Millipore, Cat. No. ES-003-D), and transferred into 4 mm gap-size electroporation cuvettes. Electroporations were performed with $3x10^6$ cells and 20 µg of DNA in a total volume of 750 µl at

250V and 500 μF using a Gene Pulser Xcell™ Total System (BioRad, Cat. No. 165-2660). Cells were rested on ice for 10 minutes before seeding wild type and mutant Cx43 transfected cells at equal ratio onto poly-L-lysine coated glass coverslips. Cells were cultured for approximately 30 hours, fixed and stained with DAPI as described above before imaging.

2.5.10. Statistical analyses

Unpaired student t-tests were performed to analyze, percentage of AP-2, Dab2, and clathrin heavy chain co-precipitated with Cx43 (**Figure 6**); percentage of Cx43/Dab2 Duolink colocalization (**Figure 7**); average number of GJs/cell pair (**Figure 8**), average time periods required for GJ plaques to form and internalize (**Figure 9**); and number of heterotypic AGJs/cell type (**Figure 11**) using the GraphPad online software package (GraphPad Software, Inc. La Jolla, CA). Data are presented as mean ± SEM. In all analyses, a p-value ≤ 0.05 (depicted with *, **, or ***) was considered statistically significant.

2.6: Figures

A

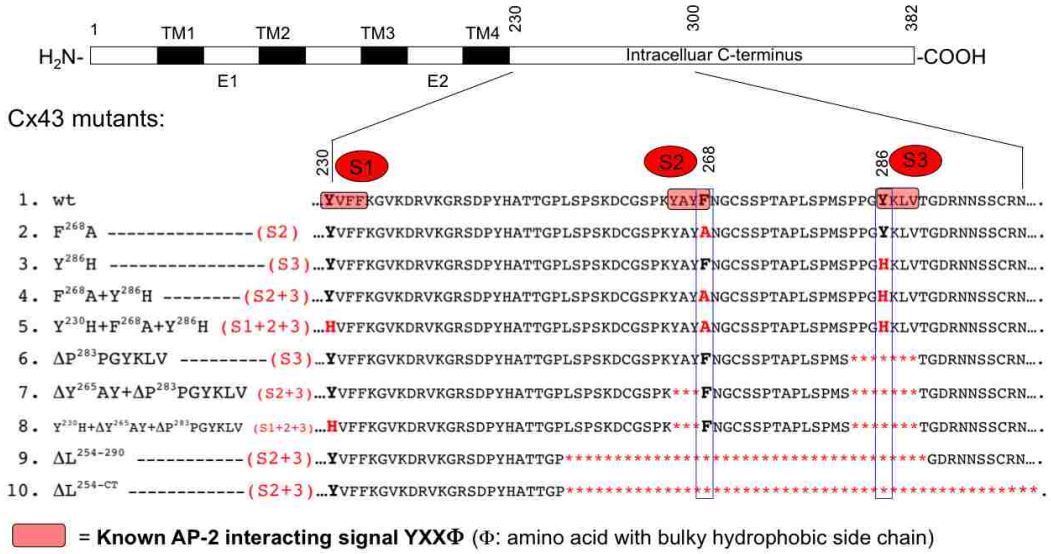

B GFP-tagged

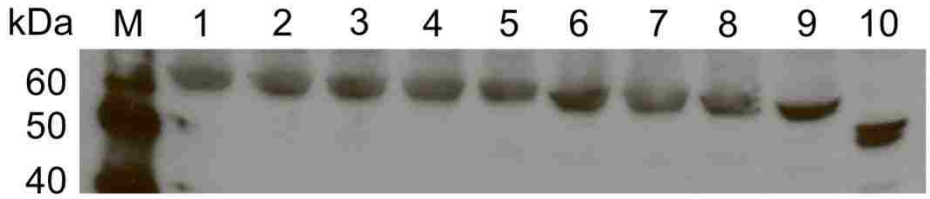

Figure 5: Cx43 mutants that interfere with AP-2/clathrin binding. **(A)** The Cx43 C-terminus harbors three canonical tyrosine-based sorting signals of the type YXXΦ at positions Y^{230}VFF, Y^{265}AYF, and Y^{286}KLV that we named S1, S2, and S3 (shown in red) that can function as putative binding sites for the classical PM clathrin adaptor, AP-2. To test their role in recruiting AP-2 to Cx43, we generated a set of mutants that abolished the AP-2 binding capacity by mutating known

critical residues of the motifs (Y or F) into H or A, or by deleting the amino acid residues of the motifs, either partially (3 amino acid residue deletions), or entirely (≥7 amino acid deletions) (depicted with asterisks, see text for details). Single, double, and triple-site mutants (depicted S1, S2, S3, S2+3, and S1+2+3) were constructed. Mutants 2 to 10 characterized in this work are shown. **(B)** Immunoblot analysis (using anti-GFP antibodies) of wild type (lane 1) and mutant Cx43-GFP constructs (lanes 2-10). Wild type and mutants produced Cx43 proteins that migrated on SDS-PAGE gels corresponding to their predicted molecular weight. M = Marker proteins.

A

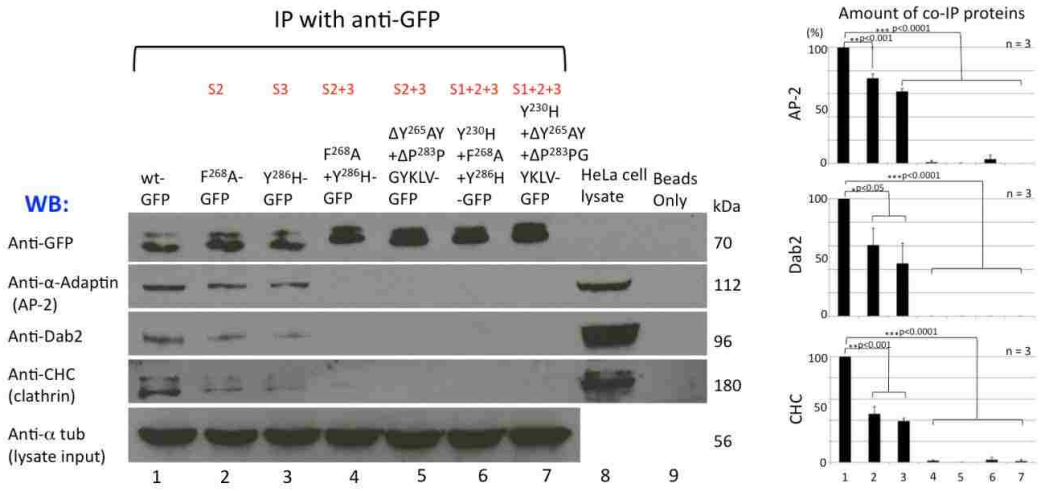

B

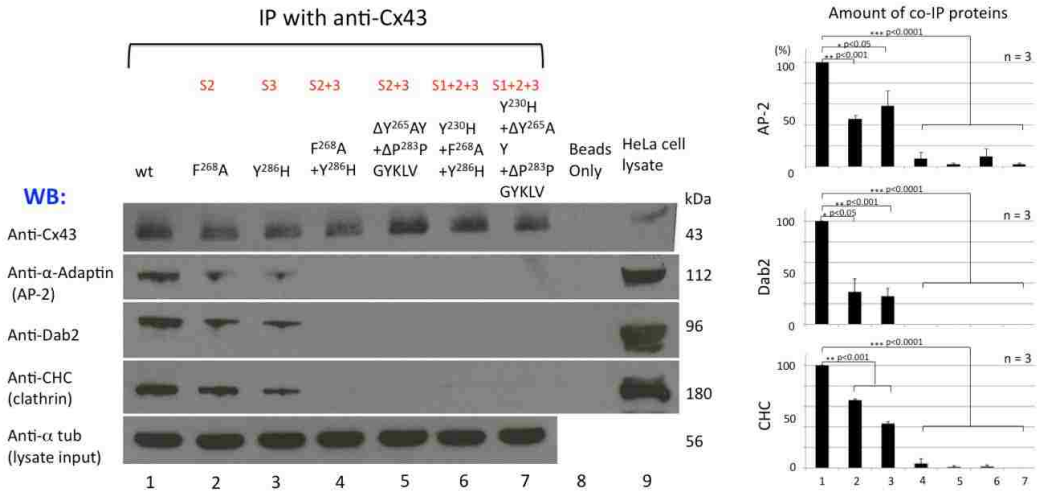

Figure 6: Cx43 mutants with AP-2 binding sites S2 or S3 mutated, co-precipitate reduced amounts, while mutants with both (S2+3) or all three sites mutated (S1+2+3) no longer co-precipitate clathrin and clathrin accessory proteins. HeLa cells were transfected with GFP-tagged **(A)** and untagged **(B)** Cx43 wt (lane 1); single $F^{268}A$ (S2), $Y^{286}H$ (S3) (lanes 2, 3); double $F^{268}A$+$Y^{286}H$ (S2+3), $\Delta Y^{265}AY$+$\Delta P^{283}PGYKLV$ (S2+3) (lanes 4, 5); and triple $Y^{230}H$+$F^{268}A$+$Y^{286}H$

(S1+2+3), $Y^{230}H+\Delta Y^{265}AY+\Delta P^{283}PGYKLV$ (S1+2+3) (lanes 6, 7) mutants. Cells were lysed in SDS-free 1x RIPA buffer, and protein complexes were immuno-precipitated using anti-GFP (in A) or anti-Cx43 (in B) magnetic beads. Bound and co-precipitated endocytic proteins were detected by Western blot analyses using antibodies specific for GFP (row 1 in A), anti-Cx43 (row 1 in B), α-Adaptin (AP-2, row 2), Dab2 (row 3), clathrin heavy chain (CHC, row 4), and α-tubulin (loading control, row 5). Cx43-wt as well as single site mutants S2 and S3 co-precipitated AP-2, Dab2, and clathrin, while double S2+3, and triple S1+2+3 mutants did not. HeLa cell lysates and beads only were analyzed in control (lanes 8, 9). Note that both single mutants S2 and S3 precipitated approximately one-half amounts of clathrin and clathrin-adaptors compared to wt Cx43 (see quantitative graphed analyses on the right). Representative blots are shown on the left, and averaged data of three independent experiments are shown on the right. Note that increasing amounts of Cx43 proteins were immunoprecipitated, correlating with the increasing stability of the mutant proteins (see Figure 6), and that a small amount of endogenous Cx43 was detected in overexposed membranes (row 1, lane 9 in B, quantified in Figure S1). Significant differences ($p < 0.05$) are shown in this and following figures. Results corroborate that motif S1 is not a functional AP-2 binding site.

A

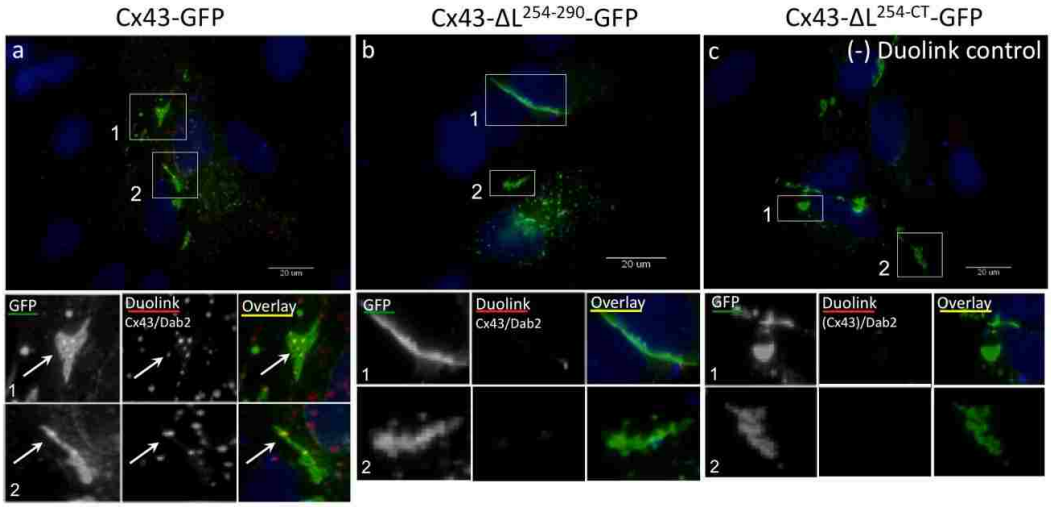

B

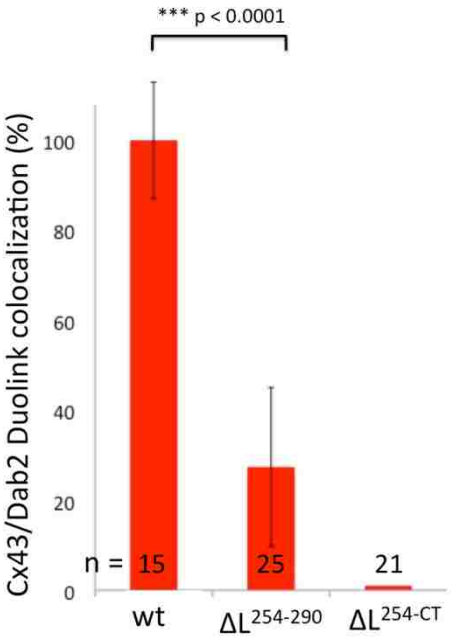

Figure 7: The accessory clathrin adaptor, Dab2, interacts indirectly with Cx43 via AP-2. **(A)** HeLa cells were transfected with wt Cx43-GFP (panel a), Cx43-$\Delta L^{254-290}$-GFP (mutant S2+3, panel b), and Cx43-ΔL^{254-CT}-GFP (mutant S2+3, panel c), and GJ plaques and AGJ vesicles were detected by their emitted fluorescence

(green). In-cell protein colocalization assays between Cx43 and Dab2 were performed with mouse anti-Dab2 and rabbit anti-Cx43 antibodies using *in situ* Duolink® technology (red fluorescence). Cx43 wt AGJ-vesicles co-localized with Dab2, detectable as red/yellow puncta in the magnified views (panel a). The Cx43-$\Delta^{L254-290}$ mutant is unable to recruit AP-2 and also does not recruit Dab2 as indicated by the negative Duolink signal (panel b). The Cx43-ΔL^{254-CT} mutant is also unable to interact with the Cx43 antibodies and served as a negative Duolink control (panel c). Representative images are shown. **(B)** Quantitative analyses of results described in (A) revealing the impaired ability of AP-2 binding-deficient Cx43 mutants to recruit Dab2. Results are consistent with co-immunoprecipitation results presented in **Figure 6**.

A

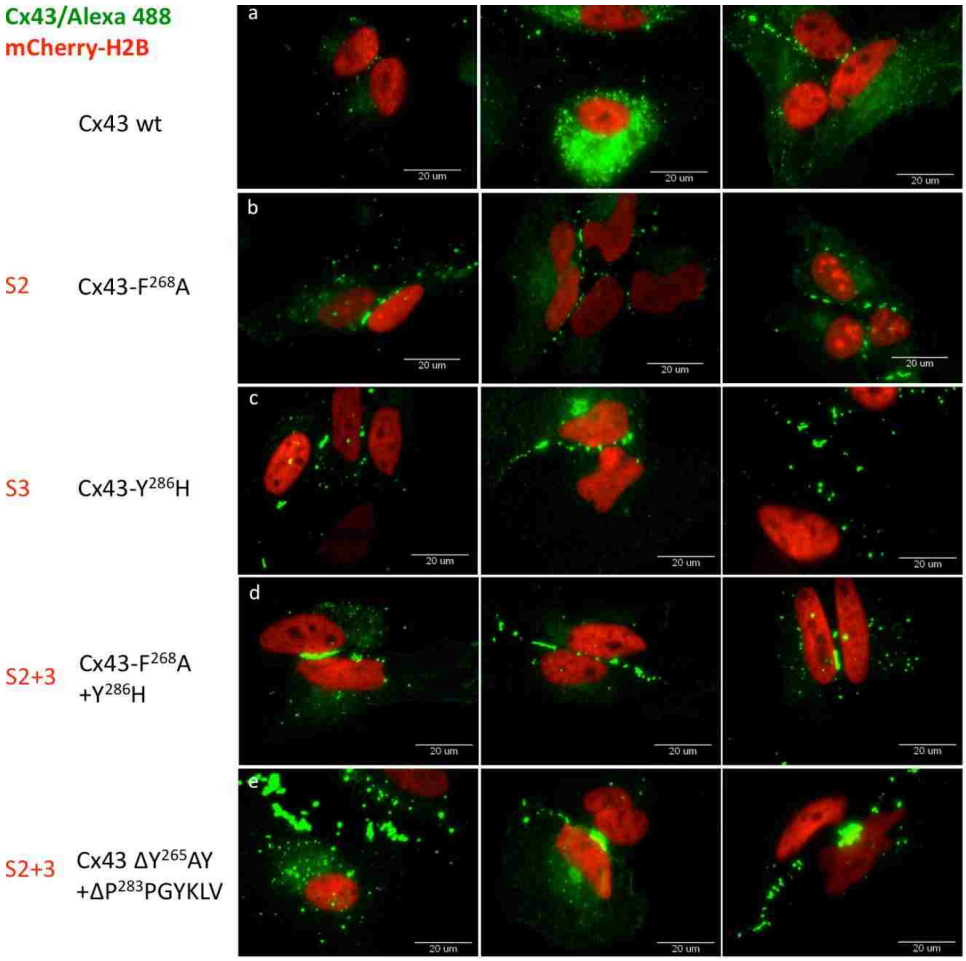
Cx43/Alexa 488
mCherry-H2B
Cx43 wt
S2
Cx43-F268A
S3
Cx43-Y286H
S2+3
Cx43-F268A
+Y286H
S2+3
Cx43 ΔY265AY
+ΔP283PGYKLV
a
b
c
d
e
20 um

B

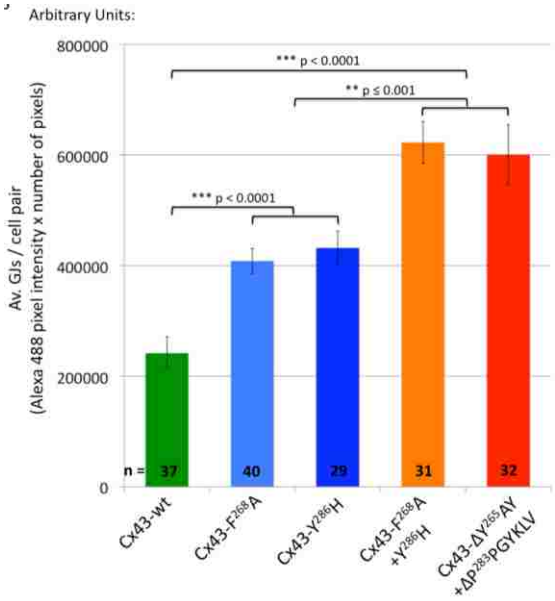
Arbitrary Units:
Av. GJs / cell pair
(Alexa 488 pixel intensity x number of pixels)
800000
600000
400000
200000
0
*** p < 0.0001
** p ≤ 0.001
*** p < 0.0001
n =
37
40
29
31
32
Cx43-wt
Cx43-F268A
Cx43-Y286H
Cx43-F268A +Y286H
Cx43-ΔY265AY +ΔP283PGYKLV

Figure 8: AP-2 binding-deficient Cx43 mutants have more GJ channels in their apposed PMs. **(A)** Untagged wt and S2, S3, and S2+3 Cx43 mutants were co-transfected with mCherry-H2B (red) (to better reveal transfected cell pairs) into HeLa cells. Cx43 was stained for immunofluorescence analyses using primary rabbit anti-Cx43 and secondary goat anti-rabbit Alexa488 (green) labeled antibodies. Images of transfected cell pairs were acquired using a 60x oil immersion objective. Three representative images of each, wt (panel a) and selected mutants ($F^{268}A$ [S2], panel b; $Y^{286}H$ [S3], panel c; $F^{268}A+Y^{286}H$ [S2+3], panel d; $\Delta Y^{265}AY+\Delta P^{283}PGYKLV$ [S2+3], panel e) are shown. **(B)** Quantitative analyses of the number of GJ channels present in apposed PMs (performed by measuring PM localized Alexa488 fluorescence intensity of wt and selected S2, S3, and S2+3 mutants) revealed a two-fold increase in Cx43-$F^{268}A$ (S2) and Cx43-$Y^{286}H$ (S3) mutants (blue bars), and a three-fold increase in Cx43-$F^{268}A+Y^{286}H$-GFP, and $\Delta Y^{265}AY+\Delta P^{283}PGYKLV$ (S2+3) mutants (orange/red bars) compared to wt Cx43 expressing cells (green bar).

A

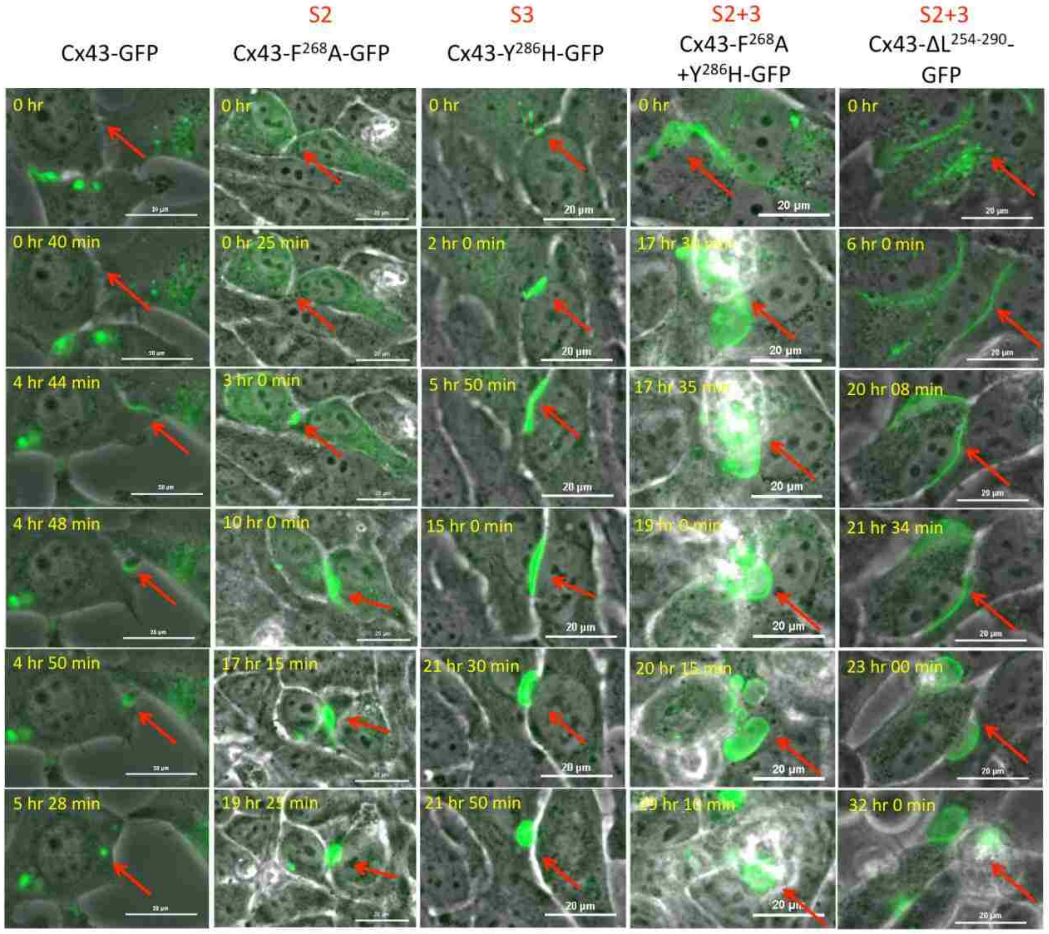
Cx43-GFP
S2
Cx43-F268A-GFP
S3
Cx43-Y286H-GFP
S2+3
Cx43-F268A +Y286H-GFP
S2+3
Cx43-ΔL254-290-GFP
0 hr
0 hr 40 min
4 hr 44 min
4 hr 48 min
4 hr 50 min
5 hr 28 min
0 hr
0 hr 25 min
3 hr 0 min
10 hr 0 min
17 hr 15 min
19 hr 25 min
0 hr
2 hr 0 min
5 hr 50 min
15 hr 0 min
21 hr 30 min
21 hr 50 min
0 hr
17 hr 35 min
20 hr 15 min
0 hr
6 hr 0 min
20 hr 08 min
21 hr 34 min
23 hr 00 min
32 hr 0 min
20 µm

B

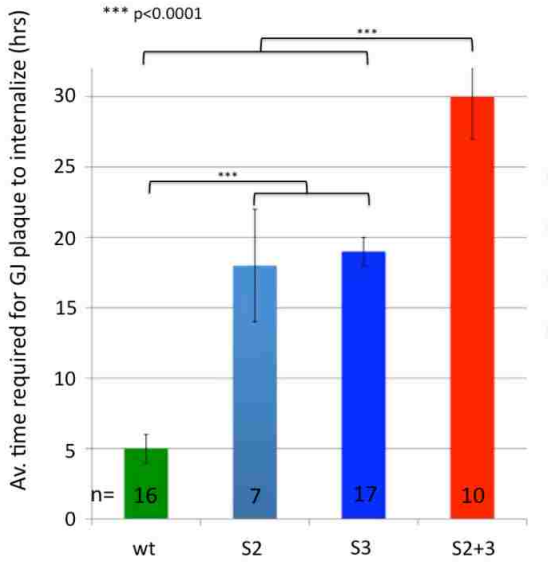
*** p<0.0001
***
***
Av. time required for GJ plaque to internalize (hrs)
30
25
20
15
10
5
0
n=
16
7
17
10
wt
S2
S3
S2+3

Figure 9: GJ plaques assembled by AP-2 binding-deficient Cx43 mutants are internalization impaired. **(A)** HeLa cells were transfected with GFP-tagged wild-type, S2, S3, and S2+3 mutant constructs and imaged every 2 or 5 minutes for up to 72 hours (phase contrast and green fluorescence channels). GJ plaque formation, maturation, and endocytosis were captured (depicted by arrows). Selected merged image frames of GFP-tagged wide-type, $F^{268}A$ (S2), $Y^{286}H$ (S3), $F^{268}A+Y^{286}H$ and $\Delta L^{254-290}$ (S2+3) are shown (also see supplementary Movies S1-5). **(B)** Quantitative analysis of time periods required for GJ plaques to constitutively turn over (form, mature, and be removed) revealed that GJ plaques assembled of wt Cx43, on average turned over in about 5 hours (green bar), while GJ plaques assembled from S2 and S3 mutants turned over in 18-19 hours (blue bars), and GJ plaques assembled from S2+3 double-mutants were removed after ~30 hours (red bar) (see Table S1 for complete data set).

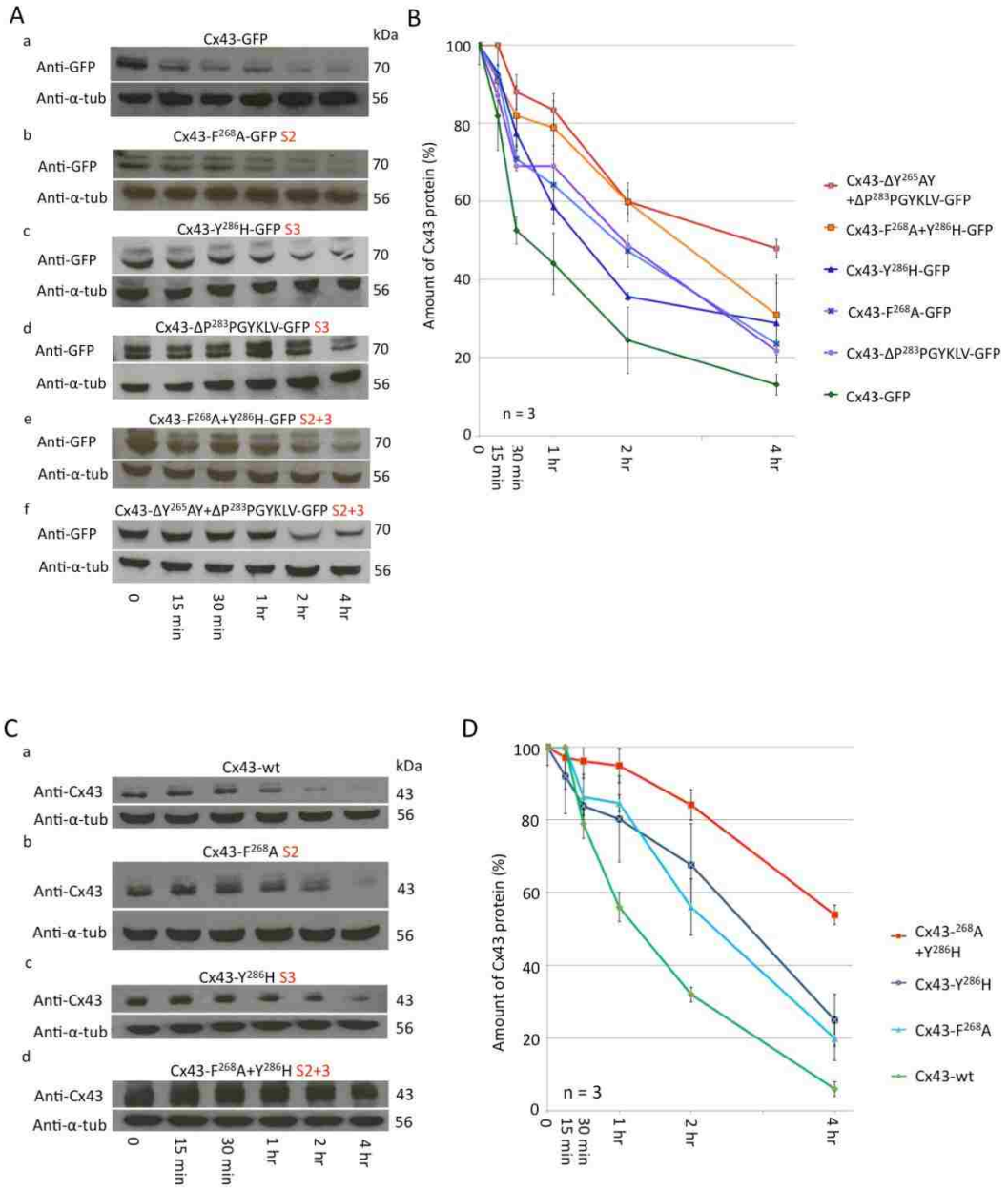

Figure 10: AP-2 binding deficient Cx43 mutant proteins exhibit longer half-lives. HeLa cells were transfected with GFP-tagged **(A)** or untagged **(B)** wt, S2, S3, and S2+3 Cx43 mutant constructs and treated with cycloheximide the following day to block protein biosynthesis. Cells were lysed at indicated time points post treatment and examined by SDS-PAGE and Western-blot analyses using anti-

GFP (in **A**) and anti-Cx43 (in **C**) antibodies. All membranes were stripped and re-probed with anti α-tubulin antibodies as a loading control. Representative Western blot analyses for Cx43 wt (panels a), $F^{268}A$ (S2, panels b), $Y^{286}H$ and $\Delta P^{283}PGYKLV$ (S3, panels c, d in A), $F^{268}A+Y^{286}H$ and $\Delta Y^{265}AY+\Delta P^{283}PGYKLV$ (S2+3, d in **C** and panels e, f in **A**) are shown. **(B and D)** Normalized quantitative analyses of Cx43 protein that remained after the indicated times in three independent analyses indicates that S2 and S3 mutant proteins have approximately doubled half-lives (~2 hours, blue curves), while double S2+3 mutants again have about doubled half-lives (~4 hours, orange/red curves) when compared with wild-type Cx43 protein (estimated half-live of ~1 hour, green curve).

A

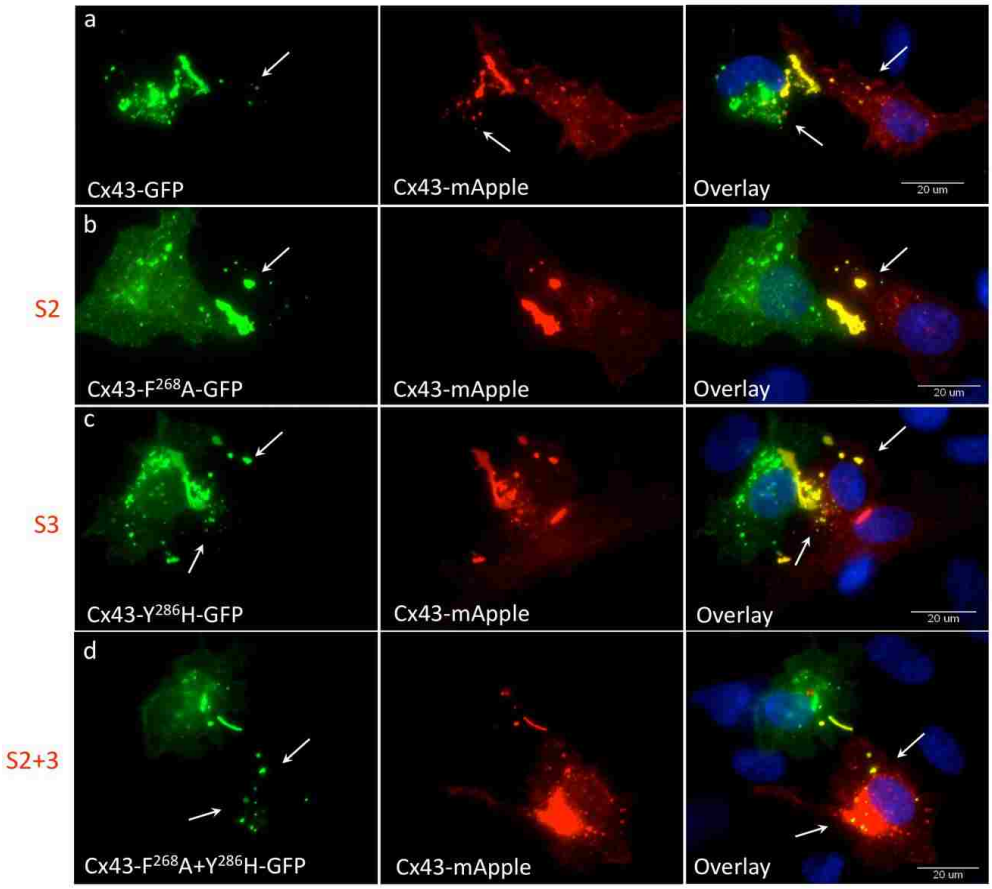
a
Cx43-GFP
Cx43-mApple
Overlay
20 um
b
S2
Cx43-F268A-GFP
Cx43-mApple
Overlay
20 um
c
S3
Cx43-Y286H-GFP
Cx43-mApple
Overlay
20 um
d
S2+3
Cx43-F268A+Y286H-GFP
Cx43-mApple
Overlay
20 um

B

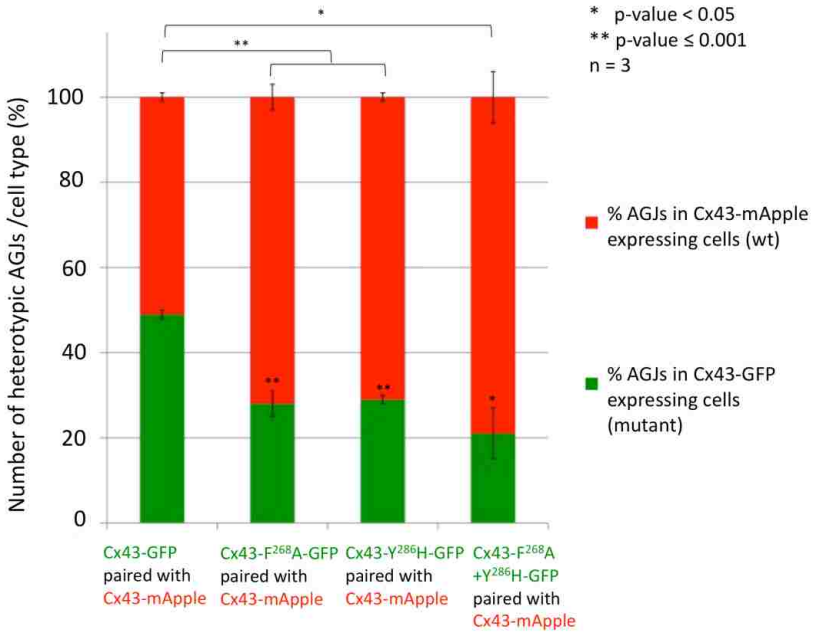
* p-value < 0.05
** p-value ≤ 0.001
n = 3
Number of heterotypic AGJs /cell type (%)
100
80
60
40
20
0
% AGJs in Cx43-mApple expressing cells (wt)
% AGJs in Cx43-GFP expressing cells (mutant)
Cx43-GFP paired with Cx43-mApple
Cx43-F268A-GFP paired with Cx43-mApple
Cx43-Y286H-GFP paired with Cx43-mApple
Cx43-F268A +Y286H-GFP paired with Cx43-mApple

Figure 11: AP-2 binding-deficient Cx43 mutants become donor cells. **(A)** HeLa cells were separately transfected with wt Cx43-mApple (red) or GFP-tagged wt, S2, S3, or S2+3 mutant constructs (green) and co-cultured. Cell pairs of wt Cx43-mApple and mutant/wt-GFP expressing cells assemble heterotypic GJs (yellow in the overlays). Heterotypic AGJs (also appearing yellow) are depicted with arrows. Representative images of wt Cx43-GFP (panel a), F^{268}A-GFP (S2, panel b), Y^{286}H-GFP (S3, panel C), and F^{268}A+Y^{286}H-GFP (S2+3, panel d) expressing cells paired with wt Cx43-mApple expressing cells of three independent experiments are shown. **(B)** Heterotypic AGJs were counted and their cellular location (either in wt Cx43-mApple expressing cells versus mutant Cx43-GFP expressing cells) was quantified. Cx43 wt/wt cell pairs exhibited an unbiased average ratio of 1:1 (bar 1), while Cx43 mutants (S2, S3, or S2+3, bars 2-4) were progressively inefficient in internalizing their plaques. Significance values between cell-pair groups, and between cell-types within groups compared to wt/wt pairs are shown above and within columns, respectively.

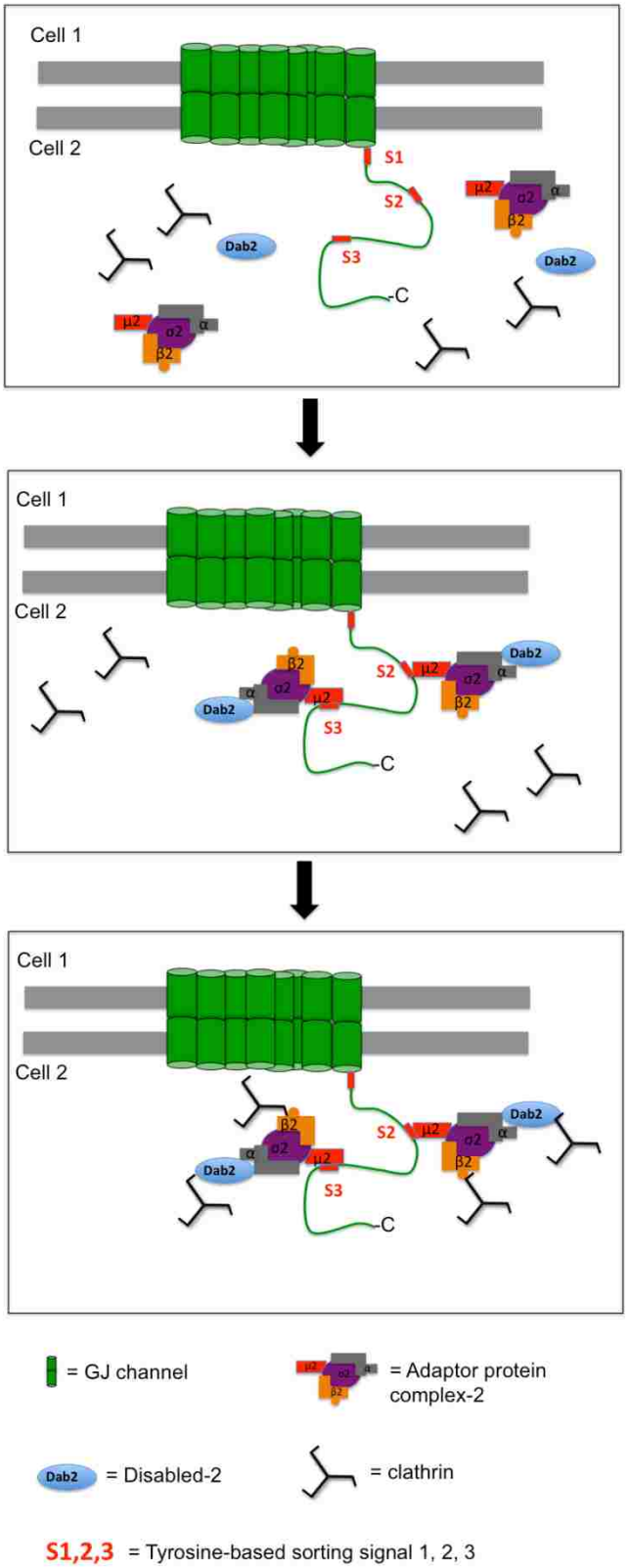
Cell 1
Cell 2
S1
S2
S3
C
Dab2
μ2
σ2
α
β2
= GJ channel
= Adaptor protein complex-2
= Disabled-2
= clathrin
S1,2,3 = Tyrosine-based sorting signal 1, 2, 3

Figure 12: Model of Cx43 recruiting clathrin and endocytic clathrin-adaptors. **(Top panel)** Cx43 encodes three canonical tyrosine-base sorting motifs of the type 'YXXΦ' in its C-terminus (S1, S2 and S3). Sorting signals, S2 and S3 both can recruit the classical clathrin adaptor AP-2 to Cx43-GJs that are destined for internalization. **(Middle panel)** Internalization-destined Cx43 binds the μ2-subunit of AP-2 via its Y^{265}AYF (S2) and/or its Y^{286}KLV (S3) motif. AP-2 then recruits clathrin either directly via its β2-subunit that binds to the terminal domain of clathrin heavy chain and/or it interacts via its α-subunit with clathrin-bound Dab2. **(Bottom panel)** As a consequence, one Cx43 polypeptide may recruit up to four clathrin molecules, potentially generating the principle molecular structure required for an efficient endocytosis of GJs.

A

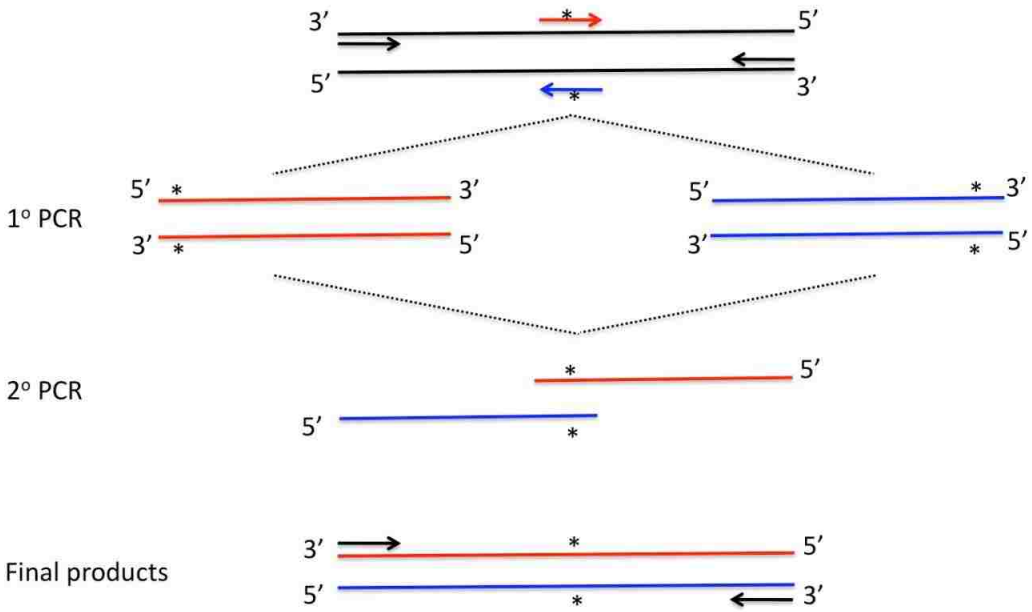

B

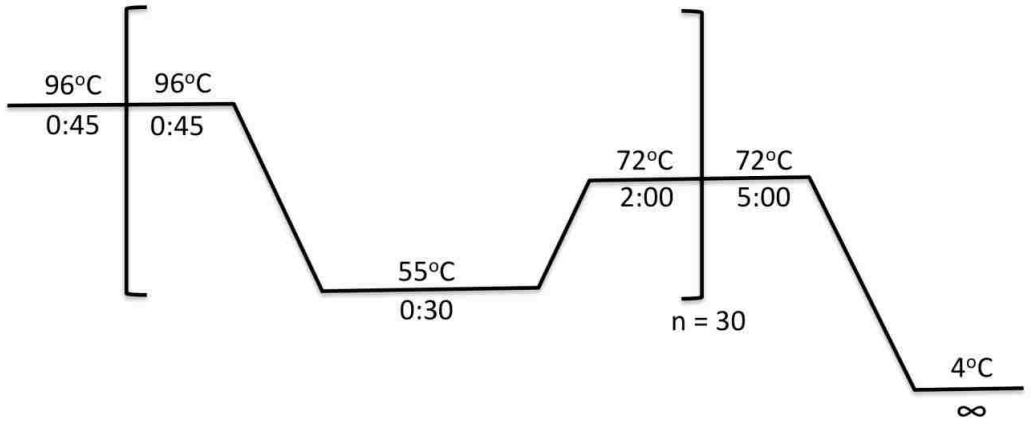

Figure 13: Scheme of site-directed mutagenesis by PCR. (a) Primary PCRs were performed by using mutagenesis primers to amplify one strand of the mutant DNA; the two PCR products from the primary PCRs (with overlapping sequences) were used as templates for the secondary PCRs. (See mutagenesis primers sequence in Appendix section). (b) Thermo cycler setting for PCR mutagenesis, 30 cycles of PCR amplifications were performed.

Chapter 3:

Cx43 phosphorylation is the signal for gap junction internalization

(A manuscript describing these results has been submitted to the journal FEBS Letters for review)

3.1. Abstract

Gap junction (GJ) channels bridge apposing membranes of neighboring cells to mediate intercellular communication by passive diffusion of signaling molecules. We have shown that GJs are internalized in whole, utilizing the endocytic clathrin machinery to form cytoplasmic double-membrane vesicles termed annular gap junctions or connexosomes. However, the signaling pathways and protein modifications that trigger GJ internalization are still unknown. Here, by treating mouse embryonic stem (mES) cells with epidermal growth factor (EGF), we found that EGF activates both MAPK and PKC signaling cascades to specifically phosphorylate the GJ protein Cx43, and that phosphorylation inhibits intercellular communication and induces GJ internalization.

3.2. Introduction

Direct intercellular communication by gap junction (GJ) channels is a hallmark of normal cell and tissue physiology. GJs are the only cell-cell junction type that allows direct cell-cell communication via the transfer of molecules

between cells. Examples include small metabolites such as glucose, amino acids, and ATP; ions such as Na^+, Ca^{2+}, and Cl^-; cell signaling molecules such as IP3 and cAMP; and potentially functional RNAs, such as miRNAs in glioma cells (Katakowski et al., 2010), and siRNAs in NRK cells (Valiunas et al., 2005; reviewed in Brink et al., 2012). In addition, based on their double-membrane configuration GJs likely contribute significantly to cell-cell adhesion. Clearly, these cellular functions require precise modulations. Complete double-membrane spanning GJ channels are formed when two hexameric hemi-channels (connexons) dock in the extracellular space. Remarkably, docked GJ channels cannot be separated into individual hemi-channels under physiological conditions (Ghoshroy et al., 1995; Goodenough and Gilula, 1974). Yet, actively proliferating cells as e.g. embryonic and somatic stem cells un-couple from their neighbors and internalize their GJs in order to undergo mitosis (Boassa et al., 2011). We have previously shown that GJs are internalized as a whole in a clathrin-mediated endocytic process (Baker et al., 2008; Fong et al., 2013; Gumpert et al., 2008; Piehl et al., 2007). However, the specific post-translational modifications such as phosphorylation, ubiquitination, etc. that render GJ protein (Connexins, Cxs) internalization competent are still poorly understood.

Twenty Cx isoforms are found in mouse with Cx43 being the most prominent isoform. Cx43 is a well-known phospho-protein. Numerous serine residues in the Cx43 C-terminus are phosphorylated to up-regulate GJ mediated intercellular communication (GJIC) (Ser325, Ser328, Ser330, Ser364/365, and Ser373) or down-regulate GJIC (Ser255, Ser262, Ser279/282, and Ser368)

(reviewed in Thevenin et al., 2013). Protein kinase C (PKC) is thought to phosphorylate Cx43 at Ser368 to down-regulate GJIC (Lampe and Lau, 2000; Solan et al., 2007). Cx43 has also been shown to be a substrate of mitogen activated protein kinase (MAPK) that upon mitogen stimulation phosphorylates Cx43 at Ser255 and Ser279/Ser282 to down-regulate GJIC (Warn-Cramer et al., 1996). Epidermal growth factor (EGF), a well-studied mitogen, can bind to the EGF receptor (a receptor tyrosine kinase [RTK] family member) to activate both the MAPK signaling cascade, and a PKC signaling pathway to promote cell proliferation. Mouse embryonic stem cells (mES cells) are actively proliferating cells with a relatively short cell cycle. They can infinitely self-renew while maintaining their pluripotency mediated via GJIC among the cells in the colony. In mES cells, expression of Cx31, Cx43, and Cx45 proteins has been described (Worsdorfer et al., 2008). However, the exact roles that GJs play in mES cell proliferation and differentiation are still unclear. In this study, we treated mES cells with EGF to induce proliferation and investigated signals, e.g. Cx43 phosphorylation events that may lead to GJ internalization.

3.3. Results

3.3.1. EGF treatment inhibits GJIC in mES cells via activation of the MAPK signaling cascade

Gap junction intercellular communication (GJIC) has been shown to play a crucial role in embryonic development, tissue function and cellular homeostasis (reviewed in Nagy et al., 2004; Wong et al., 2004). GJIC in pre-implantation

mouse embryos as early as at the 8-cell stage was described by Lo and Gilula (1979). Cx protein expression and GJIC in mES cells has also been described by the Willecke lab (Worsdorfer et al., 2008). However, regulation of GJIC in mES cells is not well understood. In 2008, inhibition of GJIC in mES cells treated with EGF has been described by (Park et al., 2008). However, the mechanisms that lead to GJIC-inhibition were not explored. EGF-induced inhibition of GJIC has also been shown in IAR20 rat liver epithelial cells (Leithe and Rivedal, 2004; Sirnes et al., 2009). Thus, to specifically examine the effects of EGF-treatment on Cx43, and to specifically test whether specific Cx43 phosphorylation events may be responsible for the inhibition of GJIC and/or GJ internalization, we pre-incubated mES cells either with or without PD98059 (a specific MEK inhibitor) in serum free media before treating cells with EGF. To assess GJIC inhibition, standard scrape loading/dye transfer assays using the GJ-permeable dye, Lucifer Yellow (LY) were performed, and GJIC-efficiency in EGF-treated cells was compared to untreated cells. GJIC in EGF-treated cells was significantly reduced to 37% ($n = 30$, SEM $\pm$ 4, $p < 0.0001$) compared to untreated controls (**Figure 15A, B**, columns 1 and 2). Cells that were pre-incubated with PD98059 exhibited a level of GJIC comparable to untreated control cells (89%, $n = 36$, SEM $\pm$ 4), suggesting that the MEK inhibitor abolished the GJIC inhibitory effect of EGF (**Figure 15A, B**, column 3). Together, these results indicate that EGF inhibits GJIC in mES cells by activating the MAPK signaling cascade.

3.3.2. EGF activates MAPK and PKC in mES cells to phosphorylate Cx43 at serines 262, 279/282, and 368

In order to examine which serine residues in the Cx43 sequence might be phosphorylated in response to EGF treatment, we implemented phospho-specific antibodies to detect the level of Cx43 phosphorylation at specific serine residues. mES cells were cultured under feeder-free conditions and serum-starved as described, then lysed at 10, 20, 30, 45, and 60 minutes post EGF treatment. Levels of phospho-Cx43 were analyzed by Western blots and intensities of protein bands were quantified using NIH ImageJ. α-tubulin was used as a loading control. Results indicate that EGF induces Cx43 phosphorylation at specific serine residues located in its C-terminus. Levels of pSer262, pSer279/282, and pSer368 at 10, 20 and 30 minutes post EGF treatment were significantly higher than in the untreated control (**Figure 16A, B**). At later time points (45 and 60 min), serine phosphorylation levels dropped to levels which were not significantly different from untreated controls. No significant increase in phospho-Ser255, another Cx43 MAPK substrate that is known to be phosphorylated in mitotic cells (Lampe et al., 1998; Sirnes et al., 2009), was detected (see Discussion in section 3.4 below).

3.3.3. EGF induces GJ endocytosis in mES cells

Down regulation of GJIC in cells may be accomplished by channel closure (Spray and Burt, 1990). However, in order to uncouple from neighboring cells, GJ channels have to be removed. GJ channel endocytosis upon onset of mitosis in rat fibroblasts and NRK cells has been described by Boassa et al., (Boassa et al.,

2011); and we have previously demonstrated that cells utilize the clathrin-mediated endocytic machinery to endocytose GJs (Baker et al., 2008; Fong et al., 2013; Gumpert et al., 2008; Piehl et al., 2007). Thus, to examine whether the EGF-induced Cx43 phosphorylation may also induce GJ internalization, mES cells were treated with EGF for 30 minutes and cultured together with appropriate untreated controls. Colonies were then fixed and stained with anti-Cx43, followed by Alexa488-conjugated secondary antibodies (Figure 3A, column 1). Alexa594-conjugated wheat germ agglutinin (WGA) was used to stain cell plasma membranes (PMs) (**Figure 17A**, column 2). Images were acquired using a 40x oil immersion objective. An increased amount of cytoplasmically located punctate Cx43 structures (presumably AGJ vesicles) were detected in EGF-treated cells (**Figure 17A**, middle panel) when compared with untreated cells (**Figure 17A**, top panel). When cells were pre-incubated with PD98059 prior to EGF-treatment, significantly less AGJs were detected (**Figure 17A**, bottom panel). Note that ES cells only have a very small cytosolic volume and hence AGJs appear to reside in close proximity to the PM.

To further support our conclusion that the cytoplasmic puncta indeed represent internalized AGJ vesicles, we treated cells with EGF or PD98059 followed by EGF, then performed EM analyses in comparison with untreated cells. Typical GJs (depicted with arrow) besides adherens type cell-cell junctions (depicted with arrowhead) were detected in the PMs between mES cell pairs (**Figure 17B**, left panel). Consistent with our immunofluorescence data, we detected an increased number of AGJ vesicles in the cytoplasm of the EGF-

treated cells (**Figure 17B**, middle panel). Note the typical, penta-laminar striped appearance of the AGJ vesicle 'wall' (depicted with arrow) that is representative of the double-membrane configuration of these structures. Also consistent, much less AGJs and more GJ plaques were detected in MEK-inhibitor and EGF-treated cells (**Figure 17B**, right panel). Taken together, our results suggest that EGF-treatment induces GJ internalization in mES cells. Representative images from 4 independent immunofluorescence experiments and 2 independent EM studies are shown.

3.3.4. More clathrin is recruited to Cx43 in EGF induced GJ-endocytosis

As described above (in chapter 2), cells utilize the clathrin endocytic mechinery to internalize their GJs (Baker et al., 2008; Fong et al., 2013; Gumpert et al., 2008; Piehl et al., 2007). Thus, the amount of clathrin that co-immunoprecipitates with Cx43 can be used as a direct measurement to quantify GJ endocytosis. We thus pre-treated mES cells in serum free media for one hour with PD98059 and/or chelerythrine-Cl (a PKC inhibitor), followed by treatment with EGF, and immunoprecipitation of Cx43 protein using magnetic beads. Untreated mES, and Mardin Darby canine kidney (MDCK) cells, known to not express endogenous Cx43 protein (Dukes et al., 2011) were included as controls. Fractions of the cell lysates were collected for input analyses of Cx43 phosphorylation, ERK1/2 activity, and protein loading (**Figure 18A**). Consistent with the results shown in Figure 16, Cx43 was highly phosphorylated at Ser262, Ser279/282, and Ser368 after 30 minutes post EGF treatment (**Figure 18A**, lanes

1 and 2). Note that the activity of the MAP kinase, ERK1/2, was significantly increased in EGF treated cells as indicated by the elevated levels of phosphorylated ERK that was detected with phospho-ERK-specific antibodies (**Figure 18A**, row 5, lane 2, 4). Also note that ERK1/2 activation/phosphorylation was effectively inhibited by PD98059 (**Figure 18A**, row 5, lane 3, 5). As a result and consistent with ERK1/2 inhibition, in PD98059 treated cells, Cx43 phosphorylation at Ser262 and Ser279/282 (known Cx43 MAPK target sites, (Warn-Cramer et al., 1996)) was inhibited (**Figure 18A**, rows 2 and 3, lanes 3 and 5). Likewise, in chelerythrine-Cl-treated cells a significant reduction of EGF-induced Ser368 phosphorylation (a known Cx43 PKC target site (Lampe et al., 2000)), was observed (**Figure 18A**, row 4, lanes 4, 5).

Proteins that co-precipitated with Cx43 under these experimental conditions were analyzed by Western blot using antibodies specific for clathrin heavy chain (CHC) (**Figure 18B**). The amount of CHC that co-immmunoprecipitated with Cx43 in EGF-treated mES cells was increased by 5.9 fold (± 1.4) when compared to untreated cells (**Figure 18B**, compare lanes 1, 2), strongly supporting our earlier finding that EGF induces GJ internalization in mES cells. Only slightly increased insignificant clathrin co-precipitation was observed in cells that were pre-incubated with PD98059 (2.7 fold ± 0.8; **Figure 18B**, lane 3), or PD98059 and chelerythrine-Cl combined (2.8 ± 0.8, **Figure 18B**, lane 5), consistent with efficient but not complete blockage of respective kinase activity in these drug-treated cells. Interestingly, when cells were pre-incubated with chelerythirne-Cl alone followed by EGF treatment, still a significant 4.9 fold

(± 1.3) increase in GJ internalization was observed (**Figure 18B**, lane 4). Thus, chelerythrine-Cl did not significantly inhibit EGF-induced GJ internalization, suggesting that PKC-mediated phosphorylation of Ser368 appears not to be sufficient to render Cx43-GJs internalization competent (see Discussion in section 3.4). No Cx43 or clathrin was immunoprecipiated in MDCK negative control cells (**Figure 18A, B**, lanes 6).

Taken together, our data (summarized in **Figure 19**) suggest that EGF induces activation of the MAPK signaling cascade (including MEK and ERK1/2), and of PKC to phosphorylate Cx43 at Ser262, Ser279/282, and Ser368. These specific phosphorylation events render Cx43 subunits in GJs clathrin-binding competent to initiate the endocytosis of GJs in mES cells. Inhibiting ERK1/2 activation by treating cells with PD98059 inhibits Cx43 phosphorylation and in consequence GJ internalization.

3.4. Discussion

EGF-mediated inhibition of GJIC in mES cells has been observed by Park and colleagues (Park et al., 2008). However, no molecular mechanisms explaining this observation have been reported. In WB-F344 and T51B rat liver epithelial cells, EGF-induced inhibition of GJIC mediated by MAPK has been described (Abdelmohsen et al., 2007; Kanemitsu and Lau, 1993). In principle, down-regulation of GJIC can be achieved by either GJ channel closure, or GJ endocytosis. Leithe and Rivedal reported evidence to suggests that by treating IAR20 rat liver epithelial cells in hypertonic medium, EGF-induced

internalization of Cx43-GJs may be mediated by a clathrin-driven endocytic process (Leithe and Rivedal, 2004). However, again detailed molecular signals that may be involved in this process have not been elucidated. In order to better understand the mechanism of EGF-induced GJIC-inhibition in mES cells, we examined specific serine residues located in the known regulatory Cx43 C-terminus that respond to EGF treatment. Implementing phospho-specific antibodies and kinase inhibitors, we uncovered that activation of ERK1/2 (MAPK signaling pathway) by EGF is required for Cx43 phosphorylation at Ser262 and Ser279/282, whereas PKC activation is responsible for Ser368 phosphorylation (**Figure 19**). Recently, Johnson et al., reported that mutations in Ser279/282 phosphorylation leads to GJ internalization deficiency in pancreatic cancer cells (Johnson et al., 2013a). Consistent with their findings, our data demonstrate that ERK1/2-mediated phosphorylation of Cx43 on Ser279/Ser282 is required for GJ internalization in mES cells. Interestingly, we did not find a significant increase in Ser255 phosphorylation (another MAPK Cx43 target site) in EGF-treated ES cells, as this was described to occur in TPA-treated epithelial IAR20 cells (Sirnes et al., 2009). TPA is a DAG-analog that is known to activate both MAPK and PKC signaling pathways and to hyper-phosphorylate and hyper-ubiquitinate Cx43 (Fykerud et al., 2012; Sirnes et al., 2009). This might be due to different experimental conditions (e.g. EGF versus TPA specificity) or might be cell type specific (mES versus rat liver epithelial cells). In addition, besides its known cell-proliferative activity, EGF might have significant yet to be characterized additional effects on mES cells that require cellular uncoupling as well as GJ

internalization (e.g. ES cell differentiation, migration, or channel-independent Cx43 signaling). In addition, our results show that EGF-receptor activation in mES cells also stimulates PKC to phosphorylate Cx43 at Ser368. However, inhibiting PKC-activation alone (by chelerythrine-Cl treatment) did not appear sufficient to inhibit EGF-induced GJ internalization, suggesting that activation of ERK1/2 (and the MAPK signaling cascade) may be more critical for EGF-induced GJ endocytosis than activation of PKC. Further studies are required to fully understand a likely crosstalk between PKC and MAPK activation pathways in regulating GJIC and GJ internalization. Although in our study the exact order of Cx43 serine phosphorylation events that occur in mES cells in response to EGF-treatment could not be determined, we provide compelling evidence that suggests that EGF activates both the MAPK signaling pathway and PKC to inhibit GJIC and induce GJ internalization. We used PD98059, a MEK inhibitor, and monitored corresponding activation (phosphorylation) of ERK1/2 (upstream and downstream kinases of the MAPK signaling cascade) to inhibit EGF-induced GJIC.

Activation of kinase signaling in ES cells to regulate self-renewal and proliferation while maintaining pluripotency is a complex matter. In recent years, the role of GJIC in mouse and human ES cell maintenance and differentiation, as well as its potential role in the reprogramming and differentiation of induced pluripotent stem (iPS) cells has attracted increasing attention. For example, it has been shown that GJIC is required for ES cells to maintain their pluripotent state (Todorova et al., 2008). In addition, Cx43 expression has recently been found to

be important for the generation of iPS cells (Ke et al., 2013). In 2008, Buehr et al., defined specific rat ES cell culture conditions that capture their authentic ES cell phenotype by using pharmacological inhibitors including MEK/ERK inhibitors (Buehr et al., 2008). Their findings together with our own results presented here indicate that ES cells utilize the EGF pathway to regulate self-renewal and proliferation by controlling GJIC within the colonies. In this context, it is fascinating to comprehend how mES cells can rapidly endocytose their GJ channels to uncouple from their neighboring cells to undergo mitosis and/or to perform other functions, and then rapidly re-establish their GJs and GJIC to maintain pluripotency. A clear understanding of the molecular mechanisms that lead to growth factor-induced inhibition of GJIC and GJ endocytosis are therefore of eminent importance.

3.5. Materials and Methods

3.5.1. Cell culture

E14TG2a mouse embryonic stem (mES) cells (ATCC, Cat. No. CRL-1821) were thawed and seeded on mouse embryonic fibroblasts (MEFs) (Millipore, Cat. No. PMEF-NL). Cells were passaged and maintained in 0.1% gelatin-coated dishes (MEF-free) in humidified atmosphere containing 5% CO_2 at 37°C in KO DMEM (Gibco, Cat. No. 10829). Media were supplemented to a final concentration of 15% with KO serum replacement (Gibco, Cat. No. 10828), 3mM L-glutamine (Gibco, Cat. No. 25030 stock 200mM), 50 I.U/ml penicillin and 50μg/ml streptomycin (Gibco, Cat. No. 15070), 1mM sodium pyvurate (Gibco,

Cat. No. 11360 stock 100mM), 1x non-essential amino acids (Millipore, Cat. No. TMS-001-C), 1x β-mercaptoethanol (Millipore, Cat. No. ES-007-E), and 1000 U/ml ESGRO mLIF (Millpore, Cat. No. ESG1106, stock 10^6U/ml) to prevent cells from differentiating. Prior to EGF treatment, media were replaced with serum free media (to starve cells of growth factors) supplemented either with 50μM PD98059 (MEK inhibitor; Sigma, Cat. No. P215), 500nM chelerythrine-Cl (PKC inhibitor; Cayman Chemical, Cat. No. 11314), or both for 1 hour and cultured under standard conditions.

3.5.2. Dye transfer assays

mES cells were cultured in 3.5 cm dishes for 2 days, then pre-incubated with serum free media as described above. Cells were treated with 100ng/ml of EGF (Sigma, Cat. No. E4127) in serum free media and cultured for 30 minutes. Media were replaced with 0.1% Lucifer Yellow (LY; Invitrogen, Cat. No. L682) in OPTIMEM (Gibco, Cat. No. 31985). mES cell colonies were cut with a sharp scalpel in the presence of LY. Cells were incubated at room temperature (RT) for 2 minutes to allow dye to transfer to neighboring cells, then were washed 3 times with OPTIMEM followed by 3.7% paraformaldehyde fixation for 10 minutes. Paraformaldehyde was removed by washing 3 times with 1xPBS containing Ca^{2+} and Mg^{2+}. Fluorescence images were acquired using a 20x objective. Dye spreading from the injured cells to the farthermost receiving cells was measured using MetaVue software version 6.1r5 (Molecular Devices, Sunnyvale, CA), averaged and plotted.

3.5.3. Immunofluorescence microscopy and image analyses

mES cell colonies were grown on glass cover slips pre-treated with 0.1% gelatin (Fisher Scientific, Cat. No. G-7); fixed and permeabilized in pure ice-cold ethanol for 10 minutes; blocked with 10% FBS in PBS at RT for 1 hour, and incubated with primary rabbit polyclonal anti-Cx43 antibodies (Cell Signaling Technology, Cat. No. 3512) at 1:500 dilution at 4°C overnight. Secondary antibodies (Alexa488-conjugated goat anti-rabbit, Molecular Probes/Invitrogen, Cat. No. A11008) were used at 1:500 dilution at room temperature for 1 hour. Plasma membranes were stained using 1 μg/ml of Alexa594-conjugated wheat germ agglutinin (WGA; Molecular Probe/Invitrogen, Cat. No. W11262). Cell nuclei were stained with 1μg/ml DAPI. Cells were mounted using Fluoromount-G™ (SouthernBiotech, Cat. No. 0100-01). Wide-field fluorescence microscopy was performed on a Nikon Eclipse TE 2000E inverted fluorescence microscope equipped with a 40x, NA 1.4, Plan Apochromat oil immersion objective. Images were acquired using MetaVue software version 6.1r5, Quantitative analyses were performed using ImageJ version 1.43u (National Institutes of Health, USA).

3.5.4. Electron microscopic analyses

mES cells were cultured under feeder-free conditions in 3.5 cm diameter dishes, then fixed with 2.5% glutaraldehyde (Sigma cat. No. G7651) in 0.1M sodium cacodylate buffer at RT for 2 hours. Cells were washed, treated with tannic acid, dehydrated, uranyl acetate-stained and flat-embedded in the dishes as

described in Falk (2000). Embedded cells were mounted, trimmed, thin-sectioned and examined with a Phillips CM100 electron microscope.

3.5.5. Western blot analyses

Denatured protein samples derived from mES cell lysates were analyzed on 10% SDS-PAGE mini-gels (BioRad). Biotinylated protein ladder (Cell Signaling Technology, Cat. No. 7727S) was used as a molecular weight marker. Proteins were transferred onto nitrocellulose membranes (Whatman, Cat. No. 10439396) on ice at 120 V for 1 hour before blocking with 5% non-fat dry milk, or 5% BSA in TBST at RT for 1 hour. Membranes were then incubated with primary antibodies at 4°C overnight. Antibodies used were: rabbit anti-Cx43 (Cell Signaling Technology, Cat. No. 3512) at 1:2500 dilution, phospho-specific rabbit anti-Cx43 Ser255 (Santa Cruz, Cat. No. sc-12899-R), phospho-specific rabbit anti-Cx43 Ser262 (Santa Cruz, Cat. No. sc-17219-R) both at 1:500, phospho-specific rabbit anti-Cx43 Ser279/282 (Solan and Lampe, 2007) at 1:1000, phospho-specific rabbit anti-Cx43 Ser368 (Cell Signaling Technology, Cat No. 3511) at 1:2000, phospho-ERK1/2 (Cell Signaling Technology Cat. No. 9102) at 1:3000, mouse anti-clathrin heavy chain (BD Transduction Laboratories, Cat. No. 610499), at 1:2000 dilution, and mouse anti-α-tubulin (Sigma, Cat. No. T9026) at 1:5000 dilution. Membranes were washed 3 times with TBST followed by incubation with HRP-conjugated secondary antibodies (Zymed Laboratories, Cat. No. 81-6520 or 81-6120) at 1:10,000 dilution at RT for 1 hour. Proteins were

detected with enhanced chemiluminescent (ECL) reagent. NIH ImageJ software was used to quantify intensity of protein bands.

3.5.6. Co-immunoprecipitation assays

mES cells were lysed with 1x SDS-free RIPA buffer (Cell Signaling Technology, Cat. No. 9806) supplemented with protease and phosphatase inhibitor cocktail (Cell Signaling Technology, Cat. No. 5872). Supernatants were incubated with rabbit anti-Cx43 antibodies (Cell Signaling Technology, Cat. No. 3512) bound to protein-G magnetic beads (Dynabeads®, Invitrogen, Cat. No.10003) at 4°C overnight or at RT for 2 hours. Beads were washed 3 times with 1x TBS. Cx43 and bound proteins were eluted from the beads using hot SDS-PAGE sample buffer containing 50 mM DTT. Samples were analyzed by Western blot as described above.

3.5.7. Statistical analyses

Unpaired student t-tests were performed to analyze the distance of dye transfer (GraphPad Software, Inc., La Jolla, CA). ANOVA with Dunnett's post-hoc tests were used to compare the levels of serine phosphorylation in Cx43, and the amount of co-precipitated clathrin heavy chains. Data are presented as mean ± SEM. In all analyses, a p-value ≤ 0.05 (depicted with *, **, or ***) was considered statistically significant.

3.6. Figures

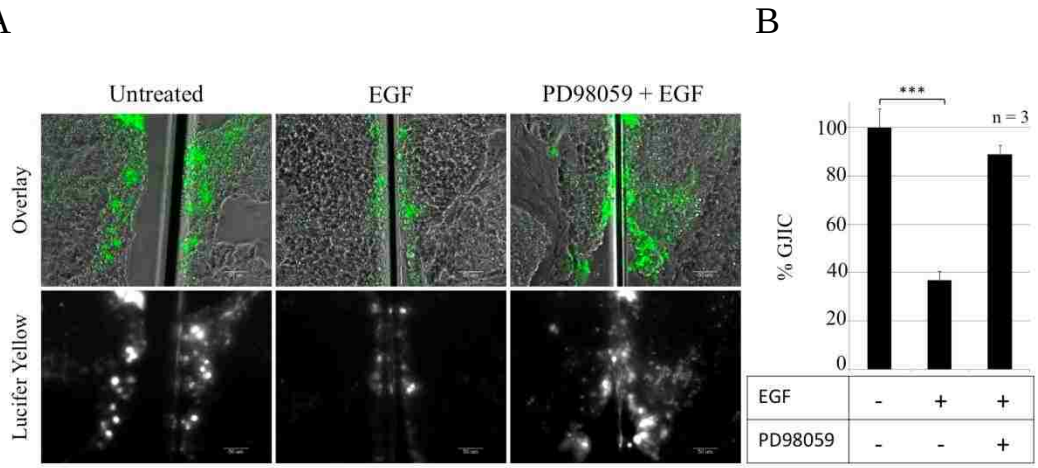

Figure 15: EGF inhibits GJIC in mES cells. mES cell colonies were treated with EGF in the presence or absence of the MEK-inhibitor PD98059 followed by Lucifer yellow (LY) scrape loading dye transfer assays. Representative images (phase contrast and fluorescence overlays on the top, LY-fluorescence alone at the bottom) of three independent experiments are shown in (A), quantitative analyses of dye transfer (representative of GJIC) are shown in (B). EGF-treatment reduced GJIC to 37% (n = 30, SEM ± 4, $p<0.0001$), while PD98059 counteracted the inhibitory EGF effect and GJIC remained at 89% (n = 36, SEM ± 4).

A

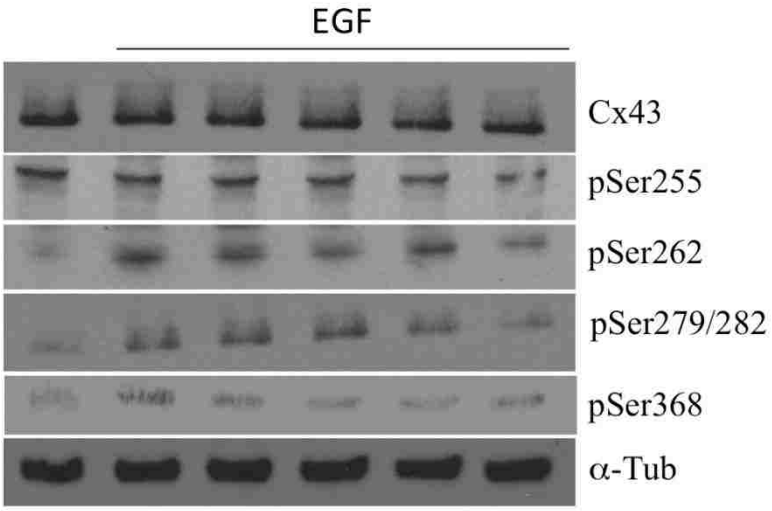

B

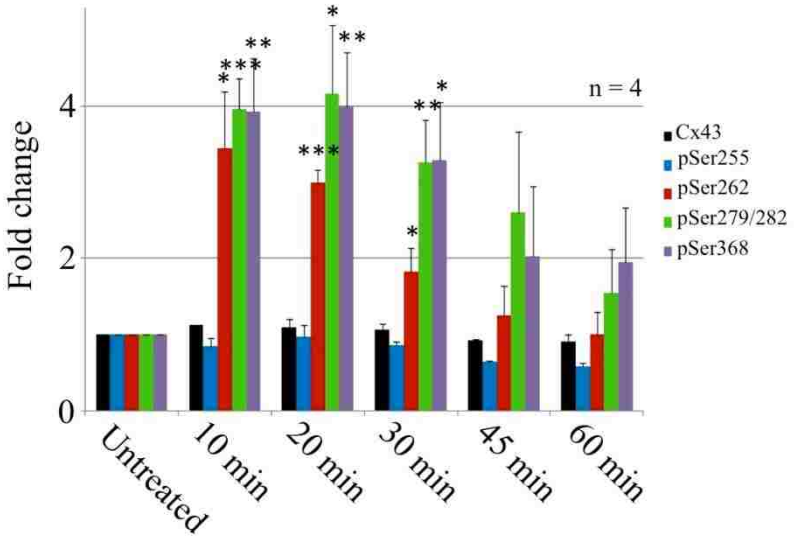

Figure 16: EGF activates MAPK and PKC signaling cascades to phosphorylate Cx43 at serine residues 262, 279/282, and 368. mES cells were treated with EGF before cell lysates were prepared at indicated times. Phosphorylated Cx43 was detected using phopho-specific antibodies directed against Ser255, Ser262, Ser279/282, and Ser368. Membranes were stripped and re-probed with anti α-

tubulin antibodies as a loading control. Representative blots of four independent experiments are shown in (A), normalized quantitative analyses of phosphorylated Cx43 are shown in (B). EGF induced a significant 4-fold increase of Cx43 phosphorylation at serines 262, 279/282 (MAPK sites), and 368 (PKC site), but not on Ser255 (another MAPK site). Phosphorylation peaked between 10-30 minutes after EGF treatment.

A

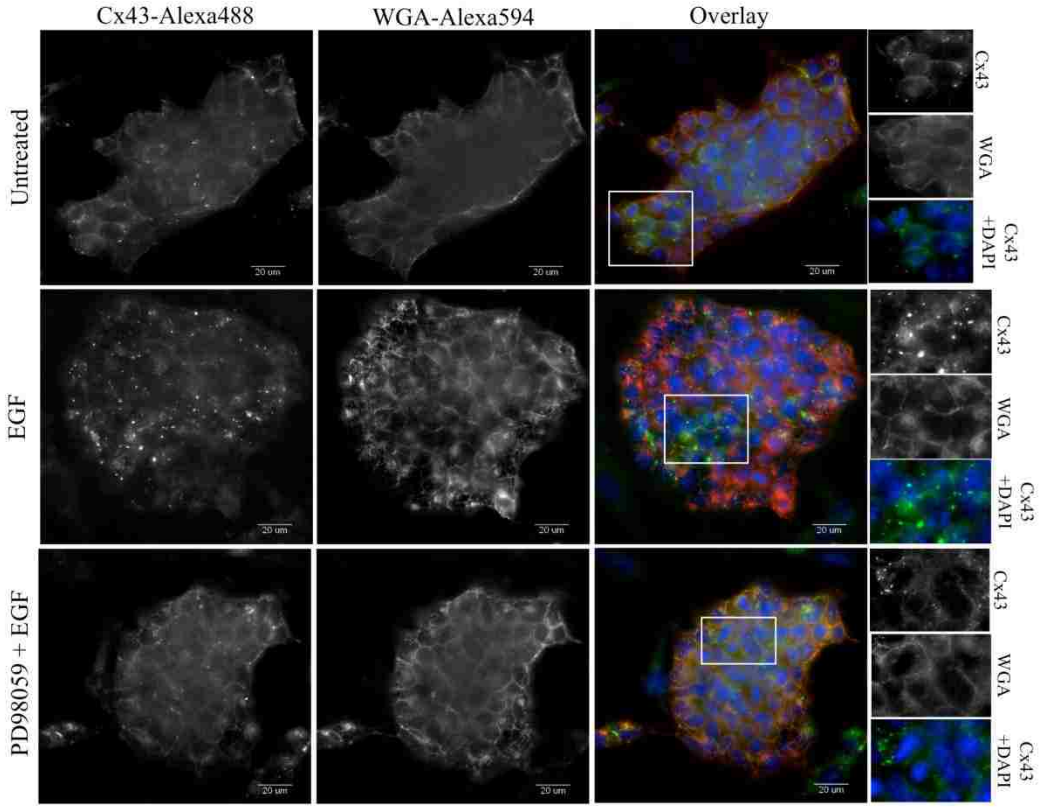

B

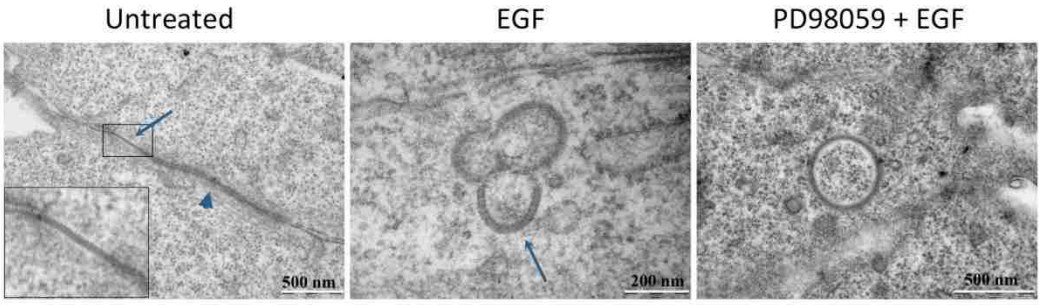

Figure 17: EGF induces GJ endocytosis in mES cells. Cell colonies grown on cover glasses were fixed and stained using antibodies specific for Cx43 (Alexa488-conjugated secondary antibodies, green). Alexa594–conjugated WGA (red) and DAPI (blue) were used to label PMs and cell nuclei, respectively. **(A)** Representative immunofluorescence micrographs from five independent

experiments are shown. Separate channels of boxed areas are shown on the right. An increased number of cytoplasmic fluorescent puncta -indicative of internalized AGJ vesicles- were observed in EGF treated cells (column 1, panel 2). **(B)** Transmission electron micrographs of treated and untreated mES cell colonies revealed typically appearing, double-membrane (penta-laminar striped) GJs and AGJs, supporting the conclusion that cytoplasmic puncta in (A) indeed are endocytosed GJs.

A

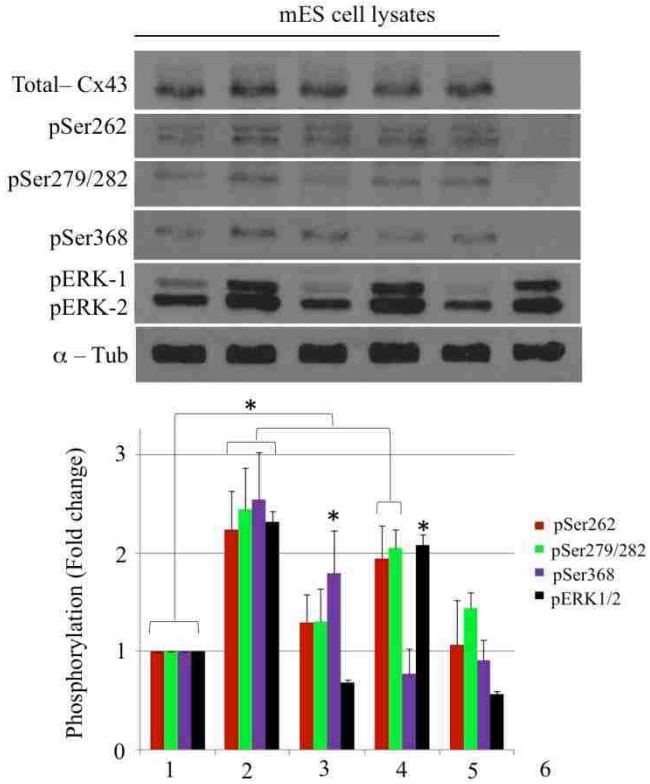
mES cell lysates
Total– Cx43
pSer262
pSer279/282
pSer368
pERK-1
pERK-2
α – Tub
Phosphorylation (Fold change)
0
1
2
3
1
2
3
4
5
6
*
*
*
pSer262
pSer279/282
pSer368
pERK1/2

B

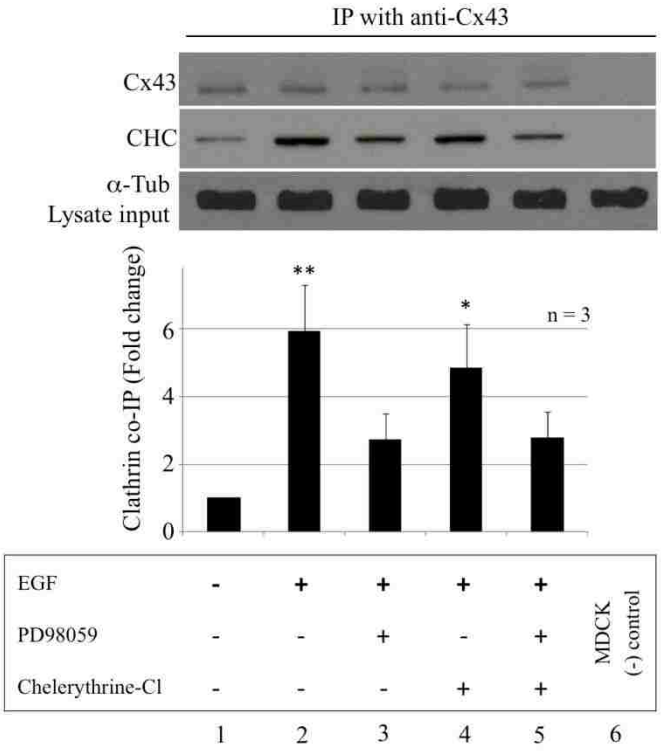
IP with anti-Cx43
Cx43
CHC
α-Tub
Lysate input
Clathrin co-IP (Fold change)
0
2
4
6
**
*
n = 3
EGF - + + + +
PD98059 - - + - +
Chelerythrine-Cl - - - + +
MDCK (-) control
1 2 3 4 5 6

Figure 18: Significantly increased amounts of clathrin, a direct indicator of GJ endocytosis, co-precipitates with Cx43 in EGF-treated mES cells. **(A)** Western blot analyses of EGF-treated cell lysates show increased activity of ERK (pERK1/2) and Cx43 phosphorylation at Ser262, Ser279/282, and Ser368 (lane 2). PD98059 inhibited phosphorylation of Ser262 and Ser279/282 (lane 3, 5), while chelerythrine-Cl (PKC inhibitor) inhibited phosphorylation of Ser368 (lanes 4, 5). Untreated mES cells and non-Cx43 expressing MDCK cells were analyzed in control (lanes 1, 6). **(B)** Cx43 from lysates in (A) were immuno-precipitated, and co-precipitated clathrin (CHC) was detected by Western blot analyses and quantified. Cx43 from EGF treated cells co-precipitated 5.9 fold ($n = 3$, SEM ± 1.5, $p < 0.01$) more clathrin than in untreated control cells (lanes 1, 2). PD98059 counteracted EGF-induced GJ internalization by inhibiting ERK1/2 (lanes 3, 5). Moderately increased levels of clathrin (4.9 fold, $n=3$, SEM $\pm$ 1.3, $p < 0.05$) co-precipitated in cells treated with chelerythrine-Cl alone (lane 4). No Cx43 or CHC was precipitated in MDCK control cells.

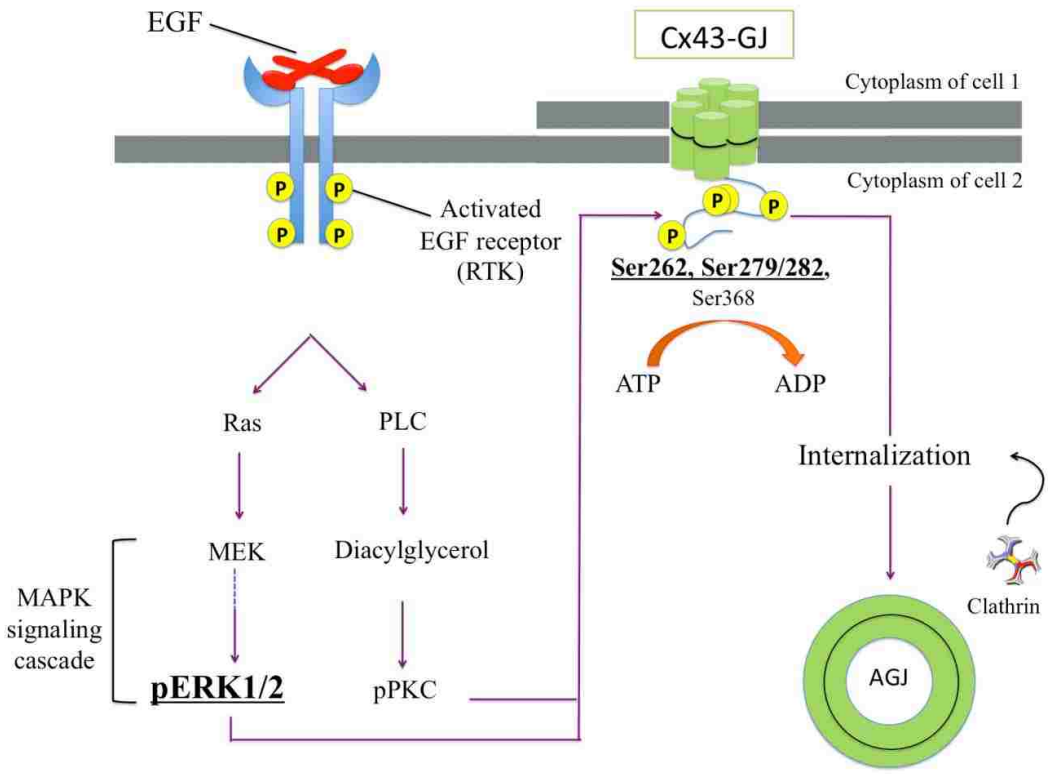

Figure 19: Schematic representation illustrating EGF-induced, MAPK/PKC-mediated GJ internalization in mES cells. EGF binds to and activates its receptor (a RTK) in the PM of cells. Active EGF-receptor activates MAPK and PKC signaling cascades to phosphorylate Cx43 at Ser262, Ser279/282, and Ser368. Phosphorylated-Cx43 recruits clathrin and clathrin-adaptors to endocytose GJs.

Chapter 4:

Conclusions and future perspectives

In chapter 2 of this dissertation, I have described that two AP-2 binding sites (S2 and S3) in the Cx43 C-terminus work cooperatively to mediate GJ internalization. In addition to Cx43 phosphorylation occurring in the C-terminal domain (described in chapter 3), other post-translational modifications that render the Cx43 C-terminus to become accessible to AP-2 may exist, such as ubiquitination, sumoylation, or acylation (palmitoylation, myristoylation). Palmitoylation is the addition of palmitate to a cysteine residue of a protein either through thioester linkage (S-palmitoylation) or amide linkage (N-palmitoylation). Protein palmitoylation (a reversible modification) has been shown to facilitate membrane interaction, trafficking, and protein-protein interaction (reviewed in (Smotrys and Linder, 2004)). Recently, two YXXΦ motifs similar to the ones we identified in the C-terminus of Cx43 were identified in the C-terminus of the G-protein coupled receptor, PAR1 (Protease-activated Receptor-1). Canto and Trejo reported that palmitoylation of the cysteine residue in the YSILC**C** motif (the proximal YXXΦ motif in the PAR1 C-terminus) is the negative regulation factor for AP-2 binding (Canto and Trejo, 2013). Cells that express a palmitoylation-deficient PAR1 mutant (CC/AA) exhibit a marked increase in internalization and lysosomal degradation. It is possible that the S2 motif in Cx43 is also regulated by palmitoylation, or by other forms of acylation such as myristoylation. There is no well-defined consensus sequence for palmitoylation other than the presence of

cysteine residues. The tyrosine-based sorting motif S2 in Cx43 also harbors a juxtaposed cysteine residue, which is situated two residues away from the YXXΦ motif (Y^{265}AYFNG**C)**. It is quite likely that the availability of this S2 binding motif is regulated by palmitoylation. This could partially explain why the Mehta group did not detect interaction of AP-2 with Cx43 through the S2 motif using a yeast-two hybrid assay (Johnson et al., 2013a), because yeast may not be able to perform this post-translational modification, at least not on the short Cx43 segment that the group used as bait. Future analyses are required to investigate the possibility of Cx43 being an acylated protein, and whether acylation may regulate clathrin access and GJ internalization.

As described in chapter 2, when cells were transfected with the double mutants (S2+3), GJ plaques that formed among these cells exhibited a significant slower rate of turnover and eventually underwent apoptosis. However, occasionally these cells were still able to eliminate their GJ plaques after a prolonged period of time (**Figure 9**, and **supplemental movies in Fong et al., 2013**). These observations suggest a potential uncharacterized mechanism for cells to remove 'unwanted' GJ plaques. Based on our findings that S2+3 Cx43 mutants were unable to recruit AP-2 and clathrin, this pathway is likely clathrin independent. Recently, ubiquitination was described to be a signal for GJ internalization and degradation (Catarino et al., 2011; Girao et al., 2009). The proline-rich PY motif (XP^{283}PXY) in the Cx43 C-terminal domain was reported to interact with the ubiquitin ligase Nedd4, via its WW domains. Once ubiquitin is conjugated to Cx43, ubiquitinated Cx43 is recognized by Esp15 through its

ubiquitin-interacting motif, proposed to result in its (clathrin-independent) internalization. A shift from CME to clathrin independent endocytosis has been described for the EGF receptor when the concentration of the ligand, EGF is increased (Sigismund et al., 2005; Traub and Lukacs, 2007). In our live-cell recordings of the Cx43 S2+3 mutants, we infrequently observed events in which cells appeared to “expel” their GJ plaques in order to un-couple from each other. This alternative pathway that might be related to exocytosis, membrane-blebbing and the initiation of apoptosis remains to be elucidated.

In addition to AP-2 and Dab2, dyanamin2 (Dyn2) has been shown to be involved in GJ internalization (Gilleron et al., 2011; Gumpert et al., 2008; Piehl et al., 2007). Moreover, when Gumpert et al. knocked down Dyn2, a significant decrease in the number of AGJs and a significant increase in GJ plaques were observed (Gumpert et al., 2008). The known functions of the GTPase dynamin include membrane bending and pinching of the formed vesicle to release it from the PM (Schmid and Frolov, 2011). These internalized AGJs occasionally undergo fission to form smaller vesicles, but the molecular machinery needed for these fissions have not been described. Recently, dynamin has been reported to play a specific role in AGJ fission (Nickel et al., 2013). Inhibiting the functions of dynamin either by siRNA knock-down or pharmacological inhibition (using the drug dynasore) resulted in infrequently release of the GJ “buds” from the PM to form AGJs. In addition, a smaller number of AGJ vesicle fission per hour was observed. Alternative roles of Dyn2 remain to be explored.

Filamentous actin attached to cytoplasmic AGJs has been observed by electron-microscopic analyses by our group (Piehl et al., 2007) and before by others (Larsen et al., 1979). In addition, Piehl et al. also observed co-localization of the retrograde actin motor, myosin VI, internalizing GJ plaques and cytoplasmic AGJ vesicles. Overexpression of a dominant-negative myosin VI mutant significantly reduced mean AGJ movement velocity and maximum distance AGJs traveled from their site of origin (on the PM) to the site of degradation (peri-nuclear cytoplasm) (Piehl et al., 2007), suggesting a specific role of myosin VI in cellular translocation of AGJs. Myosin VI can interact with the C-terminal serine residue and proline-rich region of Dab2 via its C-terminal globular tail (Piehl et al., 2007). In chapter 2 of this dissertation, I have described the indirect interaction between Dab2 and Cx43 via AP-2 (Fong et al., 2013). Thus, it is feasible to speculate that Cx43 recruits AP-2 via its YXXΦ motifs to internalize GJ plaques, while Dab2 is recruited to GJ plaques by interacting with AP-2 to also recruit myosin VI for efficient transport of the formed AGJ vesicles to cellular degradation loci. Once AP-2/Dab2 and clathrin interactions are stabilized, dynamin is recruited to the clathrin coated pit to pinch off the “buds” from the PM to form AGJs. Overall, GJ internalization appears as a highly organized process in which –as in a symphony- each protein is recruited to the GJ plaque at exactly the right time and the right order to perform its role in the pathway. Clearly, cytoskeleton components play a role in the trafficking of the internalized AGJs to their targeted compartment in the cytoplasm. The signals that trigger actin remodeling in response to GJ internalization remain to be explored.

It has been shown that treatment of cells (epithelial, endothelial, embryonic stem cells, etc.) with mitogens, such as epidermal growth factor (EGF) and vascular endothelial growth factor (VEGF), or natural inflammatory mediators such as thrombin and endothelin results in a rapid and efficient inhibition of GJIC (Baker et al., 2008; Kevil et al., 1998; Park et al., 2008; Thuringer, 2004). Another intriguing finding in this dissertation work was that I identified the serine phosphorylation events (Ser262, Ser279/282, and Ser368) in the Cx43 C-terminal domain that play a crucial role in EGF-induced GJ internalization. EGF is a growth factor that is known to stimulate cell proliferation. In order to undergo mitosis, cells need to uncouple from their neighboring cells (Boassa et al., 2011). Thus all cell-cell junctions – including GJs – need to be removed from the PM. Inhibiting the MAPK cascade by using a pharmacological inhibitor resulted in inhibition of EGF-induced GJ internalization. Furthermore, we hypothesize that when cells are stimulated with EGF, the phosphorylation of these serine residues occurs in a sequential order. The phosphorylation of the first residue will cause a conformational change to the Cx43 C-terminal domain that leads to the phosphorylation of the next residue, and so on. However, the potential phosphorylation order of these serine residues is still under investigation. By mutagenesis, we can mutate these serine residues (Ser/Ala) individually, then analyze the potential defect on phosphorylation of the other residues. These analyses will allow us to map out the Cx43 phosphorylation sequence upon stimulation. Current data in our group indicate that Cx43 phosphorylation upon stimuli is the initial event that then trigger poly-

ubiquitination of Cx43 (Kells and Falk, unpublished data). We are also investigating internalization of other GJ Cxs GJ. Results from all these ongoing projects will provide a more comprehensive understanding of GJ turnover.

The cell signals involved in EGF-induced GJ internalization are described in chapter 3. I have demonstrated that treating mES cells with MAPK inhibitor (PD98059) allows GJIC among mES cells in the colony. Interestingly, GJIC among mES cells in the colony is required to maintain their non-differentiated and proliferative state (Ke et al., 2013; Todorova et al., 2008). Moreover, it has recently been shown that GJIC between ES cells and fibroblast feeder cells is not required to maintain their pluripotent state (Kim et al., 2013). Taken together, we provide insights into possible mechanisms of how ES cells may maintain their pluripotent state (without the need for a feeder layer) by simply enhancing GJIC among ES cells in the colonies, e.g. supplementing culture media with MEK inhibitor to maintain GJIC in ES cells. In addition to inhibiting the MAPK cascade, other GJIC enhancing pathways should be explored. This information is helpful in defining novel ES cell culture conditions to generate new ES cell lines (rat ES cells) or iPS cells which can be applied to regenerative medicine.

In conclusion, research presented in this dissertation provides evidence to elucidate and understand GJ internalization on the molecular level. The results in this dissertation are novel and have greatly contributed to GJ research to drive the field forward. I have identified two YXXΦ motifs in the Cx43 C-terminus that can interact with AP-2 to recruit clathrin and other clathrin-adaptor proteins (Dab2). These findings help to explain mechanistically, how cells can endocytose

such large plasma membrane structures that can be 50 times larger than typical endocytic clathrin-coated vesicles. Since the amount of PIP2 in GJ plaques is very limited two AP-2 binding sites on the Cx43 polypeptide are likely required to initiate AP-2 stabilization and clathrin coat formation to successfully endocytose GJs. Alternative mechanisms are also possible and are discussed in chapter 3. This work also identified specific serine phosphorylation events in the Cx43 C-terminus that are mediated by ERK1/2 (the MAPK signaling cascade) and PKC that lead to GJ internalization. PD98059 (a MEK inhibitor) inhibits the activation of ERK1/2 and also prevents Cx43 phosphorylation. As a result, EGF-induced GJ internalization is inhibited. Relevant findings of my work have been (and will be) published in three primary research articles and have contributed to three published review articles.

References

Abdelmohsen, K., E. Sauerbier, N. Ale-Agha, J. Beier, P. Walter, S. Galban, D. Stuhlmann, H. Sies, and L.O. Klotz. 2007. Epidermal growth factor- and stress-induced loss of gap junctional communication is mediated by ERK-1/ERK-2 but not ERK-5 in rat liver epithelial cells. *Biochem Biophys Res Commun*. 364:313-317.

Aguilar, R.C., and B. Wendland. 2005. Endocytosis of membrane receptors: two pathways are better than one. *Proc Natl Acad Sci U S A*. 102:2679-2680.

Baker, S.M., N. Kim, A.M. Gumpert, D. Segretain, and M.M. Falk. 2008. Acute internalization of gap junctions in vascular endothelial cells in response to inflammatory mediator-induced G-protein coupled receptor activation. *FEBS Lett*. 582:4039-4046.

Batra, N., R. Kar, and J.X. Jiang. 2012. Gap junctions and hemichannels in signal transmission, function and development of bone. *Biochim Biophys Acta*. 1818:1909-1918.

Beardslee, M.A., J.G. Laing, E.C. Beyer, and J.E. Saffitz. 1998. Rapid turnover of connexin43 in the adult rat heart. *Circ Res*. 83:629-635.

Bejarano, E., H. Girao, A. Yuste, B. Patel, C. Marques, D.C. Spray, P. Pereira, and A.M. Cuervo. 2012. Autophagy modulates dynamics of connexins at the plasma membrane in a ubiquitin-dependent manner. *Mol Biol Cell*. 23:2156-2169.

Benmerah, A., C. Lamaze, B. Begue, S.L. Schmid, A. Dautry-Varsat, and N. Cerf-Bensussan. 1998. AP-2/Eps15 interaction is required for receptor-mediated endocytosis. *J Cell Biol*. 140:1055-1062.

Berthoud, V.M., P.J. Minogue, J.G. Laing, and E.C. Beyer. 2004. Pathways for degradation of connexins and gap junctions. *Cardiovasc Res*. 62:256-267.

Boassa, D., J.L. Solan, A. Papas, P. Thornton, P.D. Lampe, and G.E. Sosinsky. 2011. Trafficking and recycling of the connexin43 gap junction protein during mitosis. *Traffic*. 11:1471-1486.

Bonifacino, J.S., and L.M. Traub. 2003. Signals for sorting of transmembrane proteins to endosomes and lysosomes. *Annu Rev Biochem*. 72:395-447.

Brink, P.R., V. Valiunas, C. Gordon, M.R. Rosen, and I.S. Cohen. 2012. Can gap junctions deliver? *Biochim Biophys Acta*. 1818:2076-2081.

Buehr, M., S. Meek, K. Blair, J. Yang, J. Ure, J. Silva, R. McLay, J. Hall, Q.L. Ying, and A. Smith. 2008. Capture of authentic embryonic stem cells from rat blastocysts. *Cell*. 135:1287-1298.

Canto, I., and J. Trejo. 2013. Palmitoylation of protease-activated receptor-1 regulates adaptor protein complex-2 and -3 interaction with tyrosine-based motifs and endocytic sorting. *J Biol Chem*. 288:15900-15912.

Carnarius, C., M. Kreir, M. Krick, C. Methfessel, V. Moehrle, O. Valerius, A. Bruggemann, C. Steinem, and N. Fertig. 2012. Green fluorescent protein changes the conductance of connexin 43 (Cx43) hemichannels reconstituted in planar lipid bilayers. *J Biol Chem*. 287:2877-2886.

Catarino, S., J.S. Ramalho, C. Marques, P. Pereira, and H. Girao. 2011. Ubiquitin-mediated internalization of connexin43 is independent of the canonical endocytic tyrosine-sorting signal. *Biochem J*. 437:255-267.

Chen, B., M.R. Dores, N. Grimsey, I. Canto, B.L. Barker, and J. Trejo. 2011. Adaptor protein complex-2 (AP-2) and epsin-1 mediate protease-activated receptor-1 internalization via phosphorylation- and ubiquitination-dependent sorting signals. *J Biol Chem*. 286:40760-40770.

Cocucci, E., F. Aguet, S. Boulant, and T. Kirchhausen. 2012. The first five seconds in the life of a clathrin-coated pit. *Cell*. 150:495-507.

Collins, B.M., A.J. McCoy, H.M. Kent, P.R. Evans, and D.J. Owen. 2002. Molecular architecture and functional model of the endocytic AP2 complex. *Cell*. 109:523-535.

De Sousa, P.A., G. Valdimarsson, B.J. Nicholson, and G.M. Kidder. 1993. Connexin trafficking and the control of gap junction assembly in mouse preimplantation embryos. *Development*. 117:1355-1367.

Dukes, J.D., P. Whitley, and A.D. Chalmers. 2011. The MDCK variety pack: choosing the right strain. *BMC Cell Biol*. 12:43.

Falk, M.M. 2000. Connexin-specific distribution within gap junctions revealed in living cells. *J Cell Sci*. 113 (Pt 22):4109-4120.

Falk, M.M., S.M. Baker, A.M. Gumpert, D. Segretain, and R.W. Buckheit, 3rd. 2009. Gap junction turnover is achieved by the internalization of small endocytic double-membrane vesicles. *Mol Biol Cell*. 20:3342-3352.

Falk, M.M., J.T. Fong, R.M. Kells, M.C. O'Laughlin, T.J. Kowal, and A.F. Thevenin. 2012. Degradation of endocytosed gap junctions by autophagosomal and endo-/lysosomal pathways: a perspective. *J Membr Biol*. 245:465-476.

Fallon, R.F., and D.A. Goodenough. 1981. Five-hour half-life of mouse liver gap-junction protein. *J Cell Biol*. 90:521-526.

Fong, J.T., R.M. Kells, and M.M. Falk. 2013. Two tyrosine-based sorting signals in the Cx43 C-terminus cooperate to mediate gap junction endocytosis. *Mol Biol Cell*. 24:2834-2848.

Fong, J.T., R.M. Kells, A.M. Gumpert, J.Y. Marzillier, M.W. Davidson, and M.M. Falk. 2012. Internalized gap junctions are degraded by autophagy. *Autophagy*. 8:794-811.

Fontes, M.S., T.A. van Veen, J.M. de Bakker, and H.V. van Rijen. 2012. Functional consequences of abnormal Cx43 expression in the heart. *Biochim Biophys Acta*. 1818:2020-2029.

Fykerud, T.A., A. Kjenseth, K.O. Schink, S. Sirnes, J. Bruun, Y. Omori, A. Brech, E. Rivedal, and E. Leithe. 2012. Smad ubiquitination regulatory factor-2 controls gap junction intercellular communication by modulating endocytosis and degradation of connexin43. *J Cell Sci*. 125:3966-3976.

Gaietta, G., T.J. Deerinck, S.R. Adams, J. Bouwer, O. Tour, D.W. Laird, G.E. Sosinsky, R.Y. Tsien, and M.H. Ellisman. 2002. Multicolor and electron microscopic imaging of connexin trafficking. *Science*. 296:503-507.

Ghoshroy, S., D.A. Goodenough, and G.E. Sosinsky. 1995. Preparation, characterization, and structure of half gap junctional layers split with urea and EGTA. *J Membr Biol*. 146:15-28.

Gilleron, J., D. Carette, C. Fiorini, J. Dompierre, E. Macia, J.P. Denizot, D. Segretain, and G. Pointis. 2011. The large GTPase dynamin2: a new player in connexin 43 gap junction endocytosis, recycling and degradation. *Int J Biochem Cell Biol*. 43:1208-1217.

Gilleron, J., C. Fiorini, D. Carette, C. Avondet, M.M. Falk, D. Segretain, and G. Pointis. 2008. Molecular reorganization of Cx43, Zo-1 and Src complexes during the endocytosis of gap junction plaques in response to a non-genomic carcinogen. *J Cell Sci*. 121:4069-4078.

Girao, H., S. Catarino, and P. Pereira. 2009. Eps15 interacts with ubiquitinated Cx43 and mediates its internalization. *Exp Cell Res*. 315:3587-3597.

Gong, X., E. Li, G. Klier, Q. Huang, Y. Wu, H. Lei, N.M. Kumar, J. Horwitz, and N.B. Gilula. 1997. Disruption of alpha3 connexin gene leads to proteolysis and cataractogenesis in mice. *Cell*. 91:833-843.

Goodenough, D.A., and N.B. Gilula. 1974. The splitting of hepatocyte gap junctions and zonulae occludentes with hypertonic disaccharides. *J Cell Biol*. 61:575-590.

Govindarajan, R., S. Chakraborty, K.E. Johnson, M.M. Falk, M.J. Wheelock, K.R. Johnson, and P.P. Mehta. 2010. Assembly of connexin43 into gap junctions is regulated differentially by E-cadherin and N-cadherin in rat liver epithelial cells. *Mol Biol Cell*. 21:4089-4107.

Gullberg M., G.C., and Fredriksson S. 2011. Duolink-"In-cell Co-IP" for visualization of protein interactions in situ. *Nature Methods*. 8.

Gumpert, A.M., J.S. Varco, S.M. Baker, M. Piehl, and M.M. Falk. 2008. Double-membrane gap junction internalization requires the clathrin-mediated endocytic machinery. *FEBS Lett*. 582:2887-2892.

Helms, J.B., and C. Zurzolo. 2004. Lipids as targeting signals: lipid rafts and intracellular trafficking. *Traffic*. 5:247-254.

Hesketh, G.G., M.H. Shah, V.L. Halperin, C.A. Cooke, F.G. Akar, T.E. Yen, D.A. Kass, C.E. Machamer, J.E. Van Eyk, and G.F. Tomaselli. 2010. Ultrastructure and regulation of lateralized connexin43 in the failing heart. *Circ Res*. 106:1153-1163.

Higuchi, R., B. Krummel, and R.K. Saiki. 1988. A general method of in vitro preparation and specific mutagenesis of DNA fragments: study of protein and DNA interactions. *Nucleic Acids Res*. 16:7351-7367.

Houghton, F.D. 2005. Role of gap junctions during early embryo development. *Reproduction*. 129:129-135.

Huettner, J.E., A. Lu, Y. Qu, Y. Wu, M. Kim, and J.W. McDonald. 2006. Gap junctions and connexon hemichannels in human embryonic stem cells. *Stem Cells*. 24:1654-1667.

Hunter, A.W., R.J. Barker, C. Zhu, and R.G. Gourdie. 2005. Zonula occludens-1 alters connexin43 gap junction size and organization by influencing channel accretion. *Mol Biol Cell*. 16:5686-5698.

Hunter, A.W., J. Jourdan, and R.G. Gourdie. 2003. Fusion of GFP to the carboxyl terminus of connexin43 increases gap junction size in HeLa cells. *Cell Commun Adhes*. 10:211-214.

Johnson, K.E., S. Mitra, P. Katoch, L.S. Kelsey, K.R. Johnson, and P.P. Mehta. 2013a. Phosphorylation on Ser-279 and Ser-282 of connexin43 regulates endocytosis and gap junction assembly in pancreatic cancer cells. *Mol Biol Cell*. 24:715-733.

Johnson, K.E., S. Mitra, P. Katoch, L.S. Kelsey, K.R. Johnson, and P.P. Mehta. 2013b. Phosphorylation on Serines 279 and 282 of Connexin43 Regulates Endocytosis and Gap Junction Assembly in Pancreatic Cancer Cells. *Mol Biol Cell*.

Jordan, K., R. Chodock, A.R. Hand, and D.W. Laird. 2001. The origin of annular junctions: a mechanism of gap junction internalization. *J Cell Sci*. 114:763-773.

Kanemitsu, M.Y., and A.F. Lau. 1993. Epidermal growth factor stimulates the disruption of gap junctional communication and connexin43 phosphorylation independent of 12-0-tetradecanoylphorbol 13-acetate-sensitive protein kinase C: the possible involvement of mitogen-activated protein kinase. *Mol Biol Cell*. 4:837-848.

Katakowski, M., B. Buller, X. Wang, T. Rogers, and M. Chopp. 2010. Functional microRNA is transferred between glioma cells. *Cancer Res*. 70:8259-8263.

Ke, Q., L. Li, B. Cai, C. Liu, Y. Yang, Y. Gao, W. Huang, X. Yuan, T. Wang, Q. Zhang, A.L. Harris, L. Tao, and A.P. Xiang. 2013. Connexin 43 is involved in the generation of human induced pluripotent stem cells. *Hum Mol Genet*. 22:2221-2233.

Kenneson, A., K. Van Naarden Braun, and C. Boyle. 2002. GJB2 (connexin 26) variants and nonsyndromic sensorineural hearing loss: a HuGE review. *Genet Med*. 4:258-274.

Kevil, C.G., D.K. Payne, E. Mire, and J.S. Alexander. 1998. Vascular permeability factor/vascular endothelial cell growth factor-mediated permeability occurs through disorganization of endothelial junctional proteins. *J Biol Chem*. 273:15099-15103.

Keyel, P.A., S.K. Mishra, R. Roth, J.E. Heuser, S.C. Watkins, and L.M. Traub. 2006. A single common portal for clathrin-mediated endocytosis of distinct cargo governed by cargo-selective adaptors. *Mol Biol Cell*. 17:4300-4317.

Kim, J.S., D. Kwon, S.T. Hwang, D.R. Lee, S.H. Shim, H.C. Kim, H. Park, W. Kim, M.K. Han, and S.H. Lee. 2013. hESC Expansion and Stemness Are Independent of Connexin Forty-Three-Mediated Intercellular Communication between hESCs and hASC Feeder Cells. *PloS one*. 8:e69175.

Laing, J.G., and E.C. Beyer. 1995. The gap junction protein connexin43 is degraded via the ubiquitin proteasome pathway. *J Biol Chem*. 270:26399-26403.

Laing, J.G., P.N. Tadros, E.M. Westphale, and E.C. Beyer. 1997. Degradation of connexin43 gap junctions involves both the proteasome and the lysosome. *Exp Cell Res*. 236:482-492.

Lampe, P.D., W.E. Kurata, B.J. Warn-Cramer, and A.F. Lau. 1998. Formation of a distinct connexin43 phosphoisoform in mitotic cells is dependent upon p34cdc2 kinase. *J Cell Sci*. 111 (Pt 6):833-841.

Lampe, P.D., and A.F. Lau. 2000. Regulation of gap junctions by phosphorylation of connexins. *Arch Biochem Biophys*. 384:205-215.

Lampe, P.D., E.M. TenBroek, J.M. Burt, W.E. Kurata, R.G. Johnson, and A.F. Lau. 2000. Phosphorylation of connexin43 on serine368 by protein kinase C regulates gap junctional communication. *J Cell Biol*. 149:1503-1512.

Larsen, W.J., H.N. Tung, S.A. Murray, and C.A. Swenson. 1979. Evidence for the participation of actin microfilaments and bristle coats in the internalization of gap junction membrane. *J Cell Biol*. 83:576-587.

Lauf, U., B.N. Giepmans, P. Lopez, S. Braconnot, S.C. Chen, and M.M. Falk. 2002. Dynamic trafficking and delivery of connexons to the plasma membrane and accretion to gap junctions in living cells. *Proc Natl Acad Sci U S A*. 99:10446-10451.

Lee, M.J., I. Nelson, H. Houlden, M.G. Sweeney, D. Hilton-Jones, J. Blake, N.W. Wood, and M.M. Reilly. 2002. Six novel connexin32 (GJB1) mutations in X-linked Charcot-Marie-Tooth disease. *J Neurol Neurosurg Psychiatry*. 73:304-306.

Leithe, E., A. Kjenseth, S. Sirnes, H. Stenmark, A. Brech, and E. Rivedal. 2009. Ubiquitylation of the gap junction protein connexin-43 signals its trafficking from early endosomes to lysosomes in a process mediated by Hrs and Tsg101. *J Cell Sci*. 122:3883-3893.

Leithe, E., and E. Rivedal. 2004. Epidermal growth factor regulates ubiquitination, internalization and proteasome-dependent degradation of connexin43. *J Cell Sci*. 117:1211-1220.

Leykauf, K., M. Salek, J. Bomke, M. Frech, W.D. Lehmann, M. Durst, and A. Alonso. 2006. Ubiquitin protein ligase Nedd4 binds to connexin43 by a phosphorylation-modulated process. *J Cell Sci*. 119:3634-3642.

Lichtenstein, A., P.J. Minogue, E.C. Beyer, and V.M. Berthoud. 2011. Autophagy: a pathway that contributes to connexin degradation. *J Cell Sci*. 124:910-920.

Lin, D., J. Zhou, P.S. Zelenka, and D.J. Takemoto. 2003. Protein kinase Cgamma regulation of gap junction activity through caveolin-1-containing lipid rafts. *Invest Ophthalmol Vis Sci*. 44:5259-5268.

Lo, C.W., and N.B. Gilula. 1979. Gap junctional communication in the preimplantation mouse embryo. *Cell*. 18:399-409.

Mishra, S.K., P.A. Keyel, M.J. Hawryluk, N.R. Agostinelli, S.C. Watkins, and L.M. Traub. 2002. Disabled-2 exhibits the properties of a cargo-selective endocytic clathrin adaptor. *EMBO J*. 21:4915-4926.

Moore, C.A., S.K. Milano, and J.L. Benovic. 2007. Regulation of receptor trafficking by GRKs and arrestins. *Annu Rev Physiol*. 69:451-482.

Morell, R.J., H.J. Kim, L.J. Hood, L. Goforth, K. Friderici, R. Fisher, G. Van Camp, C.I. Berlin, C. Oddoux, H. Ostrer, B. Keats, and T.B. Friedman. 1998. Mutations in the connexin 26 gene (GJB2) among Ashkenazi Jews with nonsyndromic recessive deafness. *N Engl J Med*. 339:1500-1505.

Morris, S.M., and J.A. Cooper. 2001. Disabled-2 colocalizes with the LDLR in clathrin-coated pits and interacts with AP-2. *Traffic*. 2:111-123.

Motley, A., N.A. Bright, M.N. Seaman, and M.S. Robinson. 2003. Clathrin-mediated endocytosis in AP-2-depleted cells. *J Cell Biol*. 162:909-918.

Musil, L.S., A.C. Le, J.K. VanSlyke, and L.M. Roberts. 2000. Regulation of connexin degradation as a mechanism to increase gap junction assembly and function. *J Biol Chem*. 275:25207-25215.

Nagy, J.I., F.E. Dudek, and J.E. Rash. 2004. Update on connexins and gap junctions in neurons and glia in the mammalian nervous system. *Brain research. Brain research reviews*. 47:191-215.

Nanes, B.A., C. Chiasson-MacKenzie, A.M. Lowery, N. Ishiyama, V. Faundez, M. Ikura, P.A. Vincent, and A.P. Kowalczyk. 2012. p120-catenin binding masks an endocytic signal conserved in classical cadherins. *J Cell Biol*. 199:365-380.

Nickel, B., M. Boller, K. Schneider, T. Shakespeare, V. Gay, and S.A. Murray. 2013. Visualizing the effect of dynamin inhibition on annular gap vesicle formation and fission. *J Cell Sci*. 126:2607-2616.

Ohno, H., J. Stewart, M.C. Fournier, H. Bosshart, I. Rhee, S. Miyatake, T. Saito, A. Gallusser, T. Kirchhausen, and J.S. Bonifacino. 1995. Interaction of tyrosine-based sorting signals with clathrin-associated proteins. *Science*. 269:1872-1875.

Park, J.H., M.Y. Lee, J.S. Heo, and H.J. Han. 2008. A potential role of connexin 43 in epidermal growth factor-induced proliferation of mouse embryonic stem cells: involvement of Ca2+/PKC, p44/42 and p38 MAPKs pathways. *Cell Prolif*. 41:786-802.

Pauly, B.S., and D.G. Drubin. 2007. Clathrin: an amazing multifunctional dreamcoat? *Cell Host Microbe*. 2:288-290.

Piehl, M., C. Lehmann, A. Gumpert, J.P. Denizot, D. Segretain, and M.M. Falk. 2007. Internalization of large double-membrane intercellular vesicles by a clathrin-dependent endocytic process. *Mol Biol Cell*. 18:337-347.

Postma, F.R., T. Hengeveld, J. Alblas, B.N. Giepmans, G.C. Zondag, K. Jalink, and W.H. Moolenaar. 1998. Acute loss of cell-cell communication caused by G protein-coupled receptors: a critical role for c-Src. *J Cell Biol*. 140:1199-1209.

Qin, H., Q. Shao, S.A. Igdoura, M.A. Alaoui-Jamali, and D.W. Laird. 2003. Lysosomal and proteasomal degradation play distinct roles in the life cycle of Cx43 in gap junctional intercellular communication-deficient and -competent breast tumor cells. *J Biol Chem*. 278:30005-30014.

Quist, A.P., S.K. Rhee, H. Lin, and R. Lal. 2000. Physiological role of gap-junctional hemichannels. Extracellular calcium-dependent isosmotic volume regulation. *J Cell Biol*. 148:1063-1074.

Rhett, J.M., J. Jourdan, and R.G. Gourdie. 2011. Connexin43 Connexon to Gap Junction Transition Is Regulated by Zonula Occludens-1. *Mol Biol Cell*.

Schmid, S.L., and V.A. Frolov. 2011. Dynamin: functional design of a membrane fission catalyst. *Annual review of cell and developmental biology*. 27:79-105.

Schubert, A.L., W. Schubert, D.C. Spray, and M.P. Lisanti. 2002. Connexin family members target to lipid raft domains and interact with caveolin-1. *Biochemistry*. 41:5754-5764.

Segretain, D., and M.M. Falk. 2004. Regulation of connexin biosynthesis, assembly, gap junction formation, and removal. *Biochim Biophys Acta*. 1662:3-21.

Sigismund, S., T. Woelk, C. Puri, E. Maspero, C. Tacchetti, P. Transidico, P.P. Di Fiore, and S. Polo. 2005. Clathrin-independent endocytosis of ubiquitinated cargos. *Proc Natl Acad Sci U S A*. 102:2760-2765.

Sirnes, S., A. Kjenseth, E. Leithe, and E. Rivedal. 2009. Interplay between PKC and the MAP kinase pathway in Connexin43 phosphorylation and inhibition of gap junction intercellular communication. *Biochem Biophys Res Commun*. 382:41-45.

Smotrys, J.E., and M.E. Linder. 2004. Palmitoylation of intracellular signaling proteins: regulation and function. *Annu Rev Biochem*. 73:559-587.

Solan, J.L., and P.D. Lampe. 2005. Connexin phosphorylation as a regulatory event linked to gap junction channel assembly. *Biochim Biophys Acta*. 1711:154-163.

Solan, J.L., and P.D. Lampe. 2007. Key connexin 43 phosphorylation events regulate the gap junction life cycle. *J Membr Biol*. 217:35-41.

Solan, J.L., and P.D. Lampe. 2008. Connexin 43 in LA-25 cells with active v-src is phosphorylated on Y247, Y265, S262, S279/282, and S368 via multiple signaling pathways. *Cell Commun Adhes*. 15:75-84.

Solan, J.L., L. Marquez-Rosado, P.L. Sorgen, P.J. Thornton, P.R. Gafken, and P.D. Lampe. 2007. Phosphorylation at S365 is a gatekeeper event that changes the structure of Cx43 and prevents down-regulation by PKC. *J Cell Biol*. 179:1301-1309.

Spray, D.C., and J.M. Burt. 1990. Structure-activity relations of the cardiac gap junction channel. *The American journal of physiology*. 258:C195-205.

Thevenin, A.F., T.J. Kowal, J.T. Fong, R.M. Kells, C.G. Fisher, and M.M. Falk. 2013. Proteins and mechanisms regulating gap-junction assembly, internalization, and degradation. *Physiology (Bethesda)*. 28:93-116.

Thévenin, A.F., T.J. Kowal, J.T. Fong, R.M. Kells, C.G. Fisher, and M.M. Falk. 2013. Proteins and Mechanisms Regulating Gap Junction Assembly, Internalization and Degradation *Physiology*. 28:93-116.

Thomas, M.A., N. Zosso, I. Scerri, N. Demaurex, M. Chanson, and O. Staub. 2003. A tyrosine-based sorting signal is involved in connexin43 stability and gap junction turnover. *J Cell Sci*. 116:2213-2222.

Thuringer, D. 2004. The vascular endothelial growth factor-induced disruption of gap junctions is relayed by an autocrine communication via ATP release in coronary capillary endothelium. *Ann N Y Acad Sci*. 1030:14-27.

Todorova, M.G., B. Soria, and I. Quesada. 2008. Gap junctional intercellular communication is required to maintain embryonic stem cells in a non-differentiated and proliferative state. *J Cell Physiol*. 214:354-362.

Traub, L.M. 2003. Sorting it out: AP-2 and alternate clathrin adaptors in endocytic cargo selection. *J Cell Biol*. 163:203-208.

Traub, L.M. 2005. Common principles in clathrin-mediated sorting at the Golgi and the plasma membrane. *Biochim Biophys Acta*. 1744:415-437.

Traub, L.M., and G.L. Lukacs. 2007. Decoding ubiquitin sorting signals for clathrin-dependent endocytosis by CLASPs. *J Cell Sci*. 120:543-553.

Valiunas, V., Y.Y. Polosina, H. Miller, I.A. Potapova, L. Valiuniene, S. Doronin, R.T. Mathias, R.B. Robinson, M.R. Rosen, I.S. Cohen, and P.R. Brink. 2005. Connexin-specific cell-to-cell transfer of short interfering RNA by gap junctions. *The Journal of physiology*. 568:459-468.

Warn-Cramer, B.J., P.D. Lampe, W.E. Kurata, M.Y. Kanemitsu, L.W. Loo, W. Eckhart, and A.F. Lau. 1996. Characterization of the mitogen-activated protein kinase phosphorylation sites on the connexin-43 gap junction protein. *J Biol Chem*. 271:3779-3786.

Wayakanon, P., R. Bhattacharjee, K. Nakahama, and I. Morita. 2012. The role of the Cx43 C-terminus in GJ plaque formation and internalization. *Biochem Biophys Res Commun*. 420:456-461.

White, T.W., D.A. Goodenough, and D.L. Paul. 1998. Targeted ablation of connexin50 in mice results in microphthalmia and zonular pulverulent cataracts. *J Cell Biol*. 143:815-825.

Wolfe, B.L., and J. Trejo. 2007. Clathrin-dependent mechanisms of G protein-coupled receptor endocytosis. *Traffic*. 8:462-470.

Wong, R.C., A. Pebay, L.T. Nguyen, K.L. Koh, and M.F. Pera. 2004. Presence of functional gap junctions in human embryonic stem cells. *Stem Cells*. 22:883-889.

Worsdorfer, P., S. Maxeiner, C. Markopoulos, G. Kirfel, V. Wulf, T. Auth, S. Urschel, J. von Maltzahn, and K. Willecke. 2008. Connexin expression and functional analysis of gap junctional communication in mouse embryonic stem cells. *Stem Cells*. 26:431-439.

Xu, J., and B.J. Nicholson. 2013. The role of connexins in ear and skin physiology - functional insights from disease-associated mutations. *Biochim Biophys Acta*. 1828:167-178.

Yuan, C., J. Furlong, P. Burgos, and L.J. Johnston. 2002. The size of lipid rafts: an atomic force microscopy study of ganglioside GM1 domains in sphingomyelin/DOPC/cholesterol membranes. *Biophys J*. 82:2526-2535.

Supplemental Data

Table S1: Time in hours required for GJ plaques assembled of wild type and AP-2 binding-impaired Cx43 mutants (S2, S3, S2+3) to constitutively turn over (assemble, mature, and being removed).

	wt	S2[a]	S3[b]	S2+3[c]
	2[d]	5	8	**21**
	2	5	8	24
	2	15	**12**	**25**
	2	**19**	12	25
	4	25	12	25
	4	25	**17**	**27**
	4	30	**17**	30
	4		17	33
	5[e]		20	40
	5		22	48
	6		22	
	6		22	
	6		22	
	8		22	
	10		25	
	10		25	
			30	
n :	16	7	17	10
Mean :	5	18	19	30
SEM :	1.4	3.7	1.3	2.7

[a]S2 mutant: Cx43-F^{268}A-GFP

[b]S3 mutants: Cx43-Y^{286}H-GFP, Cx43-ΔP^{283}PGYKLV-GFP

[c]S2+3 mutants: Cx43-F^{268}A+Y^{286}H-GFP, Cx43-Δ$L^{254\text{-}290}$-GFP, Cx43-Δ$L^{254\text{-}CT}$-GFP

[d]Regular: GJ plaques already existed at start of imaging

[e]**Bold**: Recordings include GJ plaque formation and internalization

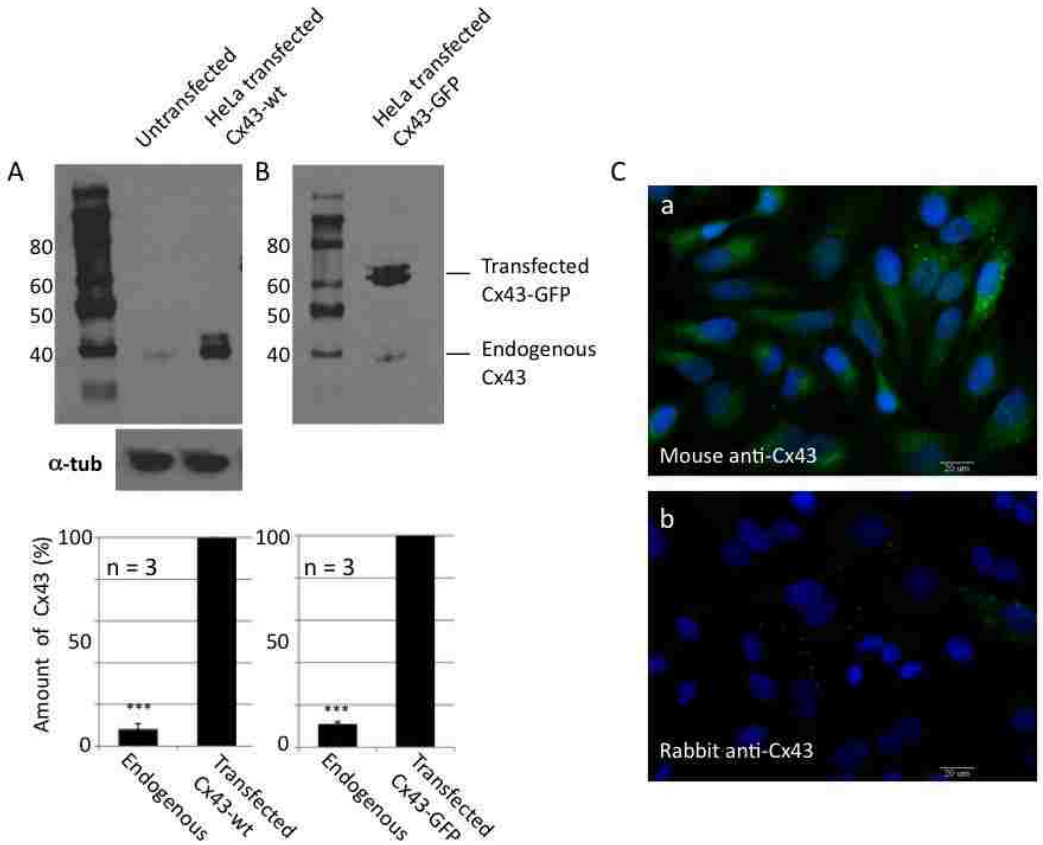

Figure S1: Basal levels of endogenous Cx43 were detected in HeLa cells (ATCC clone CCL-2). **(A)** HeLa cells were cultured in 3.5 cm diameter dishes and transfected with GFP-tagged and untagged wt Cx43 DNA constructs as described in Materials and Methods. Cells were lysed with 500 μl of protein sample buffer/dish. Transfected and endogenous Cx43 proteins from 15 μl of each sample (lysates of approximately 3000-6000 cells) were detected by Western blots using rabbit polyclonal antibodies (Cell Signaling Technology, Cat. No. 3512) **(A)**, or mouse monoclonal antibodies (Zymed, Cat. No. 138300) **(B)** directed against Cx43 as described in Materials and Methods. X-ray films were exposed to ECL in the dark for 5 minutes. Membranes were stripped and re-probed with mouse monoclonal antibodies directed against α-tubulin to control

for equal loading. Results indicate that total amount of endogenous Cx43 protein (lane 2) in the pools is ~10% (SEM ± 3, $p < 0.0001$) of the transfected Cx43 protein (CMV promoter) (lane 2, 3). Transfection efficiency in these experiments was about 20-30%. If transfection efficiency were 100%, the amount of enodogenous Cx43 in the pool would have been 1-2% compared to transfected Cx43. **(C)** Immunofluorecence staining of enodogenous Cx43 in HeLa cells using respective rabbit and mouse Cx43 antibodies performed as described in Materials and Methods. Representative images acquired using a 20x long distance lens are shown. Some GJ-like puncta and intracellular fluorescence and were detected using respective rabbit and mouse antibodies.

Appendix

7.1. Primers used for PCR mutagenesis

Forward primer pEGFP : 5'-GGC GGT AGG CGT GTA CGG-3'

Back Primer pEGFP : 5'-CGC CCT CGC CCT CGC CGG-3'

Cx43-Y^{230}H

Forward: 5'-CAT TGA GCT CTT CCA CGT GTT CTT CAA AGG C-3'

Reverse: 5'-GCC TTT GAA GAA CAC GTG GAA GAG CTC AAT G-3'

Cx43-F^{268}A

Forward: 5'-TCT CCA AAA TAT GCG TAC GCC AAT GGC TGC TCC TCA-3'

Reverse: 5'-TGA GGA GCA GCC ATT GGC GTA CGC ATA TTT TGG AGA -3'

Cx43-Y^{286}H

Forward: 5'-GTC TCC TCC TGG CCA CAA GCT GGT TAC TGG-3'

Reverse: 5'-CCA GTA ACC AGC TTG TGG CCA GGA GGA GAC-3'

Cx43-ΔY^{265}AY

Forward: 5'- TGC GGA TCT CCA AAA TTC AAT GGC TGC TCC-3'

Reverse: 5'- GGA GCA GCC ATT GAA TTT TGG AGA TCC GCA-3'

Cx43-ΔP^{283}PGKLV (generate ScaI site)

Forward: 5'-CTC TCG CCT ATG AGT ACT GGT GAC AGA AAC-3'

Reverse: 5'-GTT TCT GTC ACC AGT ACT CAT AGG CGA GAG-3'

Cx43-ΔL$^{254\text{-}290}$

Forward: 5'-GCC ACC ACT GGC CCA GGT GAC AGA AAC AAT-3'

Reverse: 5'-ATT GTT TCT GTC ACC TGG GCC AGT GGT GGC-3'

Cx43-ΔL$^{254\text{-}CT}$

Forward: 5'-GCC ACC ACT GGC CCA GCG GAT CCA CCG GTC -3'

Reverse: 5'-GAC CGG TGG ATC CGC TGG GCC AGT GGT GGC-3'

Cx43-stop (BamHI site is also eliminated)

Forward: 5'-CCT GAT GAC CTG GAG ATT **TAA** GAT CCA CCG GTC GCC ACC-3'

Reverse: 5'-GGT GGC GAC CGG TGG ATC **TTA** AAT CTC CAG GTC ATC AGG-3'

7.2. pEGFP-N1 map

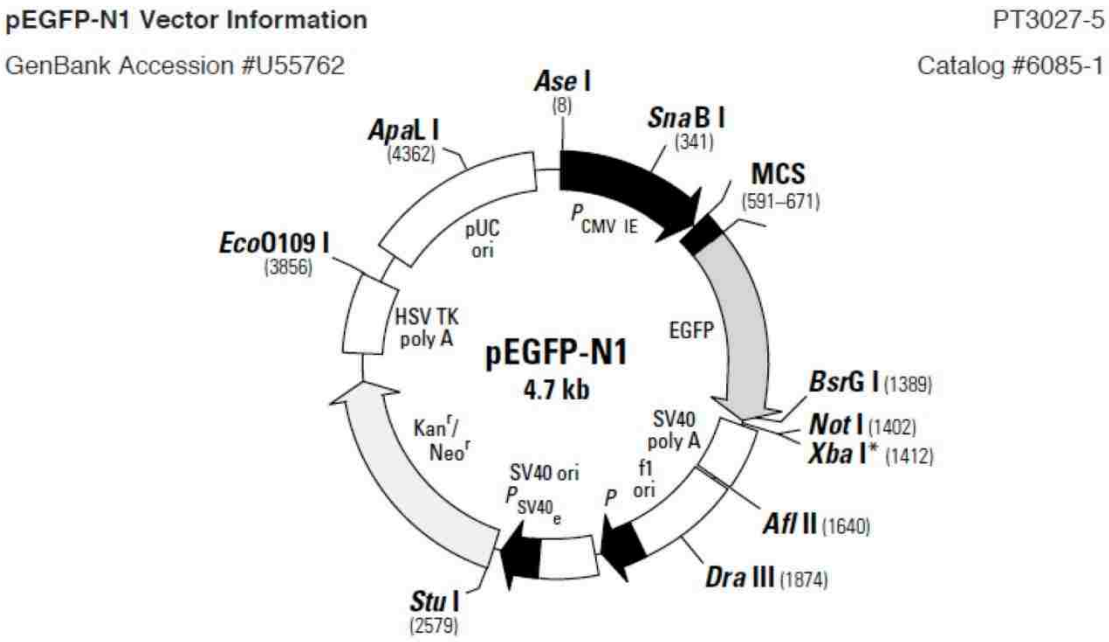

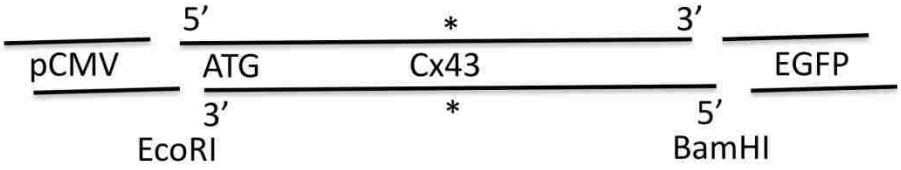

7.3. Buffers, solutions, and media used

4X SDS-sample buffer

250 mM Tris-HCl, 8% SDS, 40% glycerol, 8% beta mercaptoethanol, and 0.02% bromophenol.

SDS-PAGE running buffer

25mM Tris base, 192mM glycine, 0.1% SDS, pH 8.4.

Transfer buffer

25mM Tris, 192 mM glycine, 20% CH_3OH, pH 8.4 .

Tris buffer saline (TBS)

50 mM Tris, 150 mM NaCl, pH 7.4.

Stripping buffer

62.2 mM Tris, 2% SDS, and 0.6% beta mercaptoethanol, pH 6.8.

Phosphate buffer saline (PBS)

1 liter of PBS contain 8g of NaCl, 0.2 KCl, 0.268g $Na_2HPO_4.3H_2O$, 0.24g KH_2PO_4, pH 7.4.

Immunoprecipitation lysis buffer (RIPA)

20mM Tris-HCl (pH 7.5), 150mM NaCl, 1 mM Na_2EDTA, 1mM EGTA, 1% NP-40, 1% sodium deoxycholate, 2.5mM sodium pyrophosphate, 1mM β-glycerophosphate, 1mM Na_3VO_4, 1 μg/ml leupeptin. (additional protease and phosphatase inhibitor can be added).

Gelatin solution

0.1 % gelatin in PBS solution. Sterile by autoclave.

LB media

Dissolve 2.5 g of LB broth powder in 100ml of H_2O, sterile by autoclave.

HeLa and MEF cell culture media (prepared in sterile lamina flow hood)

High glucose DMEM were supplemented for a final concentration of 10% FBS, 2mM L-glutamine, and 1 I.U/ml penicillin and 50μg/ml streptomycin.

ES cells media (prepared in sterile lamina flow hood)

KO DMEM (Invitrogen) were supplemented for a final concentration of 15% KO serum replacement, 3mM L-glutamine, 1 I.U/ml penicillin and 50μg/ml streptomycin, sodium pyruvate, non-essential amino acids, cell culture graded β-mercaptoethanol, and LIF.

7.4. Antibodies Used

Rb anti-Cx43 (Cell Signaling Technology, Cat. No. 3512)

Mouse anti-Cx43 (Zymed Laboratories, Cat. No. 35-5000)

Rb anti-Cx43 (pS255) (Santa Cruz Biotechnology, Cat. No. sc-12899-R)

Rb anti-Cx43 (mouse pS262) (Santa Cruz Biotechnology, Cat. No. sc-17219-R)

Rb anti-Cx43 (pS279/282) gift from Dr. Paul Lampe

Rb anti-Cx43 (pS368) (Cell Signaling Technology, Cat. No.

Mouse anti-α-Adaptin (BD Transduction Laboratories, Cat. No. 610501)

Rb mAb anti-AP2M1 (Thr156) (Cell Signaling Technology, Cat. No. 7399)

Mouse anti-Dab2/p96 (BD Transduction Laboratories, Cat. No. 610464)

Rb anti-Dab2 (Cell Signaling Technology, Cat. No. 8582)

Mouse anti-clathrin heavy chain (BD Transduction Laboratories, Cat. No. 610499)

Rb mAb anti-clathrin heavy chain (Cell Signaling Technology, Cat. No. 4796)

Rb mAB anti-pERK1/2 (Cell Signaling Technology, Cat. No. 9102)

Mouse anti-GFP-HRP (Miltenyi Biotec, Cat. No. 130-091-833)

Mouse anti-α tubulin (Sigma, Cat. No. T9026)

HRP conjugated goat anti-mouse or anti-Rb (Zymed Laboratories, Cat. No. 81-6520 or 81-6120)

JOHN T. FONG

Ph.D. candidate

Curriculum Vitae

Contact Information

C250
111 Research Drive
Bethlehem, PA 18015

E-mail
Jof408@lehigh.edu
johnfong@alumni.upenn.edu

Phone: 610 507 7451

Education

Lehigh University — Bethlehem, PA
Cell and Molecular Biology, PhD program — Ph.D. candidate

University of Pennsylvania — Philadelphia, PA
Biotechnology, MS — Graduation: 08/2006

Thomas Jefferson University — Philadelphia, PA
Biotechnology, BS — Graduation: 08/2003

Honors and Awards

1. Cum Laude, Dean's list
2. Departmental Nemes Fellowship - Biological Sciences, Lehigh University – Fall 2012

Employment & Work Experience

Regeneron Pharmaceutical — 10/2006 to 08/2008 — Tarrytown, NY
Research Associate 3

- Conduct NIH Knock Out Mouse Project (KOMP).
- Perform gene targeting and ES cell culture in a high throughput manner.
- Performs sophisticated technical tasks involving a range of techniques.
- Acquire new methods to increase skills, confidence, and throughput, as well as troubleshoot and suggest improvements.
- Anticipates/recognizes potential problems with equipment and supplies and takes appropriate steps to correct or prevent.

University of Pennsylvania — 02/2005 to 10/2006 — Philadelphia, PA
Research Specialist B then promoted to Research Specialist C

- Perform Gene Targeting service, including growth, electroporation, and selection of mouse embryonic stem cells
- Perform basic molecular biological procedures: DNA isolation, Electrophoresis, karyotyping, etc.
- Assist in the design and construction of targeting vectors, conduct literature, assist in writing protocols and reports, maintain experiment records, and order supplies.

Thomas Jefferson University 09/2003 to 02/2005 Philadelphia, PA

Research Technician A

- Performed Solid Phase synthesis, chromatographic purification, and spectroscopic characterization of chelator-PNA-peptides for imaging sites of oncogene expression
- Conducted Bacterial expression, characterization of recombinant proteins
- Accelerated Grant Processing, purchasing, vendor relations, adherence to planned budgets
- Coordinated personnel and supplies among collaborating laboratories, served as liaison with university administration, and ensured compliance with safety regulations.

Teaching Experiences

Teaching assistant *Cell Biology Lab*, BIOS 368 – Fall 2011, Lehigh University, Bethlehem PA.
Teaching assistant *Biology Core II Lab, BIOS 116* – Fall 2009, Lehigh University, Bethlehem PA.
Teaching assistant *Biology Core I, BIOS 41* – Spring 2009, Lehigh University, Bethlehem PA.
Teaching assistant *Biochemistry Lab, BIOS 377* - Fall 2008, Lehigh University, Bethlehem PA.

Seminar/Invited Talks

1. International Gap Junction Conference 2013, Charleston SC, USA (2013)
2. Colloquium Seminar Series Oct. 2012, Dept. of Biological Sciences, Lehigh University

Conference Abstracts

1. **John Fong,** Rachael Kells, and Matthias Falk (2013). "Two Tyrosine-based sorting signals in the Cx43 C-terminus cooperate to mediate gap junction endocytosis." international gap junction conference." July 2013. Charleston, SC US
2. **John Fong** and Matthias Falk (2011)."Molecular mechanism of gap junction internalization: involvement of the C-terminal domain of Cx43." *51th American Society for Cell Biology annual meeting*. December 2011. Denver, CO
3. **John Fong** and Matthias Falk (2010). **"**Cx43 C-terminal domains involved in gap junction internalization." *50th American Society for Cell Biology annual meeting*. December 2010. Philadelphia, PA
4. **John Fong** and Matthias Falk (2009). **"**Connexin43 domains involved in gap junction internalization." *49th American Society for Cell Biology annual meeting*. December 2009. San Diego, CA

Publications (peer-reviewed)

1. **John T. Fong**, and Matthias Falk. EGF induces Cx43 gap junction endocytosis in mouse embryonic stem cells via phosphorylation of Ser262, Ser279/282, and Ser368. *FEBS letter* (in review).
2. **John T. Fong**, Rachael M. Kells, and Matthias Falk. Two tyrosine-based sorting signals in the Cx43 C-terminus cooperate to mediate gap junction endocytosis. *Molecular Biology of the Cell*. July 2013; 24(18): 2834-48 .
3. Anastasia F. Thévenin, Tia J. Kowal, **John T. Fong**, Rachael M. Kells, Charles G. Fisher, and Matthias M. Falk. Proteins and mechanisms regulating gap junction assembly, internalization and degradation. *Physiology*. March 2013; 28(2): 93-116.
4. Matthias M. Falk, **John T. Fong**, Rachael M. Kells, Michael C. O'Laughlin, Tia J. Kowal, and Anastasia F. Thevenin. Degradation of endocytosed gap junctions by autophagosomal and endo-/lysosomal pathway: A perspective. *J. Membr. Biol.* August 2012; 245(8):465-76.
5. **John T. Fong**, Rachael M. Kells, Anna M. Gumpert, Jutta Y. Marzillier, Michael W. Davidson, and Matthias M. Falk. Internalized gap junctions are degraded by autophagy. *Autophagy*. May 2012; 8**(**5): 794-811
6. Lynne Cassimeris, Victoria Caruso Silva, Elizabeth Miller, Quynh Ton, Cody Molner, and **John Fong**. Fueled by Microtubules: Does tubulin dimer/polymer partitioning regulate

intracellular metabolism? *Cytoskeleton* (Hoboken). March 2012; 69(3):133-43. [Epub 2012 Mar 5]

Professional Affiliations

1. American Society for Cell Biology (2009 to present)

References

Matthias M. Falk, Ph.D.
Associate Professor
Department of Biological Sciences
Lehigh University
111 Research Drive
Bethlehem, PA 18015
Phone: 610-758-5896
E-mail: mmf4@lehigh.edu

Lynne U. Cassimeris. Ph.D.
Professor
Department of Biological Sciences
Lehigh University
111 Research Drive
Bethlehem, PA 18015
Phone: 610-758-6275
E-mail: lc07@lehigh.edu

Wojtek Auerbach, Ph.D.
Director of ES cell Technology
Velocigene
Regeneron Pharmaceutical Inc.
777 Old Saw Mill River Road
Phone: 914 345 7960
E-mail: wojtek.auerbach@regeneron.com

Eric Wickstrom, Ph.D.
Professor, Biochemistry & Molecular Biology
Thomas Jefferson University
233 South 10th Street
Suite 209
Philadelphia, PA 19107
Phone: 215 955 4578
E-mail: eric@tesla.jci.tju.edu